2017-08-03

Ecohydrology of Coastal Wetland in South Florida under Sea Level Rise: A Combination of Stable Isotope Analysis, Mathematical Modeling, and Spatial Analysis

Lu Zhai
University of Miami, zhailulu@gmail.com

UNIVERSITY OF MIAMI

ECOHYDROLOGY OF COASTAL WETLANDS IN SOUTH FLORIDA UNDER SEA LEVEL RISE: A COMBINATION OF STABLE ISOTOPE ANALYSIS, MATHEMATICAL MODELING, AND SPATIAL ANALYSIS

By

Lu Zhai

A DISSERTATION

Submitted to the Faculty
of the University of Miami
in partial fulfillment of the requirements for
the degree of Doctor of Philosophy

Coral Gables, Florida

August 2017

UNIVERSITY OF MIAMI

A dissertation submitted in partial fulfillment of
the requirements for the degree of
Doctor of Philosophy

ECOHYDROLOGY OF COASTAL WETLANDS IN SOUTH FLORIDA UNDER SEA LEVEL RISE: A COMBINATION OF STABLE ISOTOPE ANALYSIS, MATHEMATICAL MODELING, AND SPATIAL ANALYSIS

Lu Zhai

Approved:

_____	_____
Leonel Sternberg, Ph.D.	Donald L. DeAngelis, Ph.D.
Professor of Biology	Research Professor of Biology
_____	_____
Carol C. Horvitz, Ph.D.	Guillermo Prado, Ph.D.
Professor of Biology	Dean of the Graduate School

_____
Robert Stephen Cantrell, Ph.D.
Professor of Mathematics

.

ZHAI, LU (Ph.D., Biology)

Ecohydrology of Coastal Wetland in South Florida under Sea Level Rise: A Combination of Stable Isotope Analysis, Mathematical Modeling, and Spatial Analysis (August 2017)

Abstract of a dissertation at the University of Miami.

Dissertation supervised by Professor Leonel Sternberg.
No. of pages in text. (107)

In southern Florida, conservation of coastal wetlands is facing two challenges under sea level rise (SLR): (1) How to estimate and predict encroachment of mangroves and other halophyte vegetation into the areas previously covered by freshwater species? (2) How to allocate more freshwater from Lake Okeechobee in middle Florida to the coastal wetlands (e.g., Everglades) to counteract increasing saltwater intrusion? Fundamental to the above challenges is saltwater intrusion associated with SLR, which can increase the soil pore water salinity to levels where freshwater species cannot survive. The overall aim of my dissertation is to access the potential changes in vegetation community structure based on different methods such as: remote sensing, using stable isotopes as a tracer and modelling the flow of these tracers through coastal wetlands.

In the second chapter of my dissertation, I investigated the persistence of mud islands in Florida Bay. Mud islands in Florida Bay are probably the most sensitive land formation in southern Florida to be affected by SLR, because they have small area and low elevation. However, surprisingly, there is no study to estimate the historical vegetation changes in these islands. More importantly, there are few human activities in these islands. Therefore they provide an appropriate setting to examine how these small island ecosystems responded to the impacts of SLR without the confounding

anthropogenic factors such as road building and land management. I used high-resolution 61-yr historical aerial images and 27-yr time-series of Landsat images to estimate changes in island areas and mangrove coverage for 15 mud islands of Florida Bay. I found, surprisingly, that these islands actually increased in their area and showed mangrove expansion under the local SLR. In addition, I observed a positive relationship between island area increase and mangrove area increase in these islands, and it indicated the contribution from the biogeomorphic feedbacks between mangroves and sedimentation to the island survival.

Large spatial scale vegetation shift from freshwater vegetation to mangroves can be estimated and even predicted by remote sensing data using the same techniques as in my second chapter. However, a more detailed prediction of vegetation shift at a relatively smaller spatial scale and even at an individual scale is required for local ecological conservation efforts. In my third chapter, I attempted to find an appropriate individual based predictor for the potential vegetation shift under SLR. I incorporated stable isotope 18O abundance of water as a tracer for various hydrologic components (e.g., vadose zone, water table) in a previously published individual based model describing ecosystem shifts between hammock and mangrove communities in southern Florida. My modelling efforts showed that freshwater hammock trees that were to be replaced by mangroves had higher δ18O values in their plant stem water than those which remained despite SLR. These tracer differences could be detected as early as 3 years before their eventual replacement by mangroves.

Much of the susceptibility of the Everglades to SLR is exacerbated by the decrease of freshwater flow into the system. To mitigate this water shortage, the water

conservation areas (WCAs) of southern Florida were constructed to serve two functions: 1) provide water to the Everglades on a regular basis and 2) remove high nutrient content from the water before the entering the naturally oligotrophic Everglades ecosystem. One critical problem of the WCA is loss of water by evaporation as they move from the Lake Okeechobee area and on to the Everglades. However, quantifying evaporation in a wetland is challenging, because it is difficult to separate evaporation from transpiration. My fourth chapter addressed this knowledge gap by using oxygen and hydrogen isotope ratios of water as a tracer for evaporation. I used a deuterium excess method based on oxygen and hydrogen stable isotope ratios ($\delta 18O$ and δD) of reservoir water to calculate the remaining fraction of water after evaporation in the Water Conservation Area-1 (WCA-1). My results showed that both vegetation coverage and distance to the discharge gate had significant effects on the remaining fraction, however the depth of the water column had no effect.

TABLE OF CONTENTS

Page

LIST OF FIGURES

Chapter 2 **Page**

Chapter 3

LIST OF TABLES

Chapter 4 **Page**

Chapter One

Introduction

Coastal Wetland Ecosystems and Sea Level Rise

Coastal wetland ecosystems are transitional lands at the terrestrial-marine interface, and this unique position makes them vulnerable to impacts of sea level rise (SLR) and other impacts of climate changes. One of the most direct effects of SLR is saltwater intrusion (SWI) which can increase the soil porewater salinity and waterlogging of coastal wetland ecosystems. SWI is accompanied by a spatial shift inland of the boundary or ecotone between salinity-tolerant (halophytic) vegetation, such as mangroves, and salinity-intolerant freshwater vegetation, such as hardwood hammocks or freshwater marshes (Ross et al., 2000). Mangroves tend to be excluded from freshwater areas because of high competition with hammock species (Silander and Antonovics, 1982; Kenkel et al., 1991; Greiner La Peyre et al., 2001) and low accessibility of mangrove propagules to the freshwater areas. But the increasing salinity due to SWI can change the balance in favor of the mangroves, causing the boundary or ecotone between the two vegetation types to shift inland (Ewe et al., 2007; Doyle et al., 2010; Saha et al., 2011). This boundary shift can result from a salinity-induced mortality of the hammocks, which is then replaced by mangroves, or by decline in growth rate of hammock vegetation, allowing it to be outcompeted by the invading mangroves. This type of vegetation shift has been observed in many field sites around world, e.g., Krauss et al. (2011) in Everglades, USA; Asbridge et al. (2016) in Gulf of Carpentaria, Australia.

Mud Islands of Florida Bay

One area in Florida for which there is a knowledge gap, in terms of the effects of SLR, are the mud islands of Florida Bay. These are Holocene carbonate mud islands with small (< 1km^2) area, low elevation (< 50cm above MSL). Therefore, these mud islands are especially vulnerable to the SLR impacts. In addition, there is little human activity, such as road building, occurring in these islands. The effects of SLR on island ecosystem include vegetation transition (Ross et al., 2009), hydrological alteration (Terry and Chui, 2012), and habitat loss (Fish et al., 2005). With these effects, islands are also of concern to conservation biologists because they harbor species with small geographic ranges and high endemicity (Wetzel et al., 2013). Mud islands should be more sensitive to the SLR and could be an early indicator of SLR influence, because of their relative homogeneous topological and climatic conditions (Courchamp et al., 2014). However, most studies focus on large-size island ecosystems with substantial human activities, which may confound SLR influences (Zhang et al. 2010). Other studies investigate a large number of islands including both large and small size types, e.g., Bellard et al. (2014) estimated 6-19% of 4447 islands which could be entirely submerged with projected SLR and may loss over 300 endemic species, however they didn't consider the potential feedbacks or adaptation of vegetation communities to SLR. Further, these mud islands have experienced very few anthropogenic influences, which can affect ecosystems more so than SLR (Gilman et al., 2008). This unique setting of the mud islands, with homogeneous environmental conditions and little anthropogenic influences, allows us to focus purely on the SLR influences by avoiding other confounding influences.

Water Conservation Areas

Another area critical to mitigating SLR effects in the Everglades are the Water Conservation Areas (WCAs) in southern Florida. The WCAs were built to maintain appropriate water flow into the Everglades and to remove nutrients from these water. In southern Florida, water resource management is critical in view of the increased competition between urbanization, agriculture and ecological conservation of the Everglades National Park (ENP). The demand for freshwater resources is rising fast with the rapid population growth of southern Florida (Obeysekera et al., 2011). One of key aims of ecological management in ENP is to improve its freshwater availability, because the freshwater inflow can counteract the increasing saltwater intrusion in ENP due to the sea level rise (Perry, 2004). For a better protection and management of freshwater resources, three Water Conservation Areas (WCAs) were built between Lake Okeechobee and ENP (Hong et al., 2010). However, estimates and control of water loss in the WCAs are still challenging, particularly for water loss by evaporation, which is a dominant form of water loss in many wetland settings, e.g., Schwerdtfeger et al. (2014) in tropical wetlands, Sánchez-Carrillo et al. (2004) in semi-arid wetlands.

Techniques used in the study

During my dissertation research, I used three major scientific tools to study issues related to SLR in southern Florida: stable isotopes as a tracer; individual based modelling and spatial analysis based on aerial and satellite images.

Stable Isotope as a Tracer of Water Flow

Chemical elements can occur in different isotopic forms, which have different numbers of neutrons, but the same number of protons in their nucleus. Because these

different forms of the same element have the same number of protons, they have the same chemical properties. The different number of neutrons, however, results in different masses for the different isotopes of the element. This mass difference can lead to partial separation of the light isotopes from the heavy ones during physiochemical processes. For example, during evaporation, the evaporation rate at a given temperature is a function of the hydrogen bond strength between the polar water molecules, and the ^{18}O-H bond is stronger than ^{16}O-H bond. A weaker hydrogen bond will make water molecules evaporate at a faster rate than the stronger one. A resulting greater flux of $H_2{}^{16}O$ leads to an enrichment of ^{16}O in the vapour phase and enrichment of ^{18}O in the remaining liquid phase. Therefore, the composition of light and heavy isotopes differs among different phases of water. During evaporation process or other physiochemical processes, the partial separation of these isotopologues (e.g., ^{16}O and ^{18}O) is called isotope fractionation, which can be quantified by different parameters, including fractionation factor (α), isotope separation (Δ) and enrichment factor (ε). These will be more precisely defined in the appropriate chapters of the dissertation. Isotope composition is quantified as a ratio of the heavier isotope to the lighter isotope, with reference to an internationally defined standard as δ (‰) = $[(R_{sample}/R_{std})-1]*1000$, where R_{sample} is the isotopic ratio of the sample (e.g., $^{18}O/^{16}O$), and R_{std} is the isotopic ratio of standard, e.g., for water, it is Vienna mean standard water.

Concepts related to isotope composition and fractionation were applied to observations in the δ^{18}O and δD values of the remaining water during evaporation in the field. These changes in isotope ratios are quantified by the Rayleigh Distillation equation. For oxygen isotopes, the equation is described by $\delta_f O = \delta_0 O - \varepsilon_O \cdot \ln f$, where $\delta_f O$ is

oxygen isotope composition of remaining water after a certain amount of evaporation, $\delta_0 O$ is oxygen isotope composition of the original water before evaporation begins, ε_O is enrichment factor (i.e., related to isotope fractionation), and f is remaining fraction of water after evaporation (i.e., the greater the evaporation, the lower the remaining faction f of water). According to the above equation, f decreases and $\delta_f O$ would increase with greater evaporation.

My study focused on application of oxygen and hydrogen stable isotope composition ($\delta^{18}O$ and δD) to predict the vegetation shift in an individual-based model and quantify evaporation in a water conservation area. The $\delta^{18}O$ value of plant stem water is an appropriate candidate of vegetation shift predictor for two reasons: (1) $\delta^{18}O$ value of water, at least in southern Florida, is indicative of its salinity, with freshwater showing less oxygen-18 enrichment than saline seawater (Sternberg and Swart, 1987; Sternberg et al., 1991). Thus, there are significant differences in $\delta^{18}O$ between various water sources, such as precipitation and sea water. (2) Although plants discriminate against salt, they do not discriminate against ^{18}O during water uptake (Dawson et al., 2002); e.g., Lin and Sternberg (1994) found that there were no significant differences in $\delta^{18}O$ values between stem water of red mangrove (*Rhizophora mangle*) and its corresponding vadose zone. As an application of quantifying evaporation (*E*) in WCA, I used $\delta^{18}O$ and δD to develop a deuterium excess (*d*) method. deuterium excess (*d*) is calculated from dual-isotope ($\delta^{18}O$ and δD) analysis of ambient water. Since *d* decreases with an increase in *E* (Huang and Pang, 2012), it serves as a proxy for *E*. This method has advantages over other traditional evaporation measurements. First, the *d* method has the potential to separate *E* from transpiration (*T*). Other methods attempted to separate *E* from *T* by estimating

evapotranspiration (*ET*) from vegetated area and comparing with that from a nearby open water area, but these methods provided unclear results (Sánchez-Carrillo et al., 2004). Second, the *d* method is relatively easy to apply in the field. It doesn't need continuous field observations with high frequency since stable isotope signatures of water integrate processes occurring through a period of time. Other methods, e.g., lysimeter method, eddy covariance method and sap flow method, require continuous survey of various environmental parameters and expensive facilities which can be only applied to appropriate environments (Drexler et al., 2004; Wu and Shukla, 2014). Third, the *d* method has a better spatial resolution than other methods, e.g., empirical methods like Penman-Monteith (PM) equation or Priestley-Taylor (PT) equation. These empirical methods have an important assumption that there is a uniform surface (e.g., uniform vegetation cover), but tropical wetland tends to have a variety of vegetation coverage, which makes these methods difficult to quantify the spatial pattern of *E* throughout a wetland (Wu and Shukla, 2014).

Mathematical Modelling

Individual-based models (IBM), which describes individual organisms in a system, have become a widely used tools in ecology, because they allow researchers to study how system level properties emerge from the adaptive behavior of individuals as well as how, on the other hand, the system affects individuals (Grimm et al., 2006). In a previously published IBM describing the dynamics of an initially mixed hardwood hammock and mangrove stand in southern Florida (Sternberg et al., 2007; Jiang et al., 2012b; Teh et al., 2015), I incorporated the $\delta^{18}O$ value of various water compartments in the model, including vadose zone, water table and plant stem water. In these compartments, their

water salinity and $\delta^{18}O$ values were followed in areas of the landscape where hammocks were replaced by mangroves in the model, and it was determined whether the change of $\delta^{18}O$ value of plant stem water preceded the replacement of a hammock species by a mangroves species.

Spatial Analysis

Spatial analysis based on aerial image and remote sensing image can directly measure the long-term changes of land surface. For example, with aerial images taken in the year of 1935 from National Archives (Washington, US), Ross et al. (1994) found that, from 1935 to 1991, the area of pine forest in Sugarloaf Key (one of the Florida Keys) decreased from 0.46 km^2 to 0.30 km^2 with a 15 cm rise in local sea level, and the areas of early pine mortality are now populated by halophytic plants. The historical aerial images used in my study of Florida Bay mud islands were made in 1953. Therefore, by a comparative spatial analysis of the aerial images in 1953 and 2014, I was able to detect the long-term changes in the island area and mangrove distribution with SLR, which is difficult to measure by field studies. Further, the precision of the island area based on aerial photo analysis may be affected by the changing position of shoreline with tides, i.e., beach area is variable with different tide levels, which can change in a very short-time period (Kadmon and Harari-Kremer, 1999). To solve this problem, the beach area was not included in my island area calculation. Further, my mapping took advantage of one vegetation landscape feature that these micro islands are surrounded by mangrove forests (Welch and Madden, 1999). Therefore, the island boundaries were represented by the ocean-side boundaries of mangrove forests in my study.

Chapter Two

Survival of Mud Islands in Florida Bay from Submergence by Sea Level Rise from 1953 to 2014: the Potential Influence of Mangrove Expansion

Summary

Long-term island submergence under sea level rise (SLR) is uncertain, and comparison between SLR and elevation increase by biogeomorphic feedbacks in vegetated coastal area showed controversial results from different studies (Craft, 2012; Lovelock et al., 2015; Kirwan et al., 2016). The controversial results may be caused by disturbing influences including human activities. Therefore, to validate long-term resilience of island ecosystems to SLR by the biogeomorphic feedbacks, there is a need for appropriate site conditions and methodology. To satisfy this purpose, mud islands in Florida Bay are unique models. The long-term changes of the mud islands were quantified by both the high-resolution 61-yr historical aerial images and 27-yr time-series of Landsat images. Two metrics were the foci of this study, island area and mangrove coverage. Here I showed that these islands have long-term increase in area under SLR, and that significant mangrove expansion on the islands may be one of the contributors to the increasing island area. Future studies about specific factors on island submergence and biogeomorphic feedbacks are required, including meteorological factors, vegetation types and topography.

Background

Submergence of island ecosystems under the SLR remains controversial, and long-term assessment of their stability tends to ignore influences of biogeomorphic feedbacks. An early global study stated that 70% of world beaches were eroding, whereas only 10%

were accreting (Bird, 1987). It is commonly accepted that long term inundation of coastal areas will be exacerbated under SLR (Kriebel et al., 2015). Therefore, a large number of studies simulate erosion and inundation impacts of SLR by mathematical models or controlled experiments. For example, Bellard et al. (2014) simulated different SLR scenarios and their threat to insular biodiversity. However, an European coastal database, "Eurosion", shows that only about 30% of European beaches are currently eroding, which is significantly less than the 70% found at global scale by Bird (1987) (Cazenave and Cozannet, 2014). Furthermore, McLean and Kench (2015) summarized multi-decadal area changes of 12 atolls, and found little evidence of reduction in island size under SLR. Recent field studies identified that keeping pace with SLR of coastal vegetated areas may be contributed from biogeomorphic feedbacks between plant growth and geomorphology (Craft et al., 2008). The proposed biogeographic feedback is caused by vegetation floor accretion, and the accretion decreases anoxic stresses of vegetation seedlings during inundation. The decreased anoxic stress further stimulates vegetation growth resulting in more sediment to build new areas for island expansion (Kirwan and Megonigal, 2013). The sediment accumulation should be improved with the increase in coastal vegetation area. Particularly in coastal mangroves, the high sediment accumulation is caused by mangroves producing excess organic carbon and plant growth which is deposited as peats, and the excess growth is based on that mangroves have higher primary production than respiration (Duarte et al., 2005). In addition, their robust aerial root structures can enhance sediment accumulation by effectively slowing water velocities and settling sediment out of the water column and onto coastal soils (Krauss et al., 2003).

The comparison between SLR and elevation increase caused by biogeomorphic feedbacks is under debate. Global measurements of elevation changes in marshes indicate that coastal marshes are increasing elevation at rates similar to or exceeding historical SLR, and simulations predict survival of the coastal marsh under different future sea level scenarios (Kirwan et al., 2016). However, tidal freshwater forest accretion cannot keep pace with sea level rise based on the rate comparison between soil accretion and sea level rise in the South Atlantic (Georgia, USA) coast (Craft, 2012). It was also observed that island surface elevation increases were less than the long-term SLR in some Indo-Pacific mangrove forests, and it was conjectured that shallow subsidence by human activities or climatic changes, e.g., compaction of surface sediments, and forest degradation (Syvitski et al., 2009; Lovelock et al., 2015), disrupted the biogeomorphic feedbacks, and decreased the rate of sediment accretion in these islands. Therefore, to validate long-term resilience of island ecosystems to SLR by the biogeomorphic feedbacks, there is a need for appropriate site conditions and methodology.

To satisfy this purpose, mud islands in Florida Bay are unique models. First, these mud islands have small area (< 1km^2) and low elevation (< 50cm above MSL) (Swart and Kramer, 2004). Therefore, they can be expected to be greatly impacted by SLR. Second, these islands are surrounded by mangrove forests (Welch and Madden, 1999), and the biogeomorphic feedbacks in the mangroves can be examined. Third, these islands have little human activities (Swart and Kramer, 2004), therefore the confounding influences from human disturbances can be minimized. Moreover, the long-term changes of the islands can be more readily quantified by spatial change analysis using historical aerial images and Landsat images (Ellison et al., 2017).

In my study, the long-term changes of the mud islands were quantified by both the high-resolution 61-yr historical aerial images and 27-yr time-series of Landsat images. Two island changes were focused on, including island area and mangrove coverage. I hypothesized that: (1) Areas of the mud islands increased under SLR; (2) Mangrove coverage of the mud islands also increased; (3) The area increases in the islands have a positive relationship with mangrove coverage increases.

Methods

1. Site condition

Florida Bay is bounded on the north by the Everglades (Fig.1A) and receives freshwater input via several streams located in the northeastern corner of Florida Bay. On the southwest, Florida Bay connects with the Gulf of Mexico, through which a large amount of wind and tidal exchange into Florida Bay. On the east, Florida Bay is bound by the Florida Keys, and has limited exchange with the coastal Atlantic Ocean. My study focused on 15 mud islands in the western Florida Bay based on the availability of the historical images. The subtropical climate of Florida Bay is characterized by warm, humid, rainy wet season during the summer and a dry season with periodic incursions of cool air during the winter. The summer wet season extends from about mid-May to November, and the winter dry season extends from about December to mid-May.

Most of the island vegetation is littoral and dominated by mangroves, and other plants include blue-green algae and low, salt-tolerant herbs (Enos, 1989). A few relatively large islands are populated by grasses, palms, buttonwoods and hardwoods. Importantly, mangroves tend to be distributed along the island shorelines surrounding these islands. This landscape feature facilitated mapping the mangrove encroachment from shoreline to

inland areas, and boundaries between islands and seawater. The island boundaries were represented by the ocean-side boundaries of mangrove canopies, which have been used in other studies (Webb and Kench, 2010; Liu et al., 2014; Albert et al., 2016) and are more stable than ground or beach boundaries. Because island area based on ground boundaries would be varied by daily-variable tidal levels (Kadmon and Harari-Kremer, 1999).

Florida Bay is experiencing SLR based on the long-term in-situ measurements around this area, e.g., the sea level data of Fig.1B was from the weather station in Key West, FL, which is located in the south end of Florida Bay. In Fig.1B, there was a clear increasing trend of the sea level from 1953 to 2014, and this period was same to my study period. In 1953, the average sea level was about 0.17 mm, but the sea level increased to about 0.35 mm in 2014. This increasing pattern of sea level was also observed in worldwide areas, and is expected to be continued in the long future (Hay et al., 2015).

2. Aerial images analysis

Mangrove mapping focused on the mangrove forests which are continually distributed from shoreline to inland areas, because these mangrove forests are experiencing direct SLR impact, and contribute directly to the area changes of the islands. More importantly, the focus on the shoreline mangrove areas improves accuracy of my results by avoiding the difficulty in distinguishing mangroves from the mixed-vegetated areas in the center of the islands. The coastal mangroves are continuously distributed, and have closed canopy without the presence of other non-mangrove species. Current mangrove forest boundaries in the islands were defined by high-resolution orthoimageries in 2014, achieved from the United States Geological Survey (USGS) Web site Earth Explorer (http://earthexplorer.usgs.gov/). The spatial resolution of the high-resolution

orthoimagery is 0.3 m, which is an appropriate resolution to identify mangrove forest in the island. In order to detect the historical distribution of mangrove forest in the islands, black and white photographs taken in 1953 by the Florida Department of Transportation (FDOT) (http://www.dot.state.fl.us) and Aerial Photography in George A Smathers Library of University of Florida (http://ufdc.ufl.edu/aerials) were used. The spatial resolution is approximately 0.3 m. The ocean- and land-side boundaries of mangrove forest were manually defined by using on-screen digitizing in ArcMap 10.1 (Esri, USA). The images were converted into NAD 1983 UTM Zone 17N coordinate system by Georeferencing Tool in ArcMap 10.1. The island images were georeferenced by using ground control points, and the total Root Mean Square Error for each image is smaller than 2 m.

3. Landsat TM images

To get time-series data of total areas of the 15 islands, Landsat Thematic Mapper (TM) data (1984 to 2011) covering cloud-free pixels of my study area were obtained from the USGS (http: //glovis.usgs.gov). The Landsat images are level 1 terrain corrected products (L1T), therefore no geo-rectification was required and image-to-image registration was omitted. Digital numbers were converted to Top-of-Atmosphere (TOA) reflectance and then corrected for atmospheric effects to get land surface reflectance. The above preprocessing steps were finished by ATMOSC module in Idrisi Selva system (Clark Labs, USA). The preprocessed images were subset by selecting a fixed polygon area covering the 15 islands. The subsetting step can reduce data volume, and increases overall image classification accuracy by reducing the spectral variation imposed by other land cover types (Giri and Long, 2016). ISODATA unsupervised classification was

performed for each image (Giri and Muhlhausen, 2008), and the generated clusters were then grouped into two classes: seawater and island. Because ISODATA algorithm is a hard classifier, pixels near island boundaries contain mixture of seawater and island area were forced into one or the other category, and this confusion is likely to be greatest for the images from low tide period. To assess accuracy of the maps, high-resolution aerial images in 1985, 1995, 1999, 2004, 2007, and 2010 obtained from USGS (National High Altitude Photography (NHAP), Digital Orthophoto Quadrangles (DOQ)), and Google Earth, were used to assess map accuracy. The assessment used more than 50 ground samples per class as recommended by Congalton (1991), and the minimum of the classification accuracies is 90% for each map. If maps didn't satisfy the standard, I manually edited the classified images to remove obvious errors using Landsat true-color images, or reclassified the images (Giri and Muhlhausen, 2008). For the other years when the aerial images are not available, I would edit the images if the total island area difference from its nearest year (choose from the above six years) is more than 10% to make sure the difference is not from the classification error. Finally, a postclassification analysis was performed to calculate total areas of the 15 islands by AREA module in Idrisi.

4. Statistical Analysis

The area increases of island and mangrove from the aerial image analysis were examined by a paired t-test, and the assumption of normal distribution of the area difference (island area and mangrove area) for each island between the two years was satisfied by a Shapiro-Wilk W test ($p>0.05$).

The relationship between change of island area and change of mangrove area was examined by a simple linear regression model. The predicted areas of the islands in 2014 without mangrove expansion were calculated by a multiple linear regression model which describes island area in 2014 as a function of island area in 1953, mangrove area change from 1953 to 2014, and their interaction. Then the island area in 2014 without mangrove expansion was predicted by setting mangrove area change to be zero. For the above two linear regression models, the assumptions about homoscedasticity and normality of residuals were satisfied, because the residual plot by the predicted values showed no trend, and Shapiro-Wilk W test cannot reject the null hypothesis about the normal distribution of the residuals ($p>0.05$).

For time series of the total areas, I first used a polynomial linear fit between total areas and year to detrend the time series data. Then residuals of the linear model follow a normal distribution (Shapiro-Wilk W Test: $p=0.4039$), the homoscedasticity of the residuals was also satisfied by checking the residual plot by the predicted values that showed homogeneous residuals with the change of predicted values, and the zero expectation of the residuals was satisfied by comparing the residual expectation with zero in the one sample t test ($p=1$). Because the linear model is based on time series data, the temporal dependence of the residuals was examined by a correlogram from sample autocorrelation function (ACF). I didn't find autocorrelation of any lags exceed two standard errors above zero. Further, no autocorrelations of the residuals was detected by Ljung–Box test ($p=0.501$). I concluded that the residuals are white noise, and the linear model is an appropriate fit to my data.

Results and Discussion

Comparative spatial analysis of their historical aerial images showed that the island area significantly increased from 1953 to 2014 (Fig. 2A, $p=0.0295$). For example, Joe Kemp Key had the largest area increase which is from 0.34 km^2 to 0.37 km^2. However, three islands, including Umbrella Key and Rankin Key, decreased in area. These islands had a large submerged area inside the island as a common feature, which may negatively impact the biogeographic feedbacks of mangrove forests. Because evaporation of these interior ponds increases the salinities to as high as 135 ppt (Swart and Kramer, 2004), and these high salinities, which are about 4 times higher than the ocean salinity, would strongly stress mangrove growth (Enos, 1989). The pattern of the island area increase was further supported by quantification of annual total areas of the 15 islands from Landsat satellite imagery (1984 to 2011), which showed significant increasing total area with time (Fig. 2B, $p=0.0029$). During the same time period from 1953 to 2014, there is also a clear increasing trend of the yearly average local sea level (Fig. 1B, $p<0.0001$). Therefore, we conclude that areas of most of the mud islands in Florida Bay expanded under sea level rise.

With expanding island area despite SLR, a strong mangrove expansion was also observed in these islands. By comparing mangrove coverages from the high resolution aerial images in 1953 and 2014, I found a significant mangrove expansion in the islands ($p<0.0001$, Fig. 3). For example, Cormorant Key had the largest mangrove coverage increase from 17% to 78%. The landward encroachment of mangroves with the concomitant retreat of freshwater species has been observed in different sites around the world, e.g., Giri and Long (2016) in southern Florida, USA; Saintilan and Wilton (2001)

in southeastern Australia; Ellison et al. (2017) in Pacific island atolls. The replacement of freshwater species by mangroves is caused by increased salinization of coastal areas, high salinity tolerance of mangrove species, and extended dispersal of mangrove propagules (Peterson and Bell, 2015; Zhai et al., 2016). However, some studies noticed that mangroves in island interiors are stressed and eventually destroyed by the following processes: sedimentation of lime mud, hypersaline conditions caused by interaction of SLR and evaporation, rapid salinity fluctuations with rainfall, and high summer water temperatures which are estimated at more than 50°C (Enos, 1989). In addition, hurricane damage can strongly affect island mangrove dynamics (Smith III et al., 2009), but mangroves also showed relatively quick recovery from the damages (Feller et al., 2015). Therefore, this long-term pattern would fluctuate in a shorter time window, and the fluctuation may be indicated by the annual total areas data in Fig. 2B.

Mangrove expansion may benefit these islands by mitigating SLR inundation, according to our analysis that the islands that increased more in area tended to have more mangrove expansion ($p=0.0001$, Fig. 4A). However, not all of the island area increase observed elsewhere is caused by the biogeomorphic feedbacks. Some atoll islands in the Pacific were also observed to have increased area under SLR (Duvat and Pillet, 2017), however, the increasing areas in some islands resulted from net lagoon-ward migration of islands, while ocean-side shorelines of the islands may still experience erosion (Webb and Kench, 2010). McLean and Kench (2015) also attributed the island area increase of the atoll islands to human activities, e.g., reclamation. Therefore, the influences of biogeomorphic feedbacks may be site specific. To further quantify the influence of mangrove expansion on the island areas, a prediction of island area in 2014 without

mangrove expansion was made by a multiple linear regression model. The model further supported that mangrove expansion had significant effect on the mangrove area in 2014 ($p=0.0003$). Without mangrove expansion, the average area decrease of the islands was 0.02 km^2 which was 9% of the average island area in 1953 (Fig. 4B). Previous studies also found that red mangrove colonization on Park Key in Florida Bay has formed striking island area growth (Enos, 1989), and mangrove expansion was also reported to reduce shoreline erosion in Hawaii (Allen, 1998).

The above effect of mangrove expansion on island area is based on the high sediment supply in seawater, which is critical to the formation of geomorphic features in Florida Bay, e.g., mud island (Swart and Kramer, 2004), and initial development of mangroves is largely dependent on physical environment with forests occupying sites once they reach a suitable elevation in the intertidal (Swales et al., 2015). The sediments in Florida Bay are characterized by high production and high unconsolidated carbonate content (~95%) (Swart and Kramer, 2004). For example, as a major form of sediment, carbonate encrustations of *Thalassia* communities have a production estimated to be as high as 118 g m^{-2} y^{-1} (Nelsen and Ginsburg, 1986). Sediment accumulation can be stimulated by the mangrove expansion, because the sediment would be trapped by mangroves with their robust aerial root structures, and sediment resuspension is decreased by mangroves (Swales et al., 2015). The sediment also benefits mud banks where the islands lie, and it is another important morphological characteristic of Florida Bay. Based on the long-term dynamics of the mud banks, western Florida Bay where my study area is located, was named Western Constructional Zone (Wanless and Tagett, 1989). Because there are excess sediments from local production and /or detrital input,

and carbon-14 dating study also indicated that mud banks in this area are actively accreting vertically and laterally (Wanless and Tagett, 1989). This sediment caused mud bank accretion may also contribute to the island area increase. In summary, there are two processes affecting the island area: above-ground biogeomorphic feedbacks in mangrove forests, and underground mud bank accretion. Both of the two processes are based on the high sediment production in Florida Bay.

Potential ground elevation increase above SLR, by mangrove caused biogeographic feedbacks, does not mean that the impact of SLR can be completely blocked out by the coastal mangroves. The aboveground processes of salt water intrusion with SLR, e.g., tidal flooding and hurricanes (White and Kaplan, 2017) can be mitigated by the increase of ground elevation. However, salt water intrusion by underground process, i.e., infiltration of seawater into coastal groundwater aquifers (Chang and Clement, 2012), may not be affected by the aboveground elevation change. Therefore, SLR can affect coastal wetlands through its influences on the groundwater, which is an important abiotic factor on the structure of coastal vegetation communities (Wilson et al., 2014). The strong mangrove expansion observed in my study also supported that SLR is still affecting the vegetation communities of the mud islands even under their increasing island areas. Further, a previous model study found that the mangrove expansion can stimulate the freshwater vegetation replacement by increasing salinity of soil pore water because of its high transpiration even under relatively high salinity condition (Zhai et al., 2016). The vegetation replacement is also exacerbated by the shallow and permeable limestone coastal aquifers of southern Florida, and the SLR effects may be seen more quickly than for less permeable clastic aquifers (Langevin and Zygnerski, 2013).

Therefore, although mangrove caused vegetation replacement might be responsible for stabilization of mud islands under SLR, it threatens the biodiversity of coastal or island ecosystems (Wetzel et al., 2013).

Although the biogeomorphic feedbacks in mangroves is important contributor to island area increase against SLR, mangroves forests are experiencing about 1%~3% area loss per year globally (Duarte et al., 2013). Therefore, there is a need to investigate the conservation of the biogeomorphic feedbacks under long-term climate changes and increasing human disturbances. For example, how to mitigate shoreline erosion caused by high tides and mangrove damages from hurricanes. Furthermore, on the basis of the spatial analysis, I am planning a soil core study to quantify the long-term soil accretion and then to compare with rate of local SLR. In addition to the low energy environment, other factors are required to be examined which may affect the comparison between SLR and biogeomorphic elevation increase, including meteorological factors, vegetation types and topography. There is also a need to investigate the tradeoff between mangrove expansion and its subsequent stabilization of mud islands versus biodiversity loss.

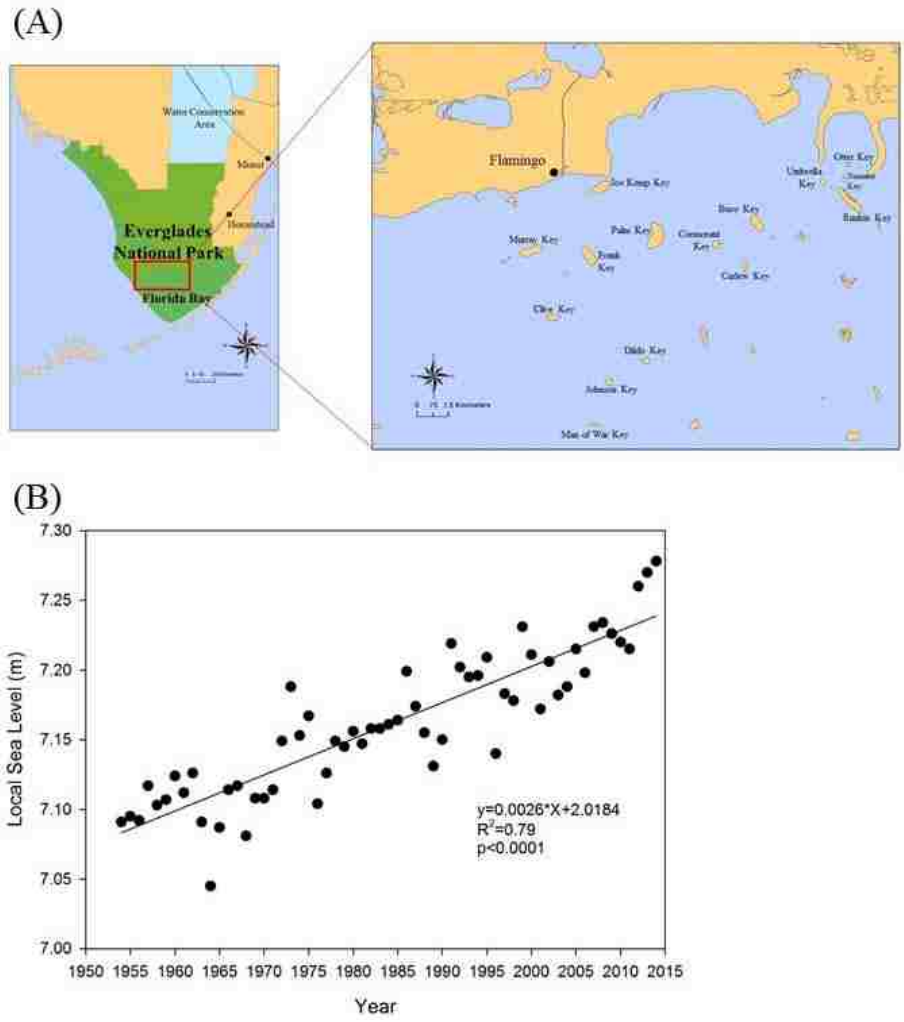

Figure 2.1: (A) Location of the 15 mud islands in Florida Bay. (B) The local sea level data were from a monitoring station of National Oceanic and Atmospheric Administration (NOAA) in Key West, FL (http://www.psmsl.org/), which is located in the south end of Florida Bay. Local sea level refers to the height of the water as measured along the coast relative to a specific point on land, which is stable vertical point (or benchmarks). There is a clear increasing trend of the local sea level from 1954 to 2014 ($p<0.0001$), which covers period of the aerial images in my study. The yearly mean sea level has increased from 7.09 m in 1954 to 7.28 m in 2014.

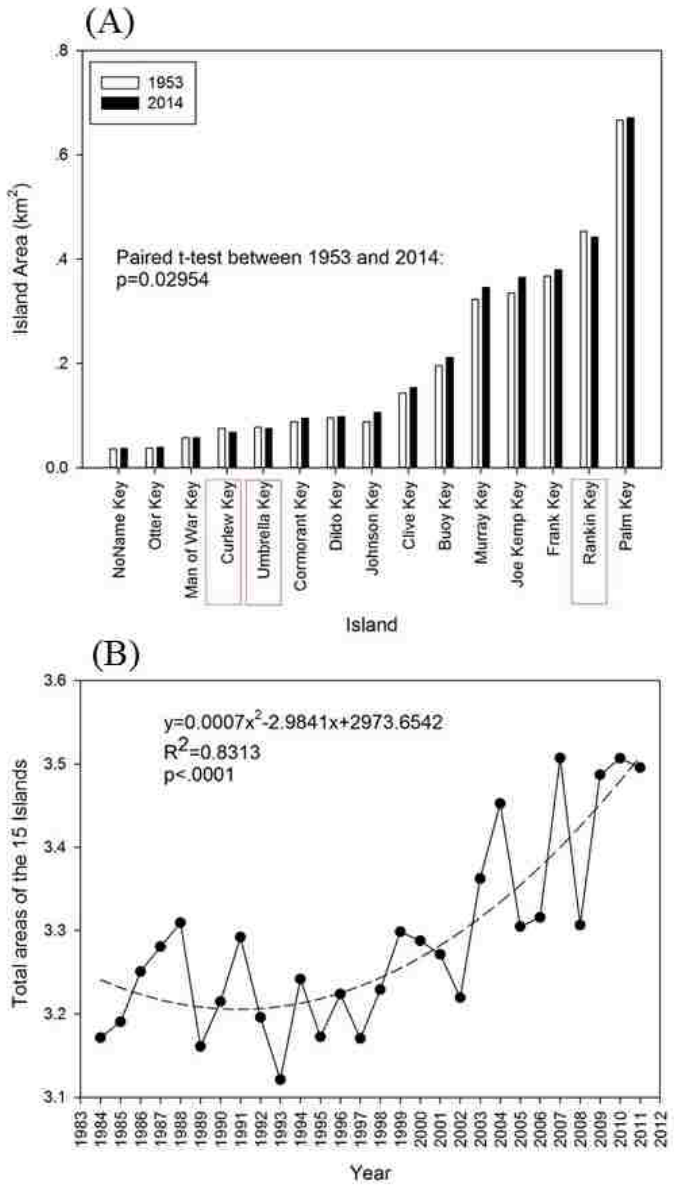

Figure 2.2: A: Island area comparison between 1953 and 2014. Area of three island decreased in this time period (thee islands in red rectangles). B: Annual total areas of the 15 islands from 1984 to 2011.

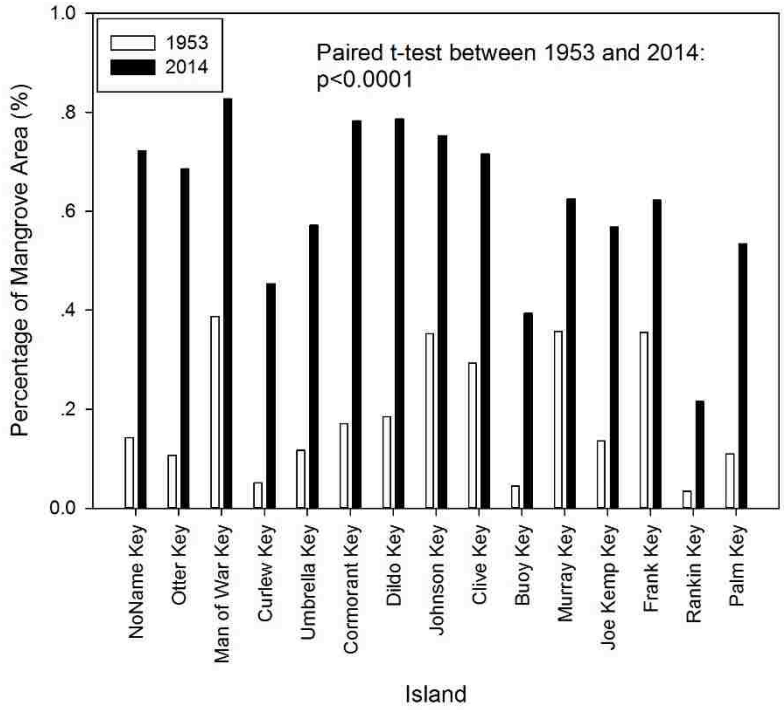

Figure 2.3: Mangrove area comparison in each island between 1953 and 2014.

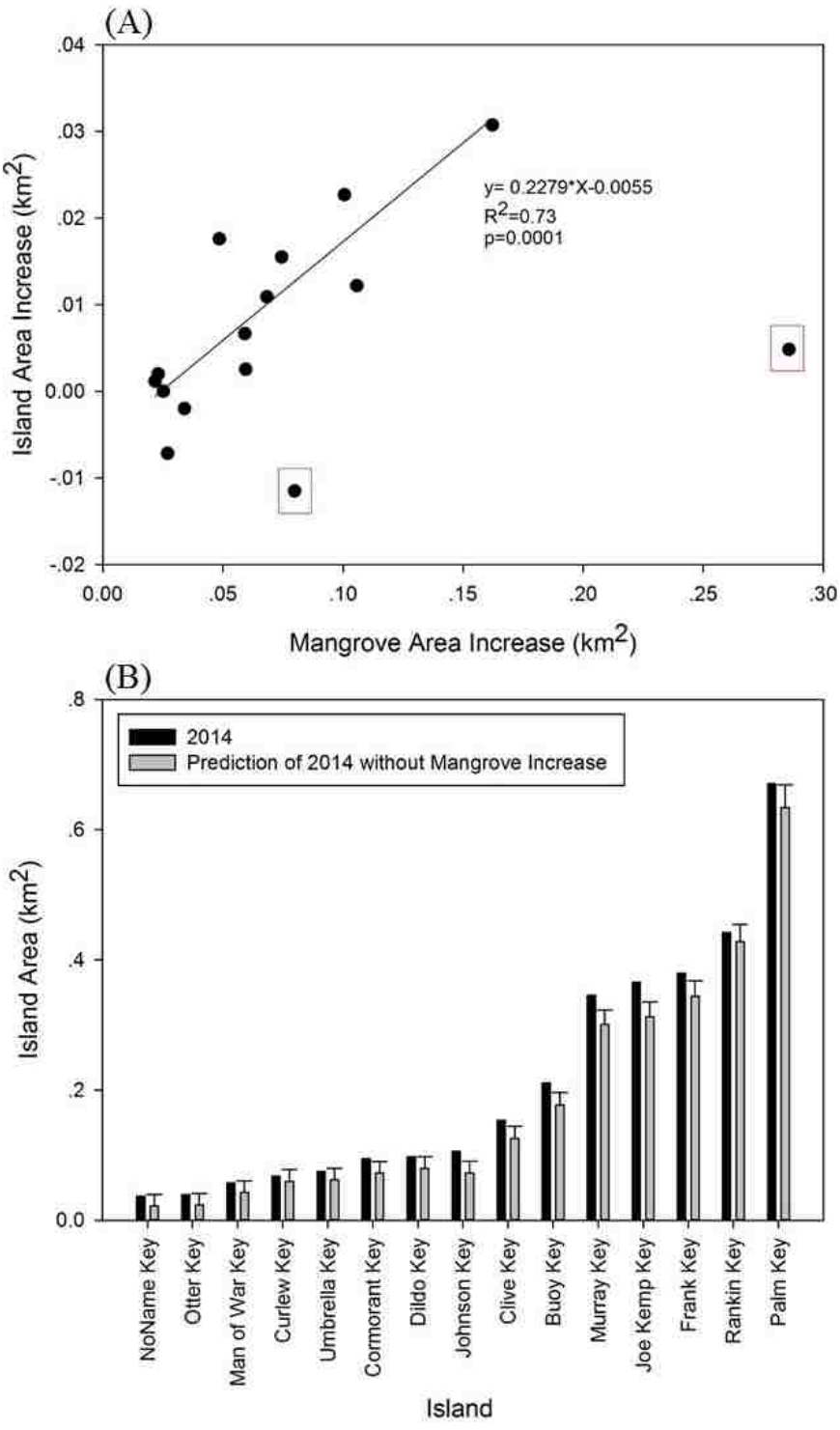

Figure 2.4: A: Linear regression between island area increase and mangrove area increase in each island. The regression analysis was based on 13 islands, because Palm Key and Rankin Key (two points in red circle) were influential point (Cook's distance = 7.0028) and outlier (standardized residual = -2.69), respectively. B: Predicted area of the islands in 2014 without mangrove area increase and their 95% prediction intervals.

Chapter Three

Prediction of Plant Vulnerability to Salinity Increase in a Coastal Ecosystem by Stable Isotopic Composition ($\Delta^{18}O$) of Plant Stem Water: a Model Study

Summary

Sea level rise and the subsequent intrusion of saline seawater can result in an increase in soil salinity, and potentially cause coastal saline-intolerant vegetation (e.g., hardwood hammocks or pines) to be replaced by saline-tolerant vegetation (e.g., mangroves or salt marshes). Although the vegetation shifts can be easily monitored by satellite imagery, it is hard to predict a particular area or even a particular tree that is vulnerable to such shift. In order to find an appropriate indicator for the potential vegetation shift, I incorporated stable isotope ^{18}O abundance as a tracer in various hydrologic components (e.g., vadose zone, water table) in a previously published model describing ecosystem shifts between hammock and mangrove communities in southern Florida. My simulations showed that: (1) there was a linear relationship between salinity and the $\delta^{18}O$ value in the water table, whereas this relationship was curvilinear in the vadose zone; (2) hammock trees with higher probability of being replaced by mangroves had higher $\delta^{18}O$ values of plant stem water, and this difference could be detected two years before the trees reached a tipping point, beyond which future replacement became certain; (3) individuals that were eventually replaced by mangroves from the hammock tree population with a 50% replacement probability had higher stem water $\delta^{18}O$ values three years before their replacement became certain compared to those from the same population which were not replaced. Overall, these simulation results suggest that it is

promising to track the yearly $\delta^{18}O$ values of plant stem water in hammock forests to predict impending salinity stress and mortality.

Background

The coastal vegetation structure of southern Florida has experienced noticeable changes over the past several decades, with encroachment of mangroves into freshwater marshes (Egler, 1952; Meeder et al., 1996; Ross et al., 2000; Smith III et al., 2010), which is mainly caused by the intrusion of brackish seawater into previously fresh-water areas (Davis et al., 2005; Saha et al., 2011). This seawater intrusion is facilitated by the flat landscape in southern Florida with shallow elevation and porous soil substrate (Hoffmeister, 1974), sea level rise (SLR) (Desantis et al., 2007; Krauss et al., 2011; Guha and Panday, 2012), and by hydrologic management along the coastal area (Fourqurean and Robblee, 1999). For example, canal systems in the Everglades diverted freshwater flow from freshwater areas (Sklar et al., 2002; Davis et al., 2005), which then experienced intrusion by more saline ocean water. Coupled with the seawater intrusion of the water table, there is an increase in salinity of the pore water of the vadose zone, the zone that is located between the soil surface and the top of the water table (Stephens, 1995), and which supplies water for the vegetation (e.g., hardwood hammocks, mangroves) in the coastal areas (Figure 1). The salinity of the vadose zone has a great influence on plant community type, as plants vary in their salinity tolerance (Ross et al., 1992).

The intrusion of brackish seawater inland is accompanied by a spatial shift inland of the boundary or ecotone between salinity-tolerant (halophytic) vegetation, such as mangroves, and salinity-intolerant freshwater vegetation, such as hardwood hammock or

freshwater marsh (Ross et al., 2000). Hardwood hammock communities occupy slightly elevated and rarely tidally inundated sites along coastal Florida (Ross et al., 1992; Gunderson, 1994) and comprise a suite of tropical tree species intolerant of high salinity (Ish-Shalom et al., 1992). Mangroves are able to utilize water having a range of salinities, from fresh water to brackish water with salinities above 30 ppt (Chapman, 1976; Sternberg and Swart, 1987; Ball, 1988). Mangroves cannot compete with hammock species in freshwater areas and are excluded from such areas (Silander and Antonovics, 1982; Kenkel et al., 1991; Greiner La Peyre et al., 2001). But the increasing seawater intrusion can change the balance in favor of the mangroves, causing the boundary or ecotone between the two vegetation types to shift inland (Ewe et al., 2007; Doyle et al., 2010; Saha et al., 2011). This boundary shift can result from a salinity-induced mortality of the hammocks, which is then replaced by mangroves, or by decline in growth rate of hammock vegetation, allowing it to be outcompeted by the invading mangroves. Conversely, vegetation shift from mangroves to hammocks is, in principle, possible if soil water become less saline, and can occur in my model. However, such shifts have not been observed empirically (Lugo, 1980) and are unlikely to occur in the current global scenario of SLR, so I limit this study to early stage detection of changes from hammocks to mangroves.

Although the two plant communities, mangroves and hardwood hammocks, occupy overlapping geographical ranges (Odum et al., 1982; Odum and McIvor, 1990; Sklar and van der Valk, 2002), they are rarely mixed and there are sharp boundaries between them (Snyder et al., 1990). Not only is there a sharp ecotone (or boundary) between the two, but the gradient in vadose zone salinity is also extremely sharp at the ecotone (Saha et al.,

2014). This results from the self-reinforcing positive feedback between the vegetation and the vadose zone below them. Both mangroves and hammock species obtain their water from the vadose zone (Sternberg and Swart, 1987). In coastal areas this vadose zone is underlain by highly saline groundwater (Fitterman et al., 1999). Plant transpiration, by depleting water in the vadose zone during the dry season, can cause infiltration of the vadose zone by more saline groundwater through capillary action. Hardwood hammock trees tend to decrease their transpiration when vadose zone salinities begin to increase, thus limiting the salinization of the vadose zone (Volkmar et al., 1998). However, mangroves can continue to transpire at relatively high salinities, resulting in high soil salinities (Passioura et al., 1992). Thus, each vegetation type, through a self-reinforcing positive feedback, tends to promote local salinity conditions that favor itself in competition. However, under the influence of SLR, the positive feedback in mangrove forests can either help the ecosytem become resilient to future changes or strengthen the landward migration of the vegetation boundary (Jiang et al., 2016). The positive feedback based on salinity can also be found in other ecosystems, for example, Armas et al. (2010) proposed that salty groundwater lift by salt-tolerant species (*Pistacia lentiscus*) in arid coastal sand dune system, can positively affect its own growth and decrease growth of competing salt-intolerant species.

It is possible that the sharp separation of the two vegetation types caused by the apparent positive feedback relationship can be formally represented as alternative stable states, in the sense of Scheffer et al. (1997); Brovkin et al. (1998); Sternberg (2001), along certain regions of a gradual gradient in groundwater salinity (Jiang et al., 2012a). There is no empirical proof of this. At present, the evidence for the existence of the

alternative stable states are from modeling studies indicating that a mixture of plants from the two communities (mangrove and hammock) may represent an unstable state and will move toward complete dominance of one type eventually (Sternberg et al., 2007; Teh et al., 2008; Jiang et al., 2012a). This vegetation dynamics pattern is also supported by modeling studies based on other ecosystem types. For example, Morris (2006) demonstrated that two marsh species with different optimum elevations for growth can move toward stable states dominated by one species or another.

Despite short-term stability of the coastal ecosystem in the Everglades, the vegetation will shift over longer time scales as highly saline groundwater intrudes farther inland due to SLR. However, there is no guarantee that this shift will have a linear and predictable response to SLR. Other factors, including precipitation and freshwater flows, also affect the vegetation dynamics, and along with the positive feedback mechanisms described above, could cause the shift process to sometimes be delayed or sometimes accelerated. More importantly, the vegetation dynamics are also vulnerable to more rapid changes from disturbances of sufficiently large size (Ross et al., 2009). For example, if a large enough pulse of salinity of storm surge is pushed inland into the region of freshwater vegetation, and high salinity remains in the soil for a long period, it may overwhelm the favorable conditions for freshwater vegetation by killing or slowing the growth of the freshwater vegetation. If the storm surge also carries mangrove seedlings into the affected freshwater region, areas of freshwater vegetation could be set on the path to irreversible replacement by halophytic vegetation and permanent salinization of the vadose zone.

There are some empirical evidence for the rapid vegetation shifts following large disturbances. For example, Baldwin and Mendelssohn (1998) used salt water inundation coupled with clipping of aboveground vegetation on two adjoining halophytic and freshwater plant communities to simulate the effects of a hurricane with a storm surge. They showed that the vegetation might shift from one type to the other, depending on the level of flooding and salinity at the time of disturbance. Hurricanes Katrina and Rita (2005), which affected the coastal areas of Louisiana, created large storm surges. Subsequent changes in the vegetation to a more saline classification have been identified in both freshwater and brackish communities due to the salinity overwash (Steyer et al., 2010), suggesting a possible regime shift. Because of the importance of freshwater habitat in affected areas of the Everglades, methods of finding indicators of rapid changes in the ecosystem will be important (Dakos et al., 2012). For example, Doering et al. (2002) used plant growth as indicator of salinity to determine the amount of needed freshwater to reduce the salinity. They used shoot density of a salt-tolerant species, *Vallisneria americana*, to estimate a minimum freshwater flow, and leaf density of *Halodule wrightii* to estimate a maximum flow, because the plant growth can indicate salinity change. Presenting a new predictive methodology is the objective of this paper.

Ecosystems may show little indication of a tipping point until change from one ecosystem type to another starts to occur (Scheffer et al., 2009), so it is hard to find an appropriate indicator which has practical use in monitoring an ecosystem transition (Dakos et al., 2012). In coastal ecosystem, water salinity of the vadose zone may be a potential indicator for the tipping point between hammock and mangrove trees. However, salinity distribution in the vadose zone is uneven. For example, a study in coastal

southwestern Florida found that the salinity varies from location to location within as little as one meter (Ewe and Sternberg, 2005). In addition to the uneven salinity distribution, the extensive and complex root system of trees in tropical forest (Sternberg et al., 1998; Kathiresan and Bingham, 2001; Sternberg et al., 2002) makes it harder to precisely determine which part of the vadose zone the roots absorb water from. A second possible approach, monitoring the salinity of xylem water, is also problematic, because plants may exclude salt during water uptake (Scholander et al., 1962; Scholander, 1968). A further potential indicator of salinity is predawn water potential, which can reflect the salinity of the water available to a plant (osmotic potential). But water potential is also affected by soil moisture (matric potential). Therefore, predawn water potential, depending on both the salinity and moisture of soil, may not precisely indicate the change in the salinity of the water available for plant uptake.

A more practical and precise indicator of a potential shift at the level of individual trees may be the oxygen isotope composition ($\delta^{18}O$ value) of plant stem water. Current methods allow for easy extraction and analysis of plant stem water for hydrogen and oxygen isotopic composition (Vendramini and Sternberg, 2007). The $\delta^{18}O$ value of plant stem water is an appropriate candidate of indicators for two reasons: (1) $\delta^{18}O$ value of water, at least in southern Florida, is indicative of its salinity, with freshwater showing less oxygen-18 enrichment than saline seawater (Sternberg and Swart, 1987; Sternberg et al., 1991). Thus, there are significant differences in $\delta^{18}O$ between various water sources, such as precipitation and sea water. (2) Although plants discriminate against salt, they do not discriminate against ^{18}O during water uptake (Dawson et al., 2002); e.g., Lin and Sternberg (1994) found that there were no significant differences in $\delta^{18}O$ values between

stem water of red mangrove (*Rhizophora mangle*) and its corresponding vadose zone. Several studies have used $\delta^{18}O$ values of stem water to quantitatively determine the utilization of plant water source, e.g., Sternberg and Swart (1987), Dawson and Ehleringer (1991), Ewe et al. (2007). The other isotopic indicator of plant water uptake, the hydrogen isotope composition value of stem water ($\delta^{2}H$), cannot be used because some salt tolerant plants discriminate against ^{2}H during water uptake (Lin and Sternberg, 1993; Ellsworth and Williams, 2007; Wei et al., 2012).

The purpose of this study was to determine if the $\delta^{18}O$ value of plant stem water can be an appropriate predictor of future replacement of hammock species by salt tolerant mangrove species in coastal ecosystem. I determined this by including the $\delta^{18}O$ value of water as a tracer in a previously published spatially explicit model describing the dynamics of an initially mixed hardwood hammock and mangrove stand in southern Florida (Sternberg et al., 2007). I incorporated the $\delta^{18}O$ value of various water compartments in the model, including vadose zone, water table and plant stem water. I then followed the water salinity and $\delta^{18}O$ value of these compartments in areas of the landscape where hammocks were replaced by mangroves in the model, and determined if the change of $\delta^{18}O$ value of plant stem water preceded the replacement of a hammock species by a mangroves species. Being able to predict this replacement using the easily measured $\delta^{18}O$ value of plant stem water has practical implications in the monitoring and conservation of coastal ecosystems, particularly in relation to a rising sea level and increasing storm surges.

Mathods

Model: General Aspects

The competition of mangroves and hardwood hammocks was modeled on a 100×100 grid of spatial cells, with each cell being roughly the size of a mature tree. The assumptions of plant physiology and factors on water movement in the vadose zone in my model were the same as in Sternberg et al. (2007) and Teh et al. (2008). Mangroves tolerate a large range of salinities from freshwater to a high salinity environment (Chapman, 1976; Sternberg and Swart, 1987; Ball, 1988). Hammocks, which are intolerant of salinity, however, are limited to freshwater areas, where they can outcompete and exclude mangroves (Silander and Antonovics, 1982; Kenkel et al., 1991; Greiner La Peyre et al., 2001). Both vegetation types utilize water from the vadose zone. Water movement in the vadose zone is mainly determined by precipitation, evaporation, plant transpiration, and tidal flooding (Figure 1). Precipitation introduces freshwater with zero salinity and low $\delta^{18}O$ values to the vadose zone, which drives the infiltration downward and decreases the salinity and $\delta^{18}O$ of the vadose zone. Tidal flooding carries saline seawater with relatively high $\delta^{18}O$ values to the vadose zone. Both evaporation and plant transpiration can cause a water deficit in the vadose zone and drive infiltration upward, which may move water with a high salinity and $\delta^{18}O$ values from the water table up into the vadose zone.

The effects of the vegetation on the salinity of the vadose zone can be spread horizontally by lateral water uptake by a tree, because a tree's roots extend beyond the location of its central stem into the locale of neighboring trees. It has been documented

by stable isotope studies that small tropical tree species can access and presumably affect areas as far as 10 meters from the central stem (Sternberg et al., 2002). Gill and Tomlinson (1977) recorded that the lengths of mangrove roots can extend over two meters, which is longer than the spatial cell length in my model. In my simulation, which is represented by 2D horizontal space with a grid of spatial cells, the transpiration by a cell containing a mangrove tree will lead to infiltration of saline water from the water table into the vadose zone. This upward water infiltration occurs not only in the immediate area of the mangrove tree, but also in neighboring areas which may not be occupied by mangroves but still have mangrove roots that extend from the focal mangrove-occupied cell. Therefore, if the above focal-neighboring interaction is sufficient to increase salinity in the neighboring area, there could potentially be a further expansion of the mangrove area. Conversely, the lateral water uptake of vegetation can enlarge hammock areas by suppressing salinity in neighboring areas. Therefore, in the model, the lateral water uptake affects soil salinity beyond the area occupied by the individual tree, and there is a tendency to eliminate lone individuals of one vegetation type surrounded by vegetation of the opposite type, which appears to be the case in nature as well. The overall effect is to sharpen the ecotone between the two vegetation types. Soil pore horizontal diffusion of salinity was ignored in my simulation, because this diffusion in soil is very small ($<0.0003 m^2$/day) (Hollins et al., 2000) compared to horizontal salinity transfer by roots.

Model: Mathematical Details

As in Sternberg et al. (2007), the hydrological components of my model include vadose zone pore water, water table and ocean water, and my study also added plant stem

water to these compartments. These hydrological components and factors responsible for water flow in the vadose zone are shown in Figure 1. I used the same initial water salinity for the first three of these compartments as in Sternberg et al. (2007) (See Appendix). In addition, I tagged the water from the above compartments with realistic isotopic signatures and followed the flow of ^{18}O as well as salinity.

I used the usual expression to describe isotopic abundance:

$$\delta^{18}O = \left[\frac{R_{sample}}{R_{standard}} - 1\right] \times 1000 \qquad Eq.(1)$$

where R represents the $^{18}O/^{16}O$ ratio of a sample and the standard, respectively. The standard is standard mean ocean water (SMOW). I labeled ocean water (O_O) and tidal influx water (O_{tide}) with a $\delta^{18}O$ value of +4‰ (Sternberg and Swart, 1987). Sea water in the bays and inlets of Florida is isotopically enriched because these systems are semi-closed and undergo extensive evaporation (Lloyd, 1964). Sea water isotopic composition did not change through time in my model. The vadose zone pore water had an initial $\delta^{18}O$ value of -3‰, but changed as a function of precipitation, infiltration and tidal input. The $\delta^{18}O$ value of precipitation (O_P) in southern Florida was calculated daily by the monthly average $\delta^{18}O$ of precipitation ($\overline{O_P}$) and the monthly standard deviation (σ_{OP}) multiplied by a normally distributed random number ranging from -1 to +1 (RN) (Price et al., 2008) (Eq. (2)). The information about precipitation and tidal flooding is shown in Figure 2, and their calculations are shown in Appendix. The equation for O_P is

$$O_P = \overline{O_P} + (RN \times \sigma_{OP}) \qquad Eq.(2)$$

The initial $\delta^{18}O$ value of water table decreased uniformly +4‰ on the seaward side to -3‰ in the landward side. The $\delta^{18}O$ values of the water table can change depending on percolation from vadose zone, water table of neighboring cells or infiltration from the underlying ocean water.

I used the same basic flux equations dictating vertical movement of water and changes of salinity as in Sternberg et al. (2007) (See Appendix). I also added equations that followed the flux of ^{18}O between the various hydrological compartments in soil. The flux of ^{18}O in and out of the vadose zone carries the signature of the $\delta^{18}O$ value from water table, ocean water, and precipitation, but the $\delta^{18}O$ value of the vadose zone is not concentrated by transpiration, as, unlike salinity, it is not excluded by the roots. It is given by:

$$\mathrm{p}H_V \frac{dO_V}{dt} \text{ (when } IF > 0 \text{ and } T_{RH} > 0)$$

$$= IF \times (O_{WT} - O_V) + P \times (O_P - O_V) + [T_{RH} \times (O_{tide} - O_V)] \qquad Eq.(3)$$

As in Sternberg et al. (2007), values of infiltration (*IF*) ($IF = Evaporation + Plant\ transpiration\ - Precipitation - Tidal\ flooding$) greater than 0 imply that water is infiltrating from the water table to the vadose zone (Figure 1). In the above equation, p, H_V and $\frac{dO_V}{dt}$ define the porosity of the vadose zone, the thickness of the vadose zone and the change in $\delta^{18}O$ value of the vadose zone per unit time respectively. The subscripted O symbols represent the $\delta^{18}O$ values of the water table (O_{WT}), the vadose zone (O_V), the precipitation (O_P), and the tidal water (O_{tide}), respectively. The water table in the model is assumed to be the upper zone of groundwater that can vary in

salinity and $\delta^{18}O$ concentrations and that can flow from high to lower elevations when there is an upstream head. The amount of precipitation and tidal height above the surface of the vadose zone are represented by P and T_{RH}, respectively. The last term of the above equation, $[T_{RH} \times (O_{tide} - O_V)]$, is only applied when T_{RH} is greater than 0, i.e. the tidal height is above the surface of the vadose zone. In the case of water infiltrating from the vadose zone to the water table ($IF < 0$), the following equation is applied:

$$\mathrm{pH}_V \frac{dO_V}{dt} (\text{when } IF < 0 \text{ and } T_{RH} > 0)$$

$$= P \times (O_P - O_V) + [T_{RH} \times (O_{tide} - O_V)] \qquad Eq.(4)$$

To determine the $\delta^{18}O$ value of plant stem water, I first determined the total transpiration (water uptake) by each plant (T_{plant}). Plant transpiration in a particular cell consists of equal contributions from the central cell and four of its adjacent cells, and is given by the following equation:

$$T_{plant}$$

$$= \left(0.20 \times TT_{plant}^{i,j}\right) + \left(0.20 \times TT_{plant}^{i+1,j}\right) + \left(0.20 \times TT_{plant}^{i-1,j}\right)$$

$$+\left(0.20 \times TT_{plant}^{i,j+1}\right) + \left(0.20 \times TT_{plant}^{i,j-1}\right) \qquad Eq.(5)$$

where the superscripted *TT*'s represent the contribution of transpiration in the central and neighboring cells by either a hammock or mangrove species, which will depend on salinity and is predicted by previously published equations (Sternberg et al., 2007). The $\delta^{18}O$ value of stem water (O_{plant}) is then given by the mean values of $\delta^{18}O$ in the water

transpiration streams from the vadose zones in center cell and four adjacent cell weighted by the size of the transpiration in each stream:

$$O_{plant} = \frac{\left[0.2 \times \left((O_V^{i,j} \times TT_{plant}^{i,j}) + (O_V^{i+1,j} \times TT_{plant}^{i+1,j}) + (O_V^{i-1,j} \times TT_{plant}^{i-1,j}) + (O_V^{i,j+1} \times TT_{plant}^{i,j+1}) + (O_V^{i,j-1} \times TT_{plant}^{i,j-1})\right)\right]}{T_{plant}}$$

$Eq.(6)$

The water table underlying the vadose zone is also subject to fluxes that might alter its salinity (See Appendix) and $\delta^{18}O$. When water percolates from the vadose zone to the water table and the water table height increases beyond that of the initial conditions, the excess water (α) flows horizontally to the next water table cell seaward to it. By mass balance principles, the changing rate of the $\delta^{18}O$ value in the water table of a particular cell should be:

$$H_{WT} \frac{dO_{WT}^{i,j}}{dt} \text{ (when } IF^{i,j} < 0) = \alpha\left(O_{WT}^{i+1,j} - O_{WT}^{i,j}\right) - IF^{i,j}\left(O_V - O_{WT}^{i,j}\right) \quad \text{Eq. (7)}$$

On the other hand, when *IF*>0, i.e. water flow is from the water table to the vadose zone, water from the underlying ocean water infiltrate upward to make up for the water table deficit. By mass balance, the $\delta^{18}O$ dynamics of the water table in a particular cell is then predicted by:

$$\mathrm{H}_{WT}\frac{dO_{WT}^{i,j}}{dt}\ \left(\text{when } IF^{i,j}>0\right)$$

$$=\alpha\left(O_{WT}^{i+1,j}-O_{WT}^{i,j}\right)+IF^{i,j}\left(O_O-O_{WT}^{i,j}\right) \qquad Eq.(8)$$

Model: Simulation

The purpose of simulations was to investigate whether given hammock occupied cells that switched to mangrove due to salinity stress could be predicted beforehand from $\delta^{18}O$ levels in the plant stemwater. If there is a particular vadose zone salinity level at which change from hammock to mangrove becomes inevitable, this is referred to as the tipping point. Simulations were based on a previously published model (Sternberg et al., 2007; Teh et al., 2008; Jiang et al., 2012a), and performed on a 2D grid of 100×100 cell landscape, which was built by an algorithm (Sternberg et al., 2007) that produces natural-looking topographies based on transect by Ross et al. (1992), and the landscape elevation increased by 10 mm per cell length along the dimension from the 1st to 100th row. The initial height of water table was assumed to increase uniformly from 50 mm to 400 mm along the same dimension. The thickness of vadose zone is the difference between cell elevation and height of water table (Figure 1). The above differential equations were discretized and applied incrementally day by day to the initial conditions.

1. Simulation Process

Initially, each spatial cell was assigned randomly as either mangrove or hammock, and the whole landscape had 50% frequency of hammocks and mangroves. On daily time step, the simulation computed the flux of water into and out of each cell, and the salinity and $\delta^{18}O$ value of each hydrological compartment. After the 1st and 2nd years, the running

average salinity of the vadose zone in each cell was used as an indicator of whether the type of tree in that cell would ultimately remain or be replaced by the other type of vegetation. If the running average salinity was $\geq$ 5 ppt in a cell, it was seen that a mangrove tree, if present, was either maintained in the cell or a mangrove replaced the hammock tree. On the other hand, if the running average salinity of a cell was <5ppt, it was seen that a hammock tree, if present, was maintained, or a hammock tree replaced a mangrove tree. (By replace I mean 'will immediately replace,' but the actual replacement of one tree type by another tree type may take decades to occur.) The simulation was continued, and the running average was calculated again at the end of each succeeding year. The vegetation distribution was updated according to the new running average of vadose zone salinity. At the end of the 10^{th} year, the final distribution of vegetation was recorded. The simulation stopped in the 10^{th} year, because there were few changes in the plant distribution after 10 years. The modeling thus artificially speeds up the rate at which the cells on the landscape sort into final vegetation types, but this still properly connects the tipping of each particular tree with the previous value of stem water $\delta^{18}O$.

2. Simulation Data Sampling

Two types of simulations were performed: 1) The purpose of the first set, in which 100 simulations were performed, was to identify specific cells on the grid that were initially populated by hammocks and that had specific probabilities (0, 25, 50, 75 and 100%) of being replaced through time by a mangrove species, when the 100 independent simulations were performed with different random number simulators (recall there is stochasticity in precipitation and tidal flux). The replacement probability was found to be related to distance of the cell from the ocean; that is, if a cell with a hammock tree was

closer to ocean, it tended to be replaced by a mangrove tree with higher probability. 2) The second set was a single data-sampling simulation where I recorded the salinity of the vadose zone water available to the plant and the $\delta^{18}O$ of hammock species stem water. In this simulation I monitored the vadose zone salinity and $\delta^{18}O$ of stem water for hammock cells showing different probabilities of being eventually replaced by mangroves. In addition, I monitored the vadose zone salinity and $\delta^{18}O$ of stem water for hammock cells with 0% probability of replacement and a subset of the set with 50% probability of replacement that were always stable as in hammock during this single 10-year simulation.

(1) Identifying hammock cells with different probabilities of being replaced by mangrove species

I performed 100 simulations (10 years each) starting with the same vegetation distribution landscape, but with daily stochastically determined precipitation and tidal flux. For each simulation I compared the plant species in each cell between the 1st and 10th year to identify which cells would ultimately shift from hammock to mangrove. After the 100 simulations, I identified particular cells that shifted from hammocks to mangroves with probabilities of 0%, 25% 50%, 75% and 100% at a 5% significance level. These cells were designated as H0, H25, H50, H75 and H100 respectively. The confidence interval of these probabilities was calculated by the following equation:

$$95\%\ \text{confidence interval of replacement probability} = \mathrm{p} \pm z_{\alpha/2}\sqrt{\frac{p(1-p)}{n}} \qquad Eq.(9)$$

in which p is the replacement probability, $z_{\alpha/2}$=1.96, and n=100 (simulation times).

(2) Data-sampling simulation

The data-sampling simulation was performed with the same initial vegetation distribution as above, where I selected subsets from every cell set of hammock cells for which specific probabilities of switching to mangroves (H0, H25, H50, H75 and H100) emerged, and I monitored the salinities and the $\delta^{18}O$ values of the hydrological compartments of these selected subsets. Hammocks in the selected subsets, in addition to passing the tipping point threshold for shifting to mangroves, had to (1) have passed this threshold exactly in the same year during the simulation, because I want to compare yearly difference in the salinity and the $\delta^{18}O$ value between the different cell types before and at the tipping point. The hammocks also had to (2) have been stable as hammocks before the shift and remained stable as mangroves after the shift. These newly identified cells, which I call 'shifting subclasses' of cells, were designated as H25→M, H50→M, H75→M and H100→M, accordingly. In the case of H0, I selected a subset of cells that remained stable as a hammock during the 10 year simulation (designated as H0→H); i.e., there is no flipping back and forth between hammock and mangrove trees before ending as hammock in the 10^{th} year. In addition, from the set of hammock cells that had a 50% replacement probability (H50), I selected a subset that was not replaced by mangroves for this particular simulation (designated as H50→H). These cells must be stable as a hammock cell during the 10 years simulation. For statistical purposes, the data sampling simulation above was carried out until at least five cells could be found in each cell subset (H0→H, H25→M, H50→M, H50→H, H75→M and H100→M). For the simulation that produces sufficient cells of each type, I recorded monthly and yearly average values of salinity and $\delta^{18}O$ of the vadose zone, water table and plant stem water

in the above cell subsets, and the vegetation distribution of landscape at the end of every year. Note that I are using 'tipping point' to represent the threshold running average of vadose zone salinity at which a single tree (or cell) will inevitably shift from hammock to mangrove.

The number of cells satisfying all the selection criteria, in which the replacement took place in the same year and remained stable before and after the replacement, are shown in Figure 3B. Although cells that were replaced in the 6^{th} year had the greatest total cell number, they just had two H75→M cells. Thus, I chose cells that passed the threshold in the 7^{th} year, because those cells had an appropriate cell number for each cell type. I examined the salinity and $\delta^{18}O$ values of their vadose zone, water table and plant stem water in detail for this selected group of cells.

Data Analysis

The data-sampling simulation was analyzed as follows. First, I compared the monthly average salinities and $\delta^{18}O$ values of the vadose zone and water table between the dry season (November through April) and wet season (May through October). For this seasonal comparison, the Mann-Whitney-Wilcoxon test was used because of the non-normal distribution of salinity and $\delta^{18}O$ values. Second, I compared the average $\delta^{18}O$ values of plant stem water from the H0→H, H25→M, H50→M, H75→M and H100→M cell subset in the 5^{th} year. The 5^{th} year was the earliest year I could identify the significant $\delta^{18}O$ value difference among the above five cell subsets. Third, I monitored the yearly average salinity and $\delta^{18}O$ values of water available to the trees from the following cell subsets; H0→H, H50→H, H50→M and H100→M, and then the yearly data were

analyzed to check when the significant differences of salinity and $\delta^{18}O$ value appear by repeated measures ANOVA.

Results

After the 10-year simulation, a clear boundary emerged between mangrove and hammock species in my model landscape (Figure 3A). I also observed that most of H25→M cells tended to pass the threshold or tipping point in the 5th and 6th years (Figure 3B). They shifted faster than most of H50→M cells, which shifted in the 7th years, and H75→M cells, which shifted in the 7th and 8th years (Figure 3B). Compared with slow shifting H50→M and H75→M cells, fast shifting H25→M cells were more landward with less salinity variation of vadose zone. It is counterintuitive for the landward cells to shift to mangroves at a faster rate than seaward cells, but this is due to the requirement for sampling noted above that the selected cells had to remain stable in their new state after the tipping. The tidal influence caused the more seaward cells to flip back and forth more frequently, delaying the time at which I declared the cells to have shift. The lower salinity variation in these plants made plant distribution of the landward area more stable (i.e. less flipping back and forth between hammocks and mangroves) allowing for a faster stabilization. My stabilization criterion is reasonable because the tree shift may not occur in such short time in nature, because mangroves usually achieve maturity in 20-30 years (Lugo et al., 1976).

Dynamics of Salinity and $\delta^{18}O$ Value of Vadose Zone and Water Table

1. Salinity

In my simulations a gradient emerged in the salinity of the vadose zone from ~30 ppt seaward to ~2 ppt landward, while the water table developed a gradient of salinity from ~20 ppt seward to ~8 ppt landward. The salinity gradient corresponded with the distinct distribution of hammocks and mangroves (Figure 3A). The comparison between hammocks and mangroves showed that under hammock forest the salinity in the water table was higher than that of the vadose zone, but under the mangrove forest the salinity in the vadose zone was higher than that of the water table (Figure 4A). I also found that there was greater variance in salinity of the mangrove soil than that of the hardwood hammock soil in figure 4A.

During the dry season, the average salinities of the vadose zone ($27.8\text{ppt} \pm 5.1$ below mangroves, $2.2\text{ppt} \pm 0.1$ below hammocks) were close to those of the wet season ($26.5\text{ppt} \pm 4.5$ below mangroves, $2.2\text{ppt} \pm 0.01$ below hammocks). However, the Mann-Whitney-Wilcoxon test showed that the vadose zone in the dry season had significantly higher salinity than that in the wet season (χ^2=3136.49, p<0.0001 for mangroves, χ^2=516.97, p<0.0001 for hammocks). The water table had significantly higher salinity in the dry season ($16.9\text{ppt} \pm 2.7$ under mangroves, $8.5\text{ppt} \pm 0.2$ under hammocks) compared to the wet season ($13.2\text{ppt} \pm 2.6$ under mangroves, $8.0\text{ppt} \pm 0.1$ under hammocks) (χ^2=20639.62, p<0.0001 for mangroves, χ^2=49199.25, p<0.0001 for hammocks). Comparing the water table with the vadose zone, I found that the water table had a greater seasonal variation of salinity (Figure 4A).

2. $\delta^{18}O$ values

In the 10th year, the $\delta^{18}O$ values of vadose zone pore water developed a gradient from ~+3.6‰ to ~-2‰ with the distance from the ocean. The gradient ranged from ~+1‰

to ~-1‰ for the water table. The average $\delta^{18}O$ values of the vadose zone in the dry season ($+1‰ \pm 1.5$ below mangroves, $-1.9‰ \pm 0.02$ below hammocks) were significantly different from those of the wet season ($+1.7‰ \pm 1.7$ below mangroves, $-1.8‰ \pm 0.01$ below hammocks) (χ^2=4569.56, p<0.0001 for mangroves, χ^2=49199.25, p<0.0001 for hammocks) (Figure 4B). In water table, the average $\delta^{18}O$ was higher during the dry season ($+0.8‰ \pm 0.4$ under mangroves, $-0.5‰ \pm 0.03$ under hammocks) relative to the wet season ($+0.1‰ \pm 0.4$ under mangroves, $-0.6‰ \pm 0.01$ under hammocks) and this seasonal difference was significant in both cases (χ^2=31642.4, p<0.0001 for mangroves, χ^2=11375.04, p<0.0001 for hammocks). During the most of the wet season, while the monthly $\delta^{18}O$ values of the water table were decreasing, the values in the vadose zone were relatively stable (Figure 4B).

The Relationship between Water Salinities and $\delta^{18}O$ Values

The range of vadose zone salinities and $\delta^{18}O$ values was ranged from 1.8 to 30 ppt and -2 to +3.5‰, respectively (Figure 5A), while the range of salinities and $\delta^{18}O$ values in the water table was 7.5 to 18.4 ppt and -0.8 to 1‰, respectively (Figure 5B). The simulation results showed that salinities of the vadose zone and water table are highly correlated with $\delta^{18}O$ values of the water, with the trend that water with higher salinity has a higher $\delta^{18}O$ value. However, the pattern of this positive correlation differed between the water table and the vadose zone. In the water table, there was a clear linear relationship between $\delta^{18}O$ value and salinity (Figure 5B). The relationship between salinity and $\delta^{18}O$ values tends to be curvilinear in vadose zone (Figure 5A). This relationship is composed of two parts: the first part (below $\delta^{18}O = 0$) is linear, while in the second part (above $\delta^{18}O = 0$), the slope asymptotes towards a maximum salinity of about 30 ppt. In the H0→H,

H50→H, H50→M and H100→M cells, from the linear relationship, it is very clear that hammock trees with higher replacement probabilities absorbed water with higher salinities and therefore higher $\delta^{18}O$ values (Figure 5C).

Prediction of Hammock Replacement by Mangroves

There were significant differences in the average $\delta^{18}O$ values of stem water from hammock trees with different replacement probabilities (H0→H, H25→M, H50→M and H100→M) two years before the tipping point for the replacement occurred (Figure 6A). The H0→H cells, i.e., no probability of shifting to mangroves, had the lowest $\delta^{18}O$ values, while the H100→M cells, i.e., a certainty of shifting, had the highest values. There were significant differences in the average $\delta^{18}O$ values of stem water in these five types of cells in the 5th year ($F=1355$, $p<0.0001$).

I also tracked yearly average salinities of the vadose zone used by individual trees (Figure 6B) and $\delta^{18}O$ values of their stem water (Figure 6C) in H0→H, H50→H, H50→M and H100→M cells. Stem water of trees in H0→H and H100→M cells generally had the lowest and highest values, respectively. Trees in H50→H and H50→M cells are from the same hammock population having a 50% replacement probability. The clear salinity difference between the two types of cells in H50→M and H50→H appeared in the 4th year ($F=4.9325$, $p=0.0290$), three years before the replacement happened (7th year) (Figure 6B). Moreover, the $\delta^{18}O$ values of plant stem water had similar trends as the salinity of the water available to the plants. Trees in H0→H and H100→M cells generally had uptake-water with the lowest and highest $\delta^{18}O$ value, respectively. There was a significant difference of ~0.1‰ in the $\delta^{18}O$ value of stem water between H50→M and

H50→H cells in the 4th year (F=6.7213, p=0.0535). In the 7th year, when the tipping point occurred, the difference increased to ~0.2‰.

Discussion

The comparison of salinity and $\delta^{18}O$ dynamics between the two vegetation types and the two seasons demonstrates the effects of plant transpiration, precipitation and tidal flooding on the coastal ecosystem. Differences in plant transpiration between the halophytic and freshwater vegetation influence the salinity of the vadose zone and water table, and this influence is indicated by the contrast of vertical salinity heterogeneity in soil between the mangrove forest (where vadose zone > water table) and hardwood hammock forest (where vadose zone < water table) (Figure 4A). The results are consistent with field observations of southern Florida where the upper soil (vadose zone) of mangrove forest has higher salinity than the water table (Ewe and Sternberg, 2005). This salt accumulation in the vadose zone under mangrove forests is caused by salt exclusion in mangrove roots during water uptake (Passioura et al., 1992; Tomlinson, 1994). The high salinity resulting from upward flow of saline groudwater by plant transpiration is also recorded in a salt marsh ecosytem in Georgia (Wilson et al., 2011). On the other hand, in hammocks of sourthern Florida, field study of Ish-Shalom et al. (1992) found that salinities of soil samples (from 0-10 cm and 20-30 cm depth) are lower than those of groundwater in both the wet and dry seasons. However, there is a limitation in my model assumption on plant transpiration that the water uptake rate is only dependent on salinity for one specific vegetation type. This rate may actually be variable through differences in energy balance, photosynthetic metabolism, and water use

efficiency (Moffett et al., 2012), which may be caused by changes of biotic and abiotic factors (e.g., temperature, nutrient, light), affecting soil salinity.

The effect of precipitaion can be detected by the significant seasonal differences of salinities in the water table under each of the vegetation types (Figure 4A). The seasonal difference is corroborated by the field study of Ewe and Sternberg (2005) in southern Florida, indicating that salinity at 50 cm belowground was lower during the end of the wet season than the dry season. This seasonal difference in salinity was mainly caused by the dilution effect of wet season precipitation. My results showed that the maximum salinity of water table occurred in April, near the end of the dry season, and the minimum salinity was in October, near the end of the wet season. The timing of the two maximum and minimum salinities match salinity measurements of a coastal hardwood hammock water table in the Everglades (Saha et al., 2014). With respect to the $\delta^{18}O$ of the vadose zone, under the hammocks, the similarities in $\delta^{18}O$ dynamics between the vadose zone water (Figure 4B) and that of rain water (Figure 2A) indicate that vadose zone is recharged by rain water and not by groundwater during the wet season. A field study in southern Florida also found that $\delta^{18}O$ values of the vadose zone water in hammocks follow temporal and seasonal patttern of rainwater $\delta^{18}O$ (Saha et al., 2009). Rainfall can change soil salinity by water input to groundwater and fresh surface water imput. Therefore, in Moreton Bay of Australia, Eslami-Andargoli et al. (2009) found that precipitation is the driving factor on the landward mangrove expansion by comparing the rainfall pattern and mangrove expansion from 1972 to 2004, and Snedaker (1995) also argued that changes in regional rainfall may have great influece on mangrove distribution in the short term.

I also noticed that there was greater variance in salinity and $\delta^{18}O$ of the mangrove soil in the model simulations (Figure 4), which might be caused by a sudden salinity and $\delta^{18}O$ increase in the area near the ocean which is under influence of the tidal flooding. This tidal flooding effect on the soil salinity was also noticed by Jiang et al. (2014), who found that salinity variance of soil porewater at the mangrove site was higher than that at the freshwater marsh site. The flooding effect on the $\delta^{18}O$ is supported by Greaver and Sternberg (2006), who found that variance of stem water $\delta^{18}O$ was negatively related to distance from the ocean. In the simulation study of salt marsh creek ecosystem, Xin et al. (2009) showed that there was a significant water table fluctuation occur in near-creek zone. From the increased salinity variance, it can be inferred that there is a significant tidal influence on the coastal ecosystem. In some specific ecosystems, tidal flooding is the only detected factor affecting vegetation dynamics in coastal ecosystem. For example, at Elkhorn Slough in California, Wasson et al. (2013) found that only increased tidal flooding has a strong relationship with upward migration of salt marsh-upland boundaries compared with other factors, including mean sea level and precipitation. At Baja California, Mexico, López-Medellín et al. (2011) found that inland mangrove colonization requires extraordinary tidal, which is main factor on establishment of the viviparous propagules of mangroves (Rabinowitz, 1978). The flooding frequency and strength can be increased by SLR (Ezer and Atkinson, 2014; Kriebel et al., 2015); therefore, the influence of tidal flooding may be enhanced in the future. The enhanced influence will tend to raise the vadose zone salinity and favor the growth of halophytic vegetation, pushing the vegetation boundary farther landward. Thus, there is a need to

forecast this vegetation shift in the coastal ecosystem, and take management steps where possible.

The positive linear relationship between salinity and $\delta^{18}O$ in the water table (Figure 5B) observed here is corroborated in many field studies of southern Florida; e.g., Sternberg et al. (1991); Lin and Sternberg (1994); Ewe et al. (2007), which may result from mixing of freshwater with low $\delta^{18}O$ values and saline seawater with high $\delta^{18}O$ values. In a tidal creek system of Australia, Wei et al. (2012) also found a similar trend, in which the water table on the creek side had higher salinities and $\delta^{18}O$ than the inland area. If the relationship between $\delta^{18}O$ value and salinity of the vadose zone pore water is affected only by the mixing of freshwater and seawater, one would also expect a linear relationship in the vadose zone (straight line in Figure 5A). However, the relationship between salinity and $\delta^{18}O$ values is curvilinear (Figure 5A) for the vadose zone and this simulation result is constistent with field studies by Swart et al. (1989) and Sternberg et al. (1991). Sternberg et al. (1991) observed a similar curvilinear relationship between salinity and $\delta^{18}O$ value for water samples at the surface of the water table in southern Florida. The linear part $\delta^{18}O$ versus salinity curve at the low salinity section (salinity < 20 ppt) might be caused purely by the mixing of freshwater and saline seawater, but the asymptotic part in the high salinity region (salinity > 20 ppt) indicates that the mangrove water uptake by excluding salts might increase the salinity of vadose zone, without changing the $\delta^{18}O$ value of vadose zone pore water. Despite the curvilinearity, the positive correlation between salinity and $\delta^{18}O$ values of the vadose zone suggests that I may be able to use the $\delta^{18}O$ value of stem water to indicate the salinity of the vadose zone water available for plant uptake.

My results indicate that the differences of vadose zone salinity among the four cell types (H0→H, H50→H, H50→M and H100→M) diverge gradually during the simulation (Figure 6B). Therefore, although the vegetation tipping point can be abrupt, it is really caused by the culmination of incremental salinity shifts. However, because of the previously stated reasons, salinity measurements of the vadose zone or of the plant xylem water in the field will not necessarily determine the probability that a hammock species will be replaced by a mangrove species. Oxygen isotope ratio of the stem water, however, might be a good candidate as an indicator of the impending vegetation shift. The $\delta^{18}O$ value ranking of the five cell types from Tukey's Post Hoc Test (Figure 6A) also suggested that I can use $\delta^{18}O$ values of stem water to determine the probability of a hammock tree being replaced by mangrove tree, with the exception for distinguishing the 25% to 50% probabilities, which were not significantly different.

Currently, measurement of the isotopic composition of stem water has a precision of approximately $\pm$0.1‰ (Vendramini and Sternberg, 2007), which is the difference observed for the $\delta^{18}O$ value of stem water from H50→M and H50→H trees three years before hammocks in the group H50→M were replaced by mangroves (Figure 6C). Thus, I may be able to analyze an appropriate number of plant stem water samples from a given hammock tree to detect the significant $\delta^{18}O$ value difference by repeated measures ANOVA. For example, an 80% certainty of detecting the significant 0.1‰ difference on $\delta^{18}O$ value of plant stem water at the 5% level of significance requires 18 replicates of stem water samples (Sokal and Rohlf, 1995).

This forecasting method based on $\delta^{18}O$ value may be applied to other ecosystems in addtion to the coastal ecosystem in southern Florida, because the similar salinity and $\delta^{18}O$

relation and the plant water use pattern can also be found in other areas. For example, Wei et al. (2012) recorded positive salinity and $\delta^{18}O$ relation and slight differences of $\delta^{18}O$ between vadose zone and stem water of *A. marina* (mangrove species) in a sub-tropical estuary in Australia. However, more research is requried to make my forecasting practical. First, to capture the topographic, geologic, and vegetative complexity of a natural site, it is important to know how to apply a general model study to a specific field conditions (Moffett et al., 2012). For example, my current model used a simplified structure of root and salinity distribution in the vadose zone. In a specific field, the root structure may vary by different plant scpecies, particularly for hardwood hammock forest which may comprise different neotropical evergreen broadleaf trees(Saha et al., 2009) with different root structure, and the salinity distribution of a site may be more complex than my current assumption. The root structure determines the location of plant water resource, and this location will be very important to my prediction in the site with a complex salinity distribution in the vadose zone. Second, there is a need to make a long-term field measurement both on salinity and $\delta^{18}O$ of the water components (vadose zone, water table and plant stem water), and on the vegetation dynamics during the same time period, as it is an appropriate way to test, elaborate and calibrate my model. Third, I need to know how much time is required to decrease the vadose zone salinity to values which prevent replacement of hammock by mangroves under current water management practices.

My predictions will be useful for improving the efficiency of current ecological restoration in southern Florida. For example, the Comprehensive Everglades Restoration Plan proposes to return freshwater flow to the Everglades to historic conditions (Perry,

2004), and the implementation of this plan will affect water salinity of the coastal ecosystems in southern Florida (Herbert et al., 2011). My study showed that $\delta^{18}O$ value of plant stem water may be a promising predictor of replacement of hammocks by mangroves three years before it occurs. The three years may be sufficient time to introduce appropriate amounts of freshwater flow to cease or slow the hammock replacement by mangroves.

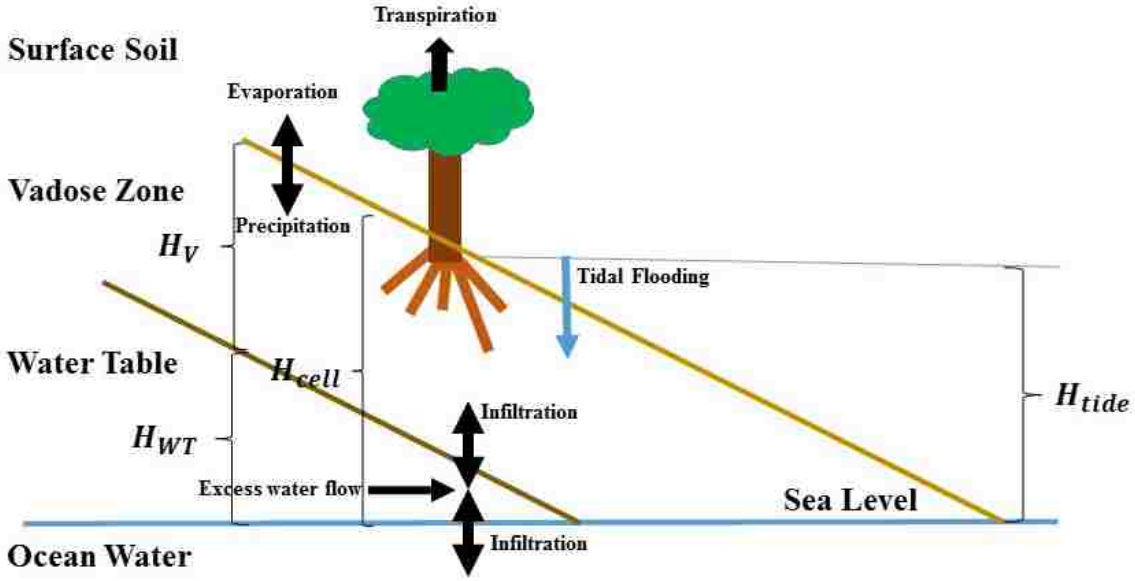

Figure 3.1: Schematic diagram of hydrological components and factors on water flow in vadose zone. H_{WT} is thickness of the water table, H_V is thickness of the vadose zone, H_{cell} is height of a spatial cell and H_{tide} is height of tidal flooding. The blue arrow denotes tidal flooding. The vertical black arrows denote evaporation, precipitation, transpiration and infiltration between the vadose zone and water table, and between water table and ocean water, respectively. The horizontal black arrow denotes excess water flow from water table in the landward neighboring cell.

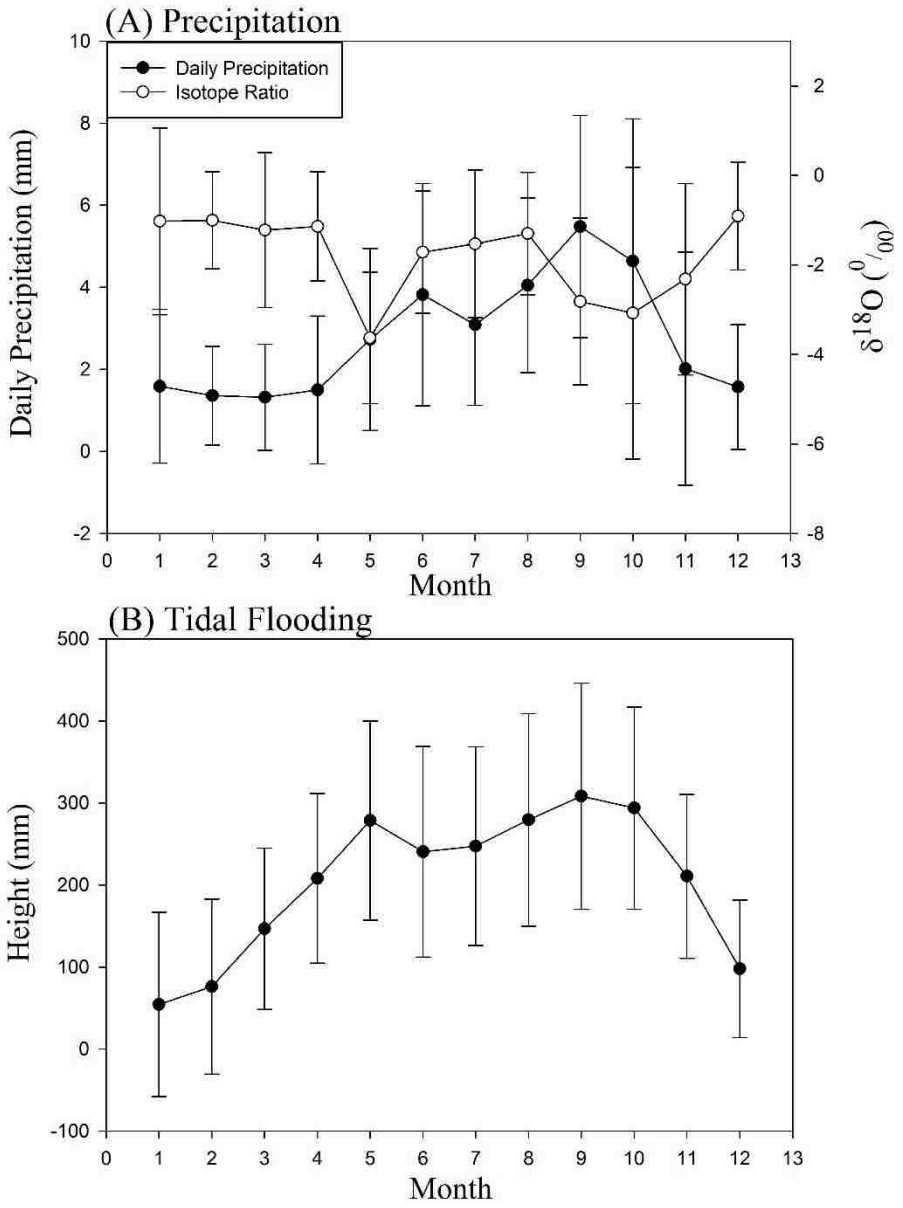

Figure 3.2: For every month, daily average and standard deviation of precipitation (mm) (NOAA, National Weather Services Forecast Office, Florida) and its $\delta^{18}O$ ($^{0}/_{00}$) (Price et al., 2008), and height of tidal flooding in Florida (NOAA, Tide & Current Historic data base, Key West Station) were derived from 162 years, 3 years and 5 years of empirical data, respectively.

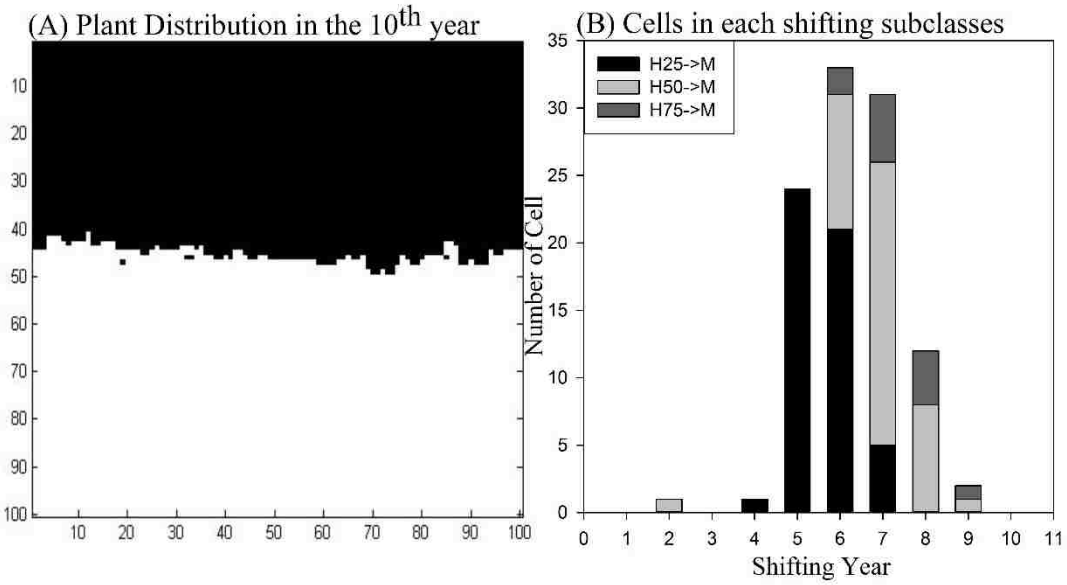

Figure 3.3: (A) Horizontal view of landscape grid with 100×100 cells showing final distribution of mangroves (black) and hammocks (white) along a topographic gradient from 85 mm above sea level (top of the panel A) to the highest inland elevation of about 1200 mm (bottom of the panel A). All cells were occupied by either one mangrove or one hammock tree. (B) Number of cells in each shifting subclass (not shown here are H100→M, H0→H etc), with only the 7th year showing enough cells of the three types of shifting subclasses.

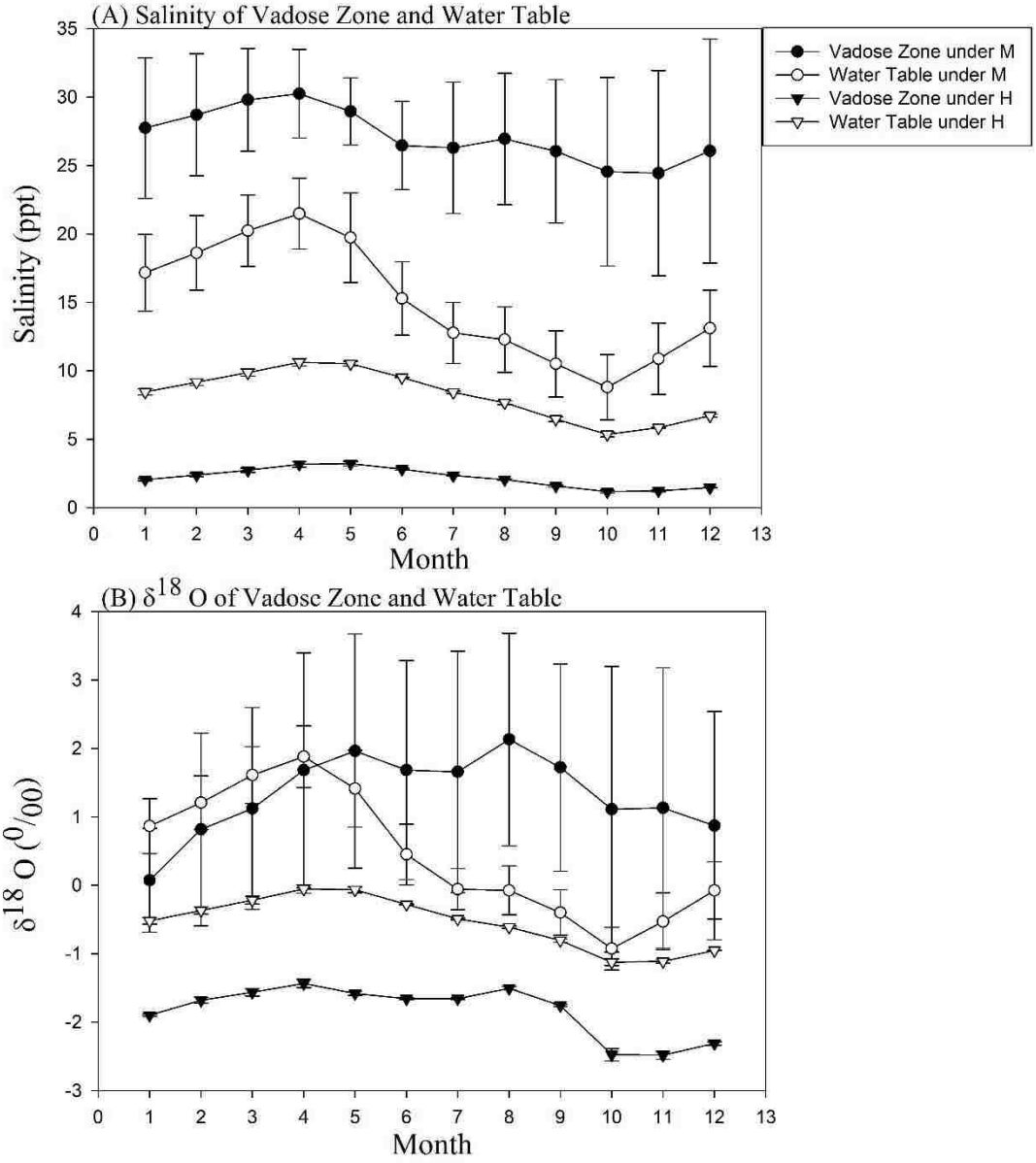

Figure 3.4: Monthly average and standard deviation of water salinities (A) and $\delta^{18}O$ values (B) of the vadose zone and the water table under mangroves (M) and hammocks (H) in the 10^{th} year of the data-sampling simulation.

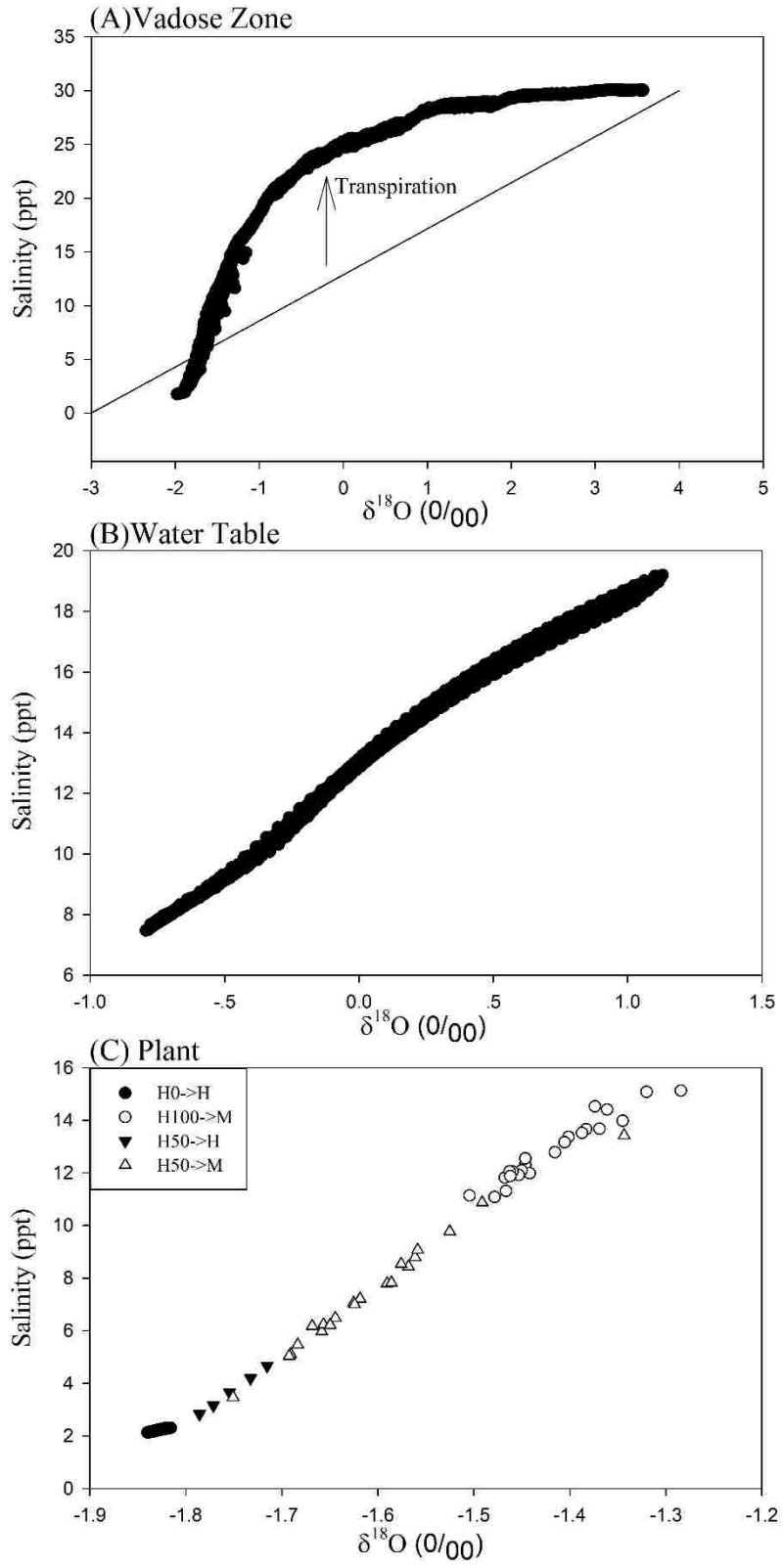

Figure 3.5: The relationship between $\delta^{18}O$ values versus salinities of water in the vadose zone (A) and water table (B) for all the cells in the landscape in the 10^{th} year. In (A), the

straight line represents ideal linear relationship between $\delta^{18}O$ and salinity expected if salinity was only determined by the mixing of freshwater and ocean water. The vertical arrow means the increase of salinity without change of $\delta^{18}O$ value in vadose zone caused by salt exclusion by mangrove roots. (C) This is the relationship between $\delta^{18}O$ values of the plant stem water and salinity of the water available for uptake in the 10th year from cell types with the different shifting probabilities (H0→H, H100→M, H50→H, and H50→M). The H0→H cells showed less variation in the bottomleft of (C).

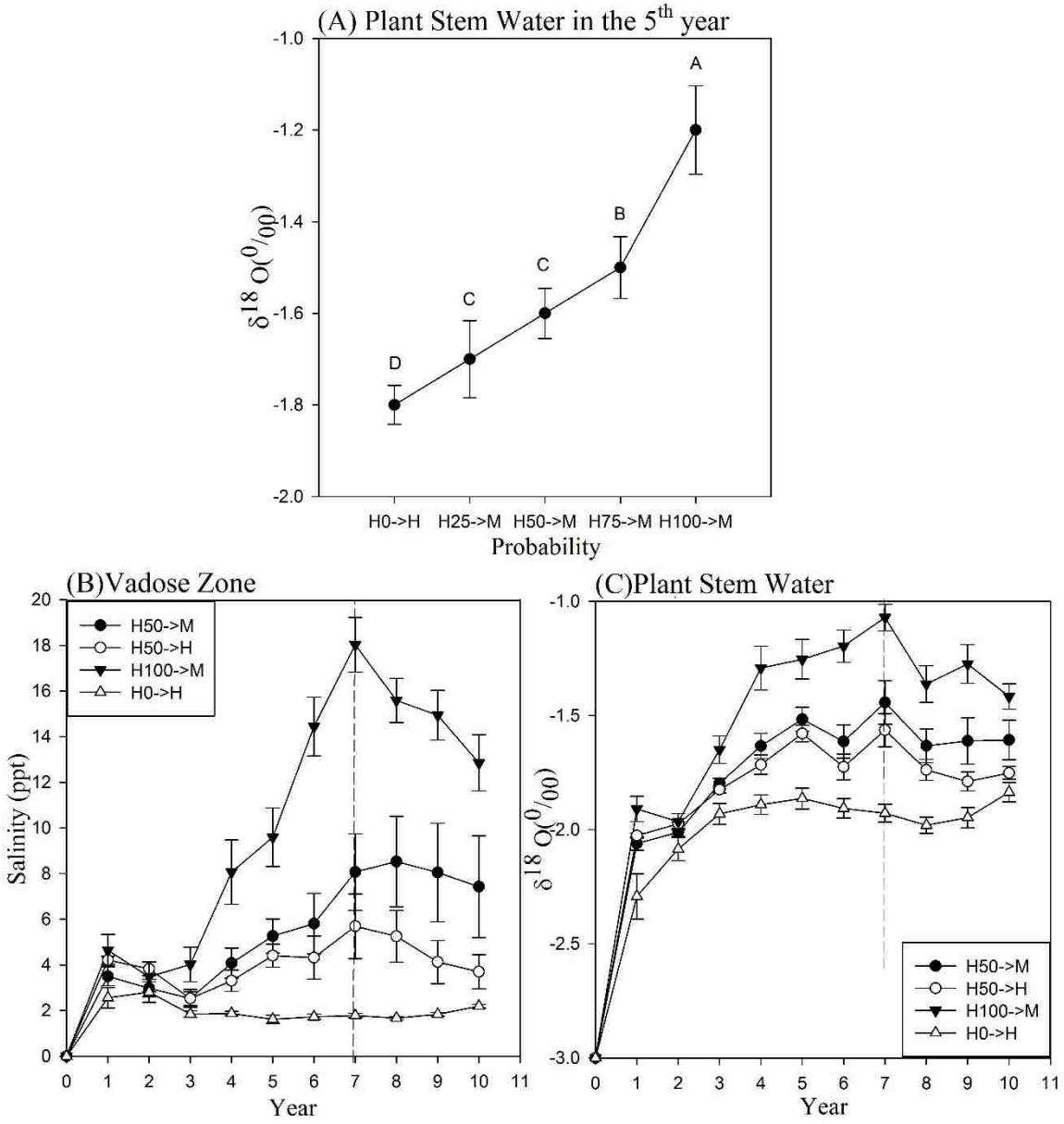

Figure 3.6: (A) The average $\delta^{18}O$ values and their standard deviations of plant stem water for hammocks in the H0→H, H25→M, H50→M, H75→M and H100→M cells. Isotope ratios of stem water were recorded two years before replacement occurred (the 7th year). Shifting subclasses having the same letter are not significantly different at the 5% level of confidence from Tukey's Post Hoc Test. (B) The yearly average and standard deviation of vadose zone salinity in the identified cell and its four neighboring cells during the data-sampling simulation. (C) The yearly average and standard deviation of $\delta^{18}O$ value of plant stem water in the identified cells during the data-sampling simulation. Error bars represent the standard deviation. The dash line indicates the year when hammocks were replaced by mangroves.

Chapter Four

Vegetation and Discharge Gate Location Affect Evaporation in a Tropical Wetland as Indicated by the Deuterium Excess Method

Summary

Evaporation (*E*) is an important part of the hydrologic cycle in tropical wetland ecosystems, because it represents the principal component of water loss. Quantifying *E* in wetlands is challenging, because it is difficult to separate *E* from transpiration (*T*). To precisely quantify the effect of *E* on water loss, my study used a deuterium excess (*d*) method based on oxygen and hydrogen stable isotope ratios ($\delta^{18}O$ and δD) of water to calculate the remaining fraction (*f*) of water in the wetland after evaporation. My study represents the first to use this method to quantify the effect of *E* in a tropical wetland environment. In addition to disentangling the effect of *E* from *T*, this method holds the advantage that it does not require knowledge of the initial isotope ratios of source water. The different sampling locations throughout my study site differed in vegetation coverage, water depth and distance to source water discharge gate which are important factors in wetland management. This sampling design offered us a unique opportunity to quantify the influences of the above three factors on loss of water by *E* with a general linear model. My results showed that: (1) there was a spatial and seasonal pattern of $\delta^{18}O$ distribution; (2) water from different locations experienced different degrees of water loss by *E*; (3) vegetation coverage had a positive effect on *f*; and (4) distance to the source water discharge gate had a negative effect on *f* for certain months of the year, while water depth had no effect on *f*. Therefore, vegetation and distance to source water discharge

gate are two important factors on the spatial pattern of water loss by *E* in this tropical wetland and my results may lead to a more informed wetland management.

Background

Evaporation (*E*), one of the most important components of a wetland hydrologic cycle, can be affected by many factors. Among these, my study considered the following factors: vegetation cover, depth of water column and proximity to source water. Although these factors have been extensively studied with respect to their impact on nutrient reduction (Kjellin et al., 2007), their influences on *E* are still unclear. Vegetation coverage may decrease water loss by *E* in a wetland area with its shading effect, e.g., reduced radiation and wind. On the other hand, it may increase water loss by transpiration (*T*) (Mykleby et al., 2016). Most conventionally based hydrology studies are not able to determine the vegetation effect on *E*. These conventionally based studies use energy-based methods such as measuring latent heat, which is residual of surface net radiation, sensible heat, and ground heat, to estimate evapotranspiration (*ET*), which sums up water loss both by evaporation (from soil, water body and rainfall intercepted by vegetation) and transpiration (Wang and Dickinson, 2012; Zhang et al., 2016). Both evaporation and transpiration are important water loss processes, but they may have different responses to changes of the wetland environment. For example, *T* would reach steady state, but *E* is seldom at steady state with increasing temperature (Dubbert et al., 2013), *T* would be decreased by increasing CO_2 at canopy level from undisturbed vegetation, but *E* may not be affected (Donohue et al., 2017), and global declining rates of wind speed may have more negative effects on *E* than *T* (McVicar et al., 2012). Other climate changes, including net radiation (Wild, 2009) and vapour pressure (Willett et al., 2008), may also

affect *E* and *T* differently. In addition, *E* and *T* may have different water sources in a wetland. The source of *E* comes directly from the water surface, but the source of *T* may come from a deeper water body or outflow seepage. From different sources, water loss may have different effects on the water balance in a wetland. For example, if *T* uses water from deep seepage, the total surface water evaporation or *ET* may be dampened (Eisenlohr, 1966). Therefore, there is a need to disentangle water loss by these two processes.

Both water depth and distance to the source water either through a channel or discharge gate are able to affect *E*, and they are important considerations for wetland management. The water depth effect has been supported by some observations in the wetlands of England and Wales, which found that with the increasing water depth, evaporation rates decreased during the higher summer temperature (Finch and Hall, 2001). Compared with shallow water, deeper water bodies may have a greater capacity for heat storage to buffer the effect of high air temperature. We are not aware of any studies considering the effect of water depth on *E* in warmer areas, such as my study site in southern Florida. Because southern Florida has a high annual mean temperature, water depth may be an important factor modulating *E* of reservoir water. Moreover, distance to the source water channel or discharge gate may affect *E* by two potentially opposing influences. Water closer to the source water suffers a shorter time exposure to radiation and wind which can decrease *E*. On the other hand, *E* would increase for water closer to a discharge gate because higher flow rates can increase *E* by: (1) decreasing the relative humidity of air above water surface by accelerating vapor transfer between areas near and far from water surface; and (2) increasing the water surface area exposed to air (Wallace

and Hobbs, 2006) by producing a great number of ripples, bubbles (Kundu et al., 2012) and tiny water droplets (Thorpe, 2007). In addition to the spatial variation of *E* caused by the above factors, there may be a strong temporal pattern of *E*. For example, Lake Okeechobee, which is close to the site studied here (Fig. 1), has higher *E* in May and lower values in December or January (Abtew, 2001; Abtew et al., 2011). This seasonal pattern may be caused by the different meteorological conditions as well as vegetation growth during different seasons, e.g., May has higher average temperature and net radiation compared to December and January in southern Florida (Fig. 2 A and E).

This study is the first to quantify loss of water by *E* using the deuterium excess (*d*) method in a semitropical wetland ecosystem. Deuterium excess (*d*) is calculated from dual-isotope ($\delta^{18}O$ and δD) analysis of ambient water (see details in Methods). Since *d* decreases with increase in evaporation (Huang and Pang, 2012), it serves as a proxy for *E*. Specifically, we use *d* to calculate the remaining fraction (*f*) of the water in a wetland after evaporation. It thus, follows that a greater *f* means a lower *E*. This method has advantages over other traditional *E* or *ET* measurements. First, the *d* method has the potential to separate *E* from *T*. The separating ability of this method is based on that $\delta^{18}O$ and δD of water would only affected by *E*, but not *T*. Because during plant uptaking water through *T*, there is no discrimination against the heavier isotopes (^{18}O and D), particularly in a freshwater environment of WCAs (Zhai et al., 2016). Other methods attempted to separate *E* from *T* by estimating *ET* from vegetated area and comparing with that from a nearby open water area, but these methods provided unclear results (Sánchez-Carrillo et al., 2004). Second, the *d* method is relatively easy to apply in the field. It doesn't need continuous field observations with high frequency since stable isotope

signatures of water integrate processes occurring through a period of time (Skrzypek et al., 2015). Other methods, e.g., lysimeter method, eddy covariance method and sap flow method, require continuous survey of various environmental parameters and expensive facilities which can be only applied to appropriate environments (Drexler et al., 2004; Wu and Shukla, 2014). Third, the *d* method has a better spatial resolution than other methods, e.g., empirical methods like Penman_Monteith (PM) equation or Priestley_Taylor (PT) equation. These empirical methods have an important assumption that there is a uniform surface (e.g., uniform vegetation cover), but tropical wetlands tend to have a variety of vegetation that makes these methods difficult to quantify the spatial pattern of *E* throughout a wetland (Wu and Shukla, 2014).

The main purpose of this study is to use the deuterium excess (*d*) method to quantify the spatiotemporal pattern of *f*, which is negatively related to *E* in a semi-tropical wetland, and test whether *f* is related to various landscape features of the wetland. Specifically, we test the hypothesis that: (1) there is a spatiotemporal variation in the isotopic enrichment of water in a wetland throughout the year; and (2) there is a greater *f* in areas with a higher vegetation cover, deeper water and closer to the source water channel or discharge gate. Because there are various site-specific factors affecting *f*, quantification of *f* for specific hydrological and ecological conditions is important for more informed decisions on water resource management.

Methods

Study site

The study site was located in the Arthur R. Marshall - Loxahatchee National Wildlife Refuge (Palm Beach County, Florida), also known as Water Conservation Area-1 (WCA-1), one of the three WCAs (Fig. 1). The major management concerns of the WCAs are flood protection, water supply to the Everglades and nutrient control (Hong et al., 2010). Water resource management in WCAs is critical in view of the increased competition between urbanization, agriculture and ecological conservation of the Everglades National Park (ENP). The demand of freshwater resource is rising fast with the rapid population growth of southern Florida (Obeysekera et al., 2011). Improving freshwater availability is one of the key aims of ecological management in ENP, because the freshwater inflow can counteract the increasing saltwater intrusion in ENP due to the sea level rise (Perry, 2004).

WCA-1 is a 145,920-acre wetland ecosystem dominated by freshwater sawgrass marshes, and it is a part of the Kissimmee River-Lake Okeechobee-Everglades-Florida Bay watershed system (Fig. 1A). The water in this reservoir originate from Lake Okeechobee and flow through the Everglades Agriculture Area before reaching WCA-1. The water flow into the WCA-1 mainly by the West Palm Beach Canal (through discharge gates: G310, G311, S362) and Hillsboro Canal (through G338). Gate G310 is one of the major gates regulating water flow into the WCA-1 (Fig. 1A). Water from WCA-1 flows through WCA-2 and 3 and eventually into the Everglades National Park and on to the Florida Bay (Fig. 1A).

The climate of southern Florida is characterized by a wet (approximately from June to October) and dry season (approximately from November to May). The wet season is characterized by a relatively high temperature (26.8 vs 21.3 ºC/day), precipitation (18.1 vs. 4.9 cm/month) and potential evapotranspiration (PET, from the Simple Method in Abtew (1996)) compared to the dry season (Fig. 2 A, C and D). During the two years of my study (2006-2007), water levels at WCA-1 were lower from March to July compared to the other months (Fig. 2B).

Water sampling and processing

Surface water samples were collected at permanent sampling stations (associated with South Florida Water Management District) throughout the WCA-1 (Fig. 1B) at 10cm depth. Hydrometereological data, such as water level, are collected at these stations on a regular basis. Because the water depth in WCA-1 is generally very shallow (~1m, Fig. 3A), It is assumed that the act of collecting water samples mixes the water column well and my 10cm deep samples are representative of the water column. The sampling dates were August, September, and November of 2006 and January, August of 2007. There were 23, 21, and 38 sampling points in August, September, and November of 2006, respectively. In 2007, 39 and 26 sampling points were collected in January and August. The differences in number of the sampling points for the different months were due to drying out of certain areas during drier periods. Water samples were placed in scintillation vials, sealed with Parafilm (Pechiney, Chicago, IL, USA) to prevent evaporation and kept refrigerated at 5ºC before analysis of oxygen and hydrogen isotope ratios. Within one month from the sampling date, oxygen and hydrogen isotope ratios of the water samples were analyzed by an Isoprime Isotope Ratio Mass Spectrometer

connected to a Multiflow system (Elementar, Germany) (Vendramini and Sternberg, 2007) at the Laboratory of Stable Isotope Ecology in Tropical Ecosystems at the University of Miami. Oxygen and hydrogen isotope ratios are expressed as $\delta^{18}O$ and δD according to the Eq.1:

$\delta^{18}O$ or $\delta D = [(R_{sample}/R_{std}) -1] * 1000$……Eq. 1

where R_{sample} and R_{std} represent the $^{18}O/^{16}O$ or D/H isotopic ratio of the sample and standard, respectively. The isotopic ratios are dimensionless. The standard used here is Vienna mean standard water (vSMOW) and the precision of analysis is $\pm$2.0‰ and $\pm$0.2‰ for δD and $\delta^{18}O$ values, respectively.

Evaporation quantified by deuterium excess method

Meteoric water line, deuterium excess and evaporative water line

Craig (1961) analyzed oxygen and hydrogen isotope ratios of global precipitation samples to derive the global meteoric water line (GMWL, Eq.2). GMWL is a global average of many local meteoric water lines (LMWL) which are controlled by local climatic factors on precipitation, e.g., origin of vapour mass, secondary evaporation during precipitation and the seasonality of precipitation (Clark and Fritz, 1997). Therefore, any LMWL may have different slope and intercept compared with the LMWL of other areas. For example, in southern Florida, the LMWL is described by Eq.3 (Price et al., 2008). The intercept of the meteoric water line (GMWL or LMWL) is called the deuterium excess (*d*), which defines the δD displacement of the precipitation line from that of seawater. The deuterium excess (*d*) of the LMWL in southern Florida is 11 (Eq.3) and the deuterium excess of any water sample collected in southern Florida is described by Eq.4.

$\delta D = 8\delta^{18}O + 10$……Eq. 2

$\delta D = 8.6\delta^{18}O + 11$……Eq.3

$d = \delta D - 8.6\delta^{18}O$……Eq.4

In addition to the meteoric water line, there are local evaporative water lines (EWL) which are derived from the relationship between oxygen and hydrogen isotope ratios of water bodies undergoing evaporation. Because of additional fractionation factors, EWL tends to have a slope lower than that of the LMWL. Meanwhile, EWL will extrapolate and intersect the LMWL at the hydrogen and oxygen isotope ratios of the original source of water before evaporation.

Equilibrium and kinetic isotope effects during evaporation

I define here isotope fractionation as the unequal preference of one isotope over the other during physical and chemical processes. Total isotope fractionation (α) during evaporation is a combination of two types isotopic fractionations: (1) equilibrium fractionation, which happens within the boundary layer, i.e., vapour layer with 100% relative humidity located right above the water surface; and (2) kinetic fractionation, which is the effect of the diffusivity of different water isotopologues through the boundary layer (Clark and Fritz, 1997). The separation factor denoted as Δ is the difference in the isotope ratio (Eq.1) between a product and a substrate in a physical or chemical process undergoing isotopic fractionation, i.e., the difference in isotope ratio between vapor and liquid water in equilibrium, and Δ is approximated by 1000(α-1) or $10^3 \ln\alpha$ in Eq.6 and 7.

During evaporation, the source (liquid water) has higher $\delta^{18}O$ and δD values than that of the generated vapour. The separation factor ($\Delta^{18}O$ or ΔD, Eq.5) between liquid

water and vapour is sum of the differences of both the respective equilibrium separation factors ($\Delta_E^{18}O$ or $\Delta_E D$, Eq.6-7) and kinetic separation factors ($\Delta_K^{18}O$ or $\Delta_K D$, Eq.8-9) (Majoube, 1971; Gonfiantini, 1986). For the calculation of the equilibrium separation factor (Eq.6 and 7), it is necessary to have the water temperature, while relative humidity (h) is necessary for the calculation of the kinetic separation factor (Eq. 8 and 9). If relative humidity is unavailable, it can be calculated by Eq.10 (Gonfiantini, 1986).

$\Delta = \Delta_E + \Delta_K$……Eq.5

$\Delta_E^{18}O \approx 10^3 \ln \alpha^{18}O = 1.137(10^6/T^2) - 0.4156(10^3/T) - 2.0667.$ Eq.6

$\Delta_E D \approx 10^3 \ln \alpha D = 24.844(10^6/T^2) - 76.248(10^3/T) + 52.612.$ Eq.7

$\Delta_K^{18}O = 14.2(1-h).$ Eq.8

$\Delta_K D = 12.5(1-h).$ Eq.9

$h = 1 - (\Delta_E D - S \cdot \Delta_E^{18}O)/(14.2 \cdot S - 12.5)$ Eq.10

where *T* is surface water temperature in [K], *h* is relative humidity (%), and S is the dimensionless slope of evaporative water line. Here, the calculated *h* (Eq.10) was compared with *h* from the closest weather station, and no significant difference was found (p=0.13 from a paired t-test of the five-month data). In my study, only air temperature was available, but the temperature differences between surface water and air tend to be no more than 5 K (Livingstone and Lotter, 1998). Therefore, we made a sensitivity test and found that 5 K temperature difference only caused less than 5% change of the final *f* values.

Calculating the remaining fraction (*f*) of water after evaporation with the deuterium excess (*d*) method

During evaporation of a water body, the remaining water becomes progressively enriched in heavy stable isotopes (^{18}O and D), and the enrichment can be predicted by the Rayleigh distillation equation (Eq.11) (Clark and Fritz, 1997), where δ_f and δ_0 are either δ^{18}O or δD values of the remaining water during evaporation, and that of initial source water, respectively. The deuterium excess (d_i) of the ith water sample from the WCA-1 can be calculated by using the slope of the LMWL (Eq.4). The remaining fraction (f_i) of water from ith sample point after evaporation can be calculated by Eq.13, which is derived from Eq. 11-12.

$\delta_f \approx \delta_0 - \Delta \cdot lnf$……Eq.11

$d_i = \delta D_i - 8.6\delta^{18}O_i$……Eq.12

$f_i = e^{[(d_i - d_{LMWL})/(8.6\Delta^{18}O - \Delta D)]}$……Eq.13

where d_{LMWL} is the deuterium excess of the LMWL (see Eq.4) and has a value of 11. As it can be seen, it is not necessary to know the isotope ratios of the original source water with this method. The only prerequisite is that the source water originated from local rainfall with its oxygen and hydrogen isotope ratios following the relationship of the LMWL.

Mapping δ^{18}O values, vegetation coverage and water depth

The isoscape (West et al., 2010) of water δ^{18}O values in WCA-1 were calculated by a kriging algorithm. Here we map the δ^{18}O values rather than the δD, because ^{18}O abundance is much more sensitive to evaporation compared to D abundance resulting from the stronger kinetic isotope effect on ^{18}O compared to that of D during evaporation

(Clark and Fritz, 1997). The $\delta^{18}O$ distribution maps were made by using the GPS locations of sampling points within in the boundaries of WCA-1 in ArcMap (ESRI, USA). The distances between sample locations and the discharge gate were determined by the GPS information. Distribution data of water depth and vegetation (Fig. 3) were obtained from Conceptual Design of the Everglades Depth Estimation Network (EDEN) (Jones and Price, 2007) and High Accuracy Elevation Data Project of USGS (Desmond, 2007), respectively. Vegetation coverage of each water sample point was calculated by average percentage of open water within 50m radius around the corresponding point. Further, a vegetation type map of WCA-1 was obtained from Bancroft et al. (2002) which recoded and combined the multispectral SPOT satellite images of WCA-1.

Statistical analysis

Evaporative water line (EWL) by Model II regression

The slope and intercept of the EWL was calculated by Model II regression, because both $\delta^{18}O$ and δD are measured values with random errors (Sokal and Rohlf, 1995). The model II regression was calculated by the major axis (MA) method, which is based on certain assumptions including (Legendre, 1998): (1) data distribution is bivariate normal, which is checked by MVN package in R (Korkmaz et al., 2014); (2) both $\delta^{18}O$ and δD are dimensionless; (3) it can be reasonably assumed that the error variances of $\delta^{18}O$ and δD are approximately equal. Note that two outliers in September 2006 were removed from the analysis.

General linear model

To examine the influences of the three numerical factors (vegetation cover, water depth, and distance to the discharge gate) and one category factor (month) on *f*, we used a

general linear model (Eq. 13) to describe f_i of ith sampling point as a function of vegetation cover (V_i), water depth (W_i), and distance to the canal station (D_i) of i^{th} point.

$$f_{ij} = M_j + V_i + W_i + D_i + \varepsilon_{ij} \ldots\ldots \text{Eq. 13}$$

where f_{ij} is the remaining fraction of the reservoir in the j^{th} month at i^{th} point, M_j is the effect of jth month (j = 1, 2, 3, 4, and 5) including August, September and November in 2006, and January and August in 2007, and ε_{ij} is the random error of the ith sample in the jth month.

The statistical analysis and examination of the analysis assumptions were conducted in the linear regression framework in JMP statistic program (Sall et al., 2012). The assumption of residual normality was satisfied (Shapiro-Wilk W test: p=0.3474). The assumption about the zero expectation of the residuals was satisfied by comparing the residual expectation with zero in the one sample t test (p=1). The homoscedasticity assumption was also satisfied by checking the residual plot by the predicted values that showed homogeneous residuals with the change of predicted values. Then, the linearity assumption of the relationship between *f* and the main factors was satisfied by checking the plot of the actual values versus the predictive values of the *f* (p<.001). Next, the collinearity between the main factors was small by checking the values of variance inflation factor (VIF) which were less than 10 (Neter et al., 1996). For significance levels of statistical tests in this study, we considered p<0.05 to be significant, and p<0.001 to be highly significant (Sokal and Rohlf, 1995).

Results

Evaporation and $\delta^{18}O$

Plots of δD versus $\delta^{18}O$ values of reservoir water for each sampling month fell along EWLs with slopes ranging from 5.05 to 6.43 (Fig. 4), and these slopes are lower than the slope (~8.6) of LMWL (Fig. 4A) of southern Florida (Wilcox et al., 2004; Price et al., 2008). Therefore, isotope ratios of water in WCA-1 were isotopically enriched by evaporation. In 2016 August and September, the average *f* value was 90%. Therefore, on the basis of the average water depth (18 cm) of the similar time period (Fig. 3A) and WCA-1 area (564 km^2), evaporation consumed about 2.2×10^7 m^3 water during the two month period.

The $\delta^{18}O$ values of water within WCA-1 were spatially or temporally heterogeneous. The range of $\delta^{18}O$ values from different locations in the WCA-1 can be as large as 3‰ for any sampling date. The general spatial pattern of $\delta^{18}O$ values is that higher values distributed in the middle-eastern area and decreased towards the northwestern area (Fig. 5A-D). The average $\delta^{18}O$ values for the different months were also significantly different ($p<.001$), with September 2006 having the significantly lower average value compared with that of other months (Fig. 5F).

Correlation between *f* and vegetation, water depth, and discharge gate

Vegetation coverage was highest on the edge of the WCA-1 (Fig. 1B). The major component species of this coverage are Sawgrass (*Cladium jamaicenses*) and Cattail (*Typha domingensis*) (Bancroft et al., 2002) (Fig. 3B). Reservoir *f* values were significantly correlated with vegetation coverage ($p<.001$, Table 1). Vegetation coverage

effect explained 18~37% of the variation in *f* for the three months in 2006 (Fig. 6A-C), but not for the two months of 2007 (Fig. 6 D-E).

The remaining fraction of water (*f*) is also correlated with the distance to the discharge gate, but not with the water depth. Water depth in WCA-1 ranged from about 0m to 1.2m (Fig. 3A), but its correlation with *f* was not significant for all the sampling months ($p=.9112$, Table 1). The distance to the discharge gate had a significant correlation with the *f* ($p<0.001$, Table 1), and this correlation was significantly negative with *f* in August ($p<0.05$) and November ($p<0.001$) in 2006, January ($p<0.05$) in 2007 (Fig. 6 A, C and D). The distance to the discharge gate explains 19% to 39% variation in the *f* for the months with significant correlations (Fig. 6).

Discussion

The monthly variation of $\delta^{18}O$ values in WCA-1 corresponded to changes in meteorological and hydrological factors that affect evaporation. These factors, including temperature, precipitation, water level, etc., can affect evaporation, which in turn is reflected in the $\delta^{18}O$ values of the remaining water (Gat, 1995). Both temperature and net radiation tend to have a positive effect on evaporation. Indeed, the isotopic measurements for August of the two years, which had the highest temperature and net radiation during the study period (Fig. 2A and E), had relatively higher values compared with other months (Fig. 5F). High $\delta^{18}O$ values in the summer have been also observed in other wetlands. For example, Pham et al. (2009) found that most lakes of the Canadian Prairies revealed a greater $\delta^{18}O$ enrichment during the summer months. Increase in temperature alone, however, does not explain ^{18}O enrichment of WCA-1 water. Other factors, such as precipitation and humidity, can also affect $\delta^{18}O$ and *E*. For example, September 2006 had

a relatively high temperature (Fig. 2A), however the reservoir water had the lowest $\delta^{18}O$ value and *E* compared to the other months (Fig. 5B and F). Lower $\delta^{18}O$ values for September 2006 may be caused by a dilution effect of increasing incoming water with low $\delta^{18}O$ into WCA-1. This explanation is supported by the high precipitation and water level observed during the month of September 2006 (Fig. 2B-C). September is also close to the end of wet season in southern Florida which would cause a greater influx of isotopically depleted rain water (Price et al., 2008). The high water input from the discharge gate may have increased water flow rate so as to decrease the time of water is stagnant and undergoing evaporation in WCA-1. The lag period between the low $\delta^{18}O$ value in September, and the antecedent high precipitation during the wet season indicates the cumulative effect of precipitation and its consequential dilution of $\delta^{18}O$ values of the WCA-1 water. In addition, the lower $\delta^{18}O$ values during the month of September can be also caused by decrease in *E*, which is due to the high precipitation and humidity (data not shown) observed during this month.

The spatial distribution of *f* is correlated with vegetation coverage in WCA-1 (Table 1 and Fig. 6). Water had lower $\delta^{18}O$ values and higher *f* (i.e., lower *E*) in areas where the vegetation cover was high compared to areas where the vegetation coverage was low. This negative influence on *E* may be caused by solar radiation interception (Mengistu et al., 2014; Thompson et al., 2015) and wind reduction on the water surface (Helfer et al., 2009) by the vegetation. The reduction of the solar radiation and wind will decrease *E* which in turns suppresses ^{18}O enrichment of the remaining water and water loss through evaporation. However, the negative relationship between *f* and vegetation cover was not significant in the two months of 2007. The non-significant relationship may be caused by

relatively dry weather in the two months comparing with the other study months. This dry condition may decrease *f* (or increase *E*) of WCA-1 throughout a large spatial range, which overrides the vegetation influence. This explanation is supported by the $\delta^{18}O$ distribution map for the two months, and the high enrichment values over larger areas in these two months compared to those of the other months (Fig. 5 D and E). Further studies are necessary to determine how meteorological factors may override the vegetation influence.

Evaporation suppression by vegetation does not necessarily mean a lowering of the total water loss (i.e., *ET*). Transpiration (*T*), which can account for 60–80% of *ET* on land (Schlesinger and Jasechko, 2014), can also increase the water loss in areas of high vegetation cover. For example, one study in a swamp forest of southeastern Louisiana found that water loss from areas covered with vegetation is higher than open water (Allen et al., 2016). Abtew and Melesse (2013) concluded that *ET* rates of wetland areas covered with vegetation range from slightly less than to several times higher than *E* rates of open water areas. The effect of vegetation on wetland water loss may vary depending on the vegetation types characterized by different physiological or biophysical features, which can regulate proportion of *T* to *E* in the water budget (Mohamed et al., 2012). Therefore, to determine the proportion of *T* to *E*, the deuterium excess (*d*) method would be useful by quantifying *E* directly from wetland environment, particularly in conjunction with other methods, such as eddy covariance method which measure total *ET*.

My results indicated that location of the inflow discharge could be a major factor on the spatial distribution of $\delta^{18}O$, *f* and *E*. Water from sampling points closer to the discharge gate tended to have a higher *f* or lower *E*. This result supports the hypothesis

that shorter distances from the water source decrease the exposure time of water to radiation and wind, and ultimately reduce *E*. In addition, because the flow of water at my study site is directional (from the discharge gate at the northern end to the exit canal at the south end), there may be progressive cumulative evaporation as a function of distance from the discharge gate. In the beginning of the cumulative evaporation or areas near the discharge gate, *f* values of all the months were close to 100%, except for August 2007. The high *f* values near the gate indicated that water may have experienced very little evaporation before entering WCA-1 which validates my method of quantifying how different factors in WCA-1 affect evaporation. However, the effect of distance to the discharge gate on *E* was not significant in September 2006 and August 2007. The lack of correlation between distance to the discharge gate and *f*, as discussed previously, may be also caused by meteorological factors. Meteorological variability could be a major regulator of the wetland hydrology and this has been supported in many long-term studies, e.g., Sánchez-Carrillo et al. (2004). From water loss point of view, decreasing exposure time of water in WCAs to evaporation can be a potential method to minimize evaporation and raise the freshwater supply to the Everglades. However, in addition to providing adequate water supply to the Everglades, another ecological function of WCA-1 is to remove nutrients or other potentially harmful elements from the water. The removal process requires sufficient time for sedimentation or absorption of the elements before water enters the Everglades (Schoumans et al., 2014) which would increase water loss by *E*. Therefore, the tradeoff between freshwater quantity and quality to the Everglades needs management attention.

The relationship between *f* and water depth may be confounded by a high vegetation cover on the northern and eastern edges of WCA-1 where there were both shallow water and high vegetation cover (Fig. 3). We previously hypothesized that the shallow water would have a higher evaporation resulting in a higher water $\delta^{18}O$ values and lower *f* (or high *E*). However, any increase in *E* in shallow areas around the edges of WCA-1 might have been counteracted by lowering of *E* caused by the greater vegetation cover in these areas.

Evaporation estimated by the *d* method in WCA-1, which is located in subtropical area, was comparable with evaporation estimated by other stable isotope based methods in other subtropical areas. For example, in the subtropical areas of South America, Kosten et al. (2009) used Gat-Bower model to quantify Inlet/Evaporation (I/E) ratios of 16 lakes during warmer season (December to March). The I/E ratios were transformed to the *f* values in my study by f=1-E/I, and its average value is 77% ±2% which is lower than average *f* value (88% ±3%) of WCA-1 from my study during the months (August in 2006 and 2007, September in 2006) of the similar "warmer season" in Florida. The *f* difference may be caused by different biotic or abiotic conditions even though both of the two studies are from subtropical areas. Future studies can compare evaporation estimates by these different isotope based methods under similar conditions. Application of the *d* method to a specific wetland has two potential limitations: (1) The *d* method requires the parameters of the LMWL which are estimated from a statistical regression, and high accuracy of the regression analysis requires large number of rainfall samples with different water isotope values; (2) The *d* method assumes that all types of inflow water have similar isotope values as precipitation. In addition to precipitation, inflows may also

include surface water inputs through rivers or canals, and groundwater seepage. Prior-evaporation of surface water inflow before entering the wetland may confound the calculation of *f*. This influence, however, can be estimated by examining trends in *f* as a function of distance to discharge gate. My study found that the prior-evaporation before surface water entering the WCA-1 was negligible. Groundwater seepage may also confound the calculation of *f*, but previous studies near my study area support that the shallow groundwater, which might seep into WCA-1, has a similar isotope composition as precipitation (Price and Swart, 2006; Harvey and McCormick, 2009).

Distance to the source water discharge gate and vegetation coverage had significant effects on *f* and *E* in WCA-1. However, we did not observe any significant relationship between water loss by evaporation and depth of the water. Control of water loss could potentially be achieved by high vegetation coverage. However, it would be necessary to determine which species would have a transpiration regime such that the overall loss of water by evapotranspiration is diminished. There are other proposed evaporation mitigation techniques which mimic in part the shading by vegetation coverage, including continuous coverings of the entire reservoir by shade-cloth (Finn and Barnes, 2007), and floating modular devices (Hassan et al., 2015). These suggested methods, however, would have a high initial cost as well as a high maintenance costs. Further, compared with vegetation, it is not clear whether these methods would remove nutrients from the water to minimize the impact in the Everglades oligotrophic system. In addition to vegetation, location of discharge gate is also an important factor on spatial distribution of *E* at WCA-1.

Table 4.1: Summary of associated degrees of freedom, F ratios, and p values from the general linear model determining the importance of month (M), vegetation cover (V), water depth (W), and distance to discharge gate (D) on the remaining fraction of the water at each sampling point after evaporation.

Effect	df		water $\delta^{18}O$ value	
	Numerator	Denominator	F	p[a]
Month	4	131	-3.44	**.0008**
V	1	131	3.03	**.0030**
W	1	131	0.11	.9112
D	1	131	-3.6	**.0004**

[a] p-values which are significant at the 95% level of confidence are shown in bold type.

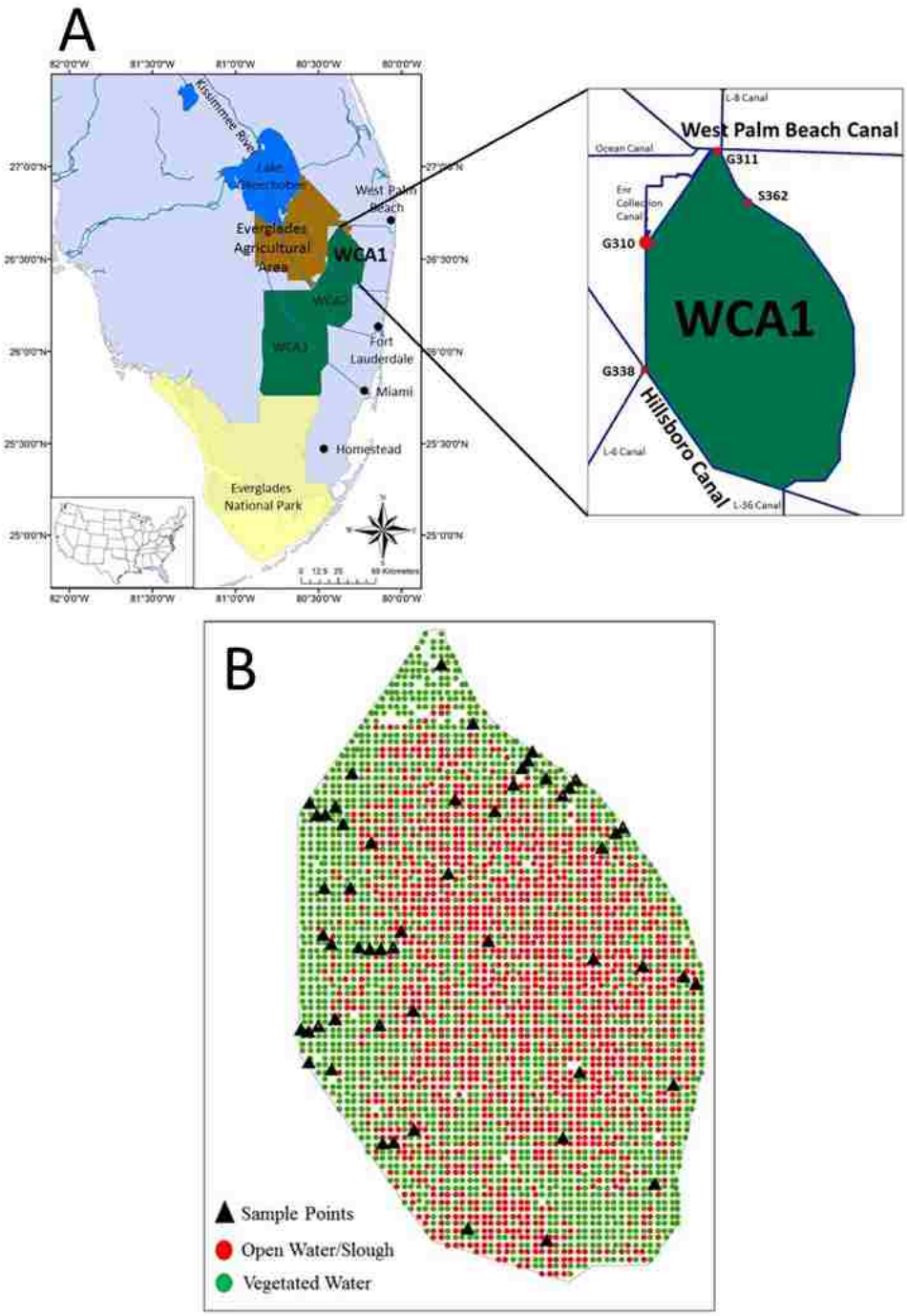

Figure 4.1: A, Location of the research area (WCA-1). Blue lines are canals, and red dots are discharge gates. B, Distribution of water sampling points, open-water and vegetated-water areas in WCA-1 from Desmond (2007).

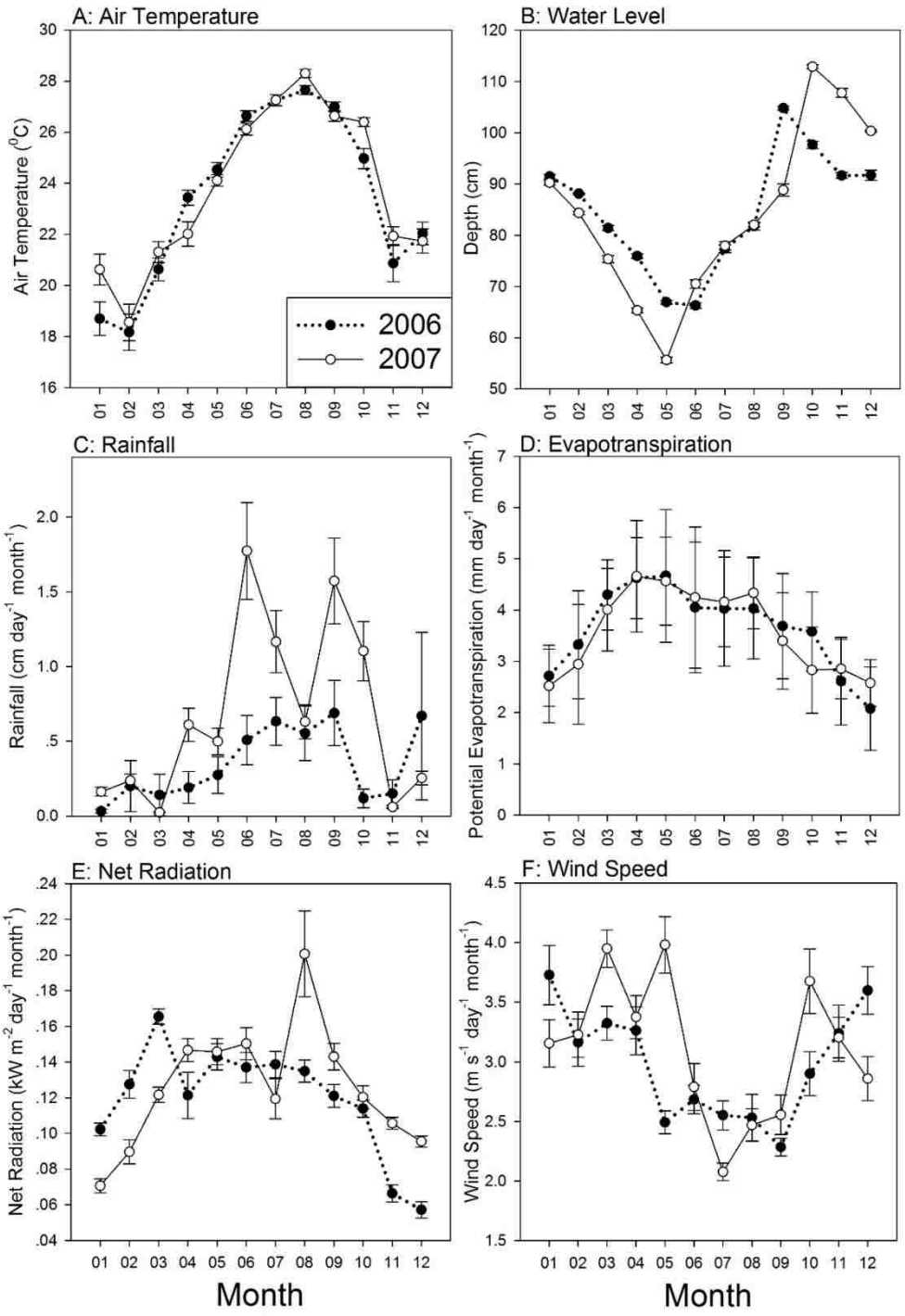

Figure 4.2: A, Temperature; B, Water Depth; C, Rainfall; D, Potential Evapotranspiration; E, Net Radiation; F, Wind speed. Data are from DBHYDRO database of South Florida Water Management District. Note: Potential Evapotranspiration is computed by A Simple or Abtew Method (Abtew, 1996).

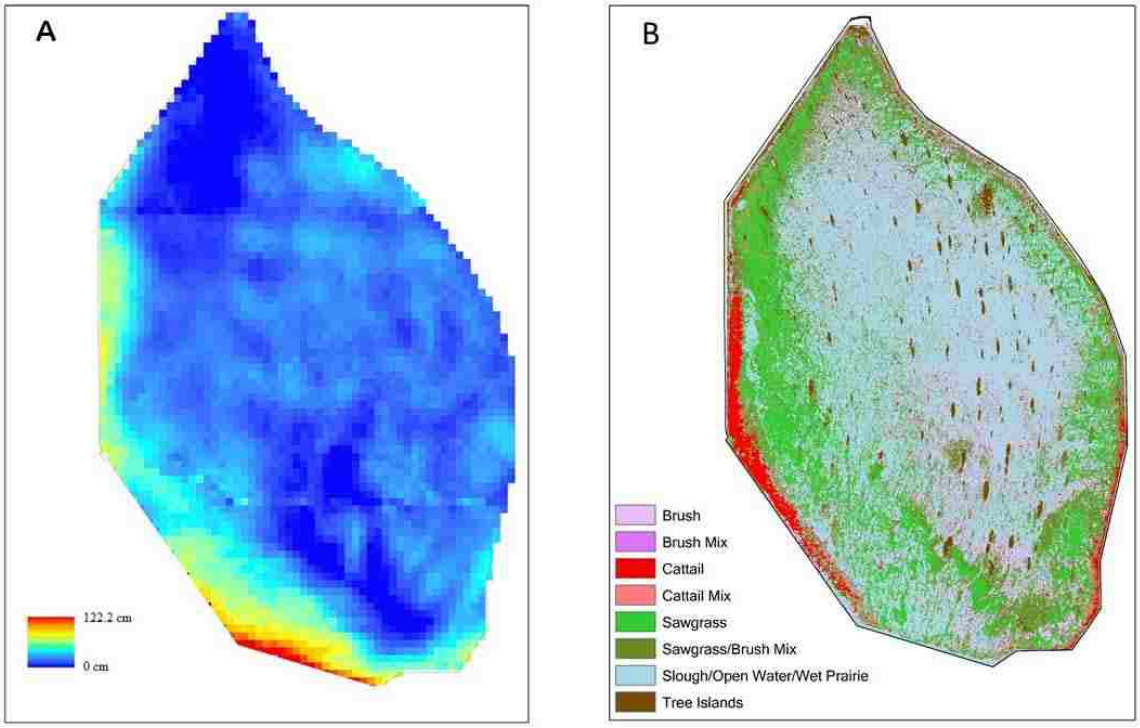

Figure 4.3: A: Average water depth map (in centimeter) of WCA-1 in the third quarter of 2006 calculated from Jones, et al, (2007). B: Vegetation map of WCA-1 calculated from data of Bancroft, et al (2002).

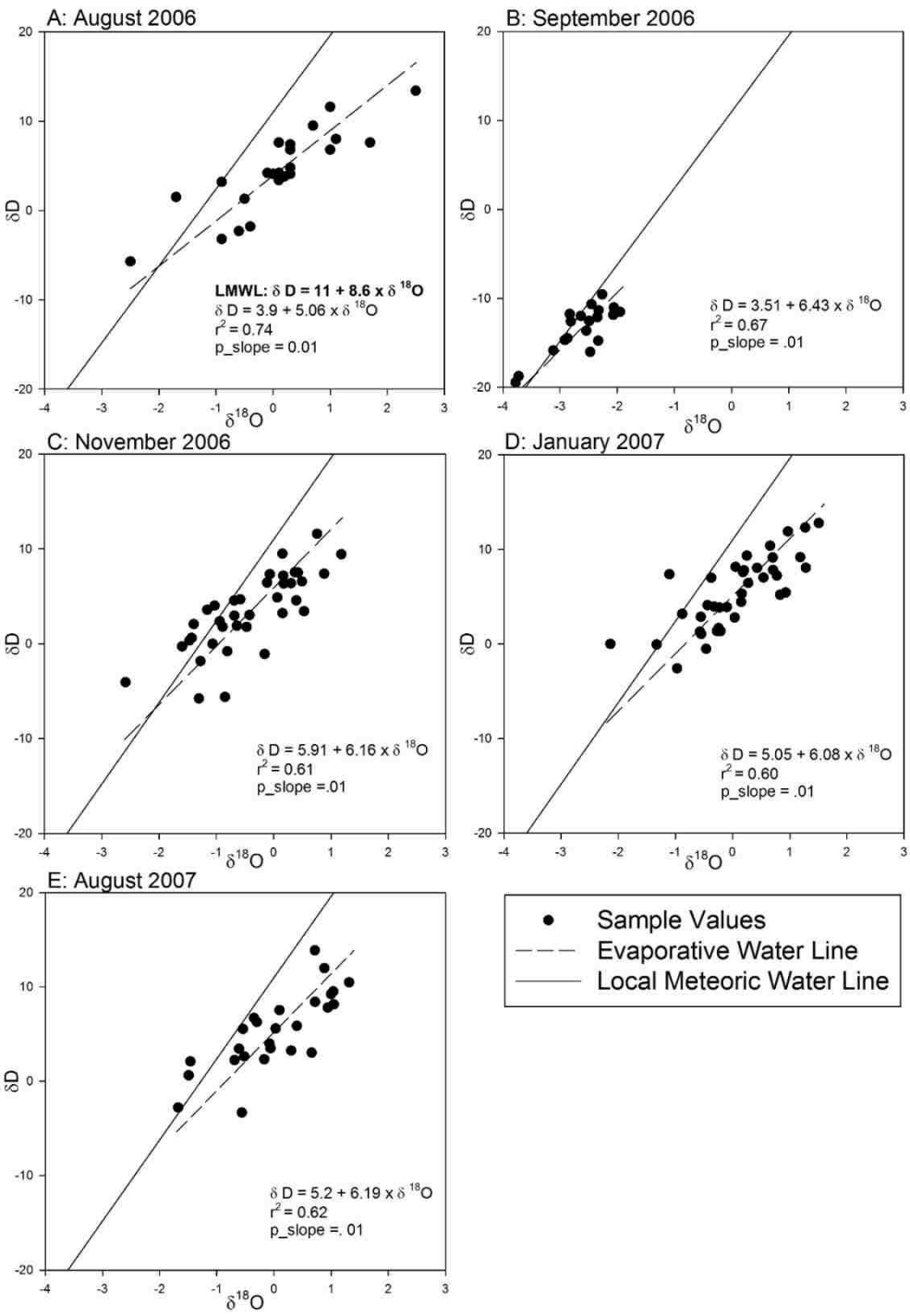

Figure 4.4: δD versus $\delta^{18}O$ of water from various sampling points in WCA-1 in the months of: A, August 2006; B, September 2006; C, November 2006; D, January 2007; E, August 2007. The local meteoric water line (LMWL) from precipitation is shown as solid lines, while the dashed lines represent the evaporative water line (EWL) for each month.

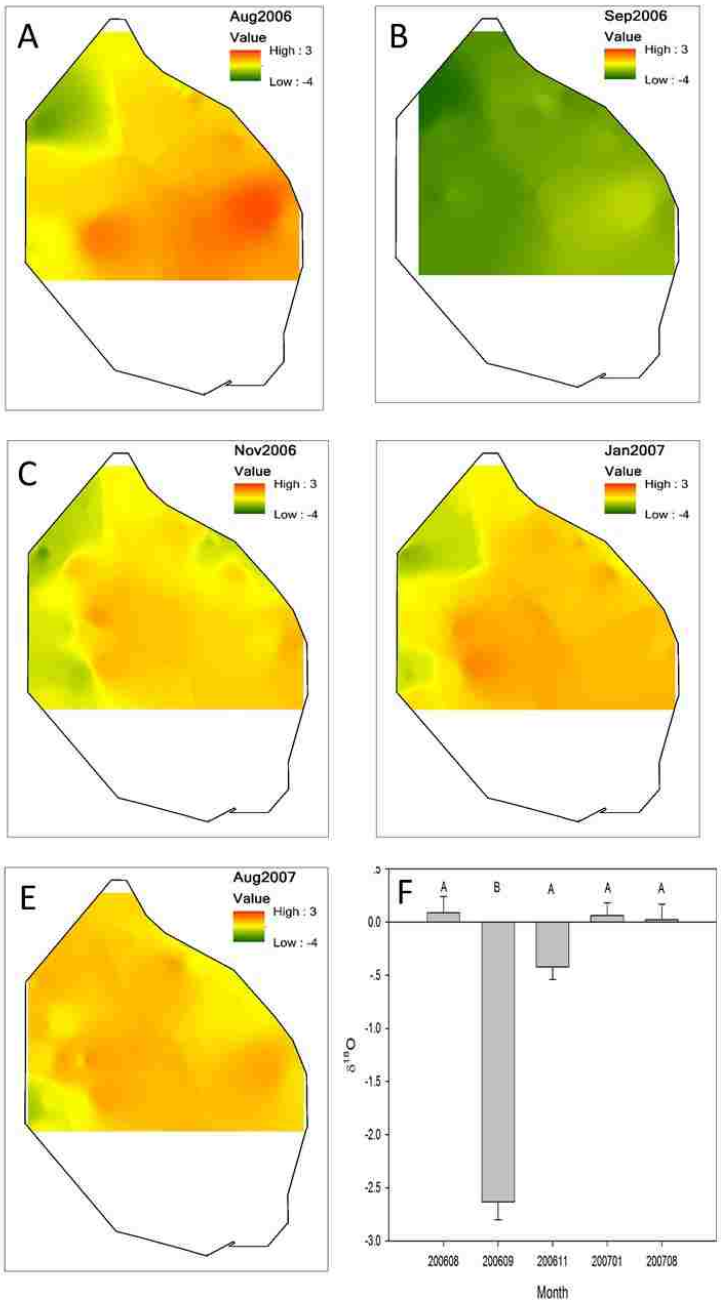

Figure 4.5: Distribution of water $\delta^{18}O$ values (‰) in WCA-1 in the months of: A, August 2006; B, September 2006; C, November 2006; D, January 2007; E, August 2007. And F: Average $\delta^{18}O$ values of water from WCA-1 for each month. Significant differences between months are represented with letters where months having a different letter have water $\delta^{18}O$ values significantly different from the other months. Data for the white part of maps (e.g., southern zone of the reservoir) was not considered, as there were several missing values. Water samples for all designated sampling locales could not be collected at all times since several sampling areas dried out during the sampling period.

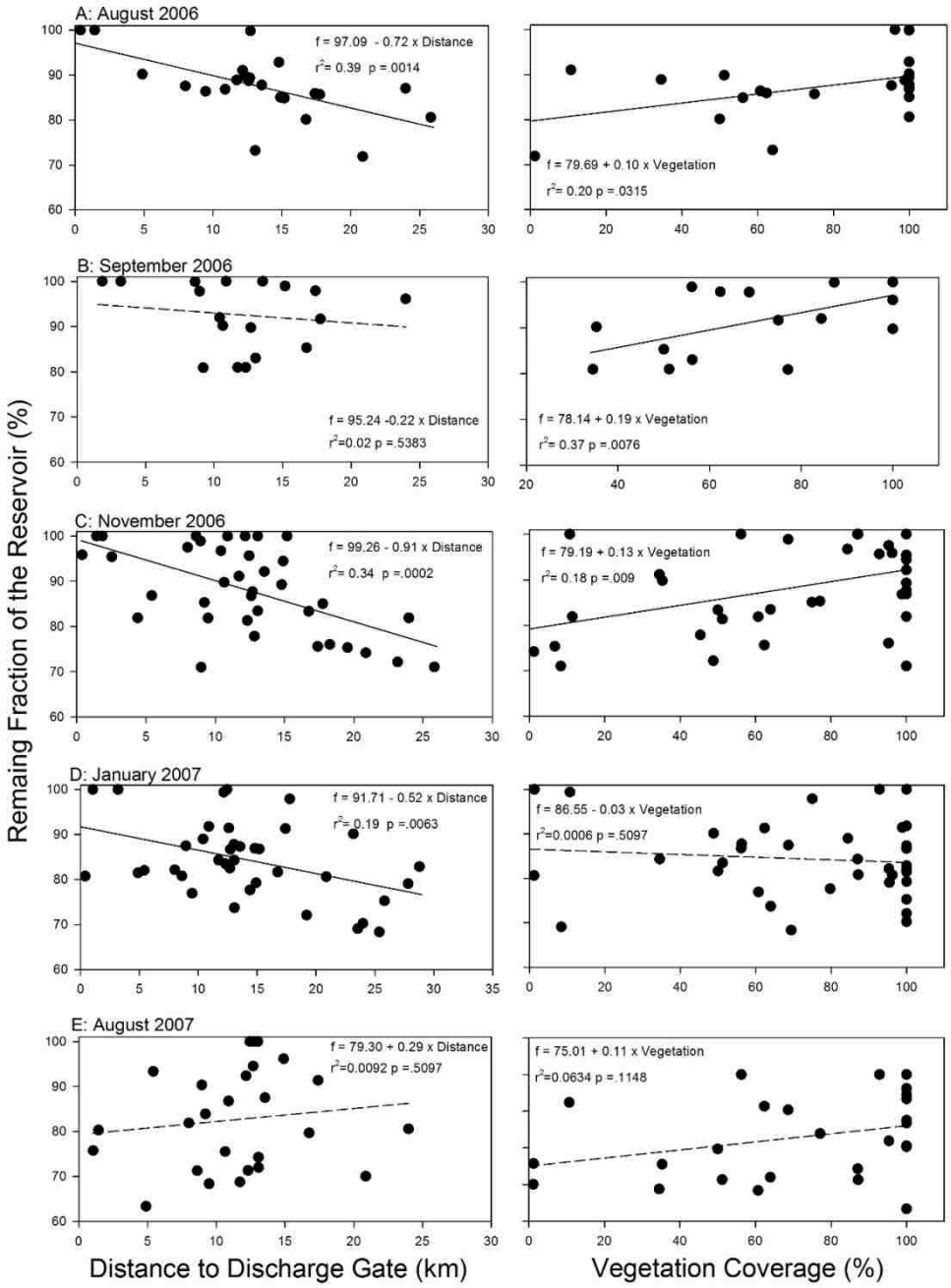

Figure 4.6: Relationship between *f* values and distance to discharge gate and vegetation coverage for: A, August 2006; B, September 2006; C, November 2006; D, January 2007; E, August 2007. The relationship was not significant (shown with a dashed line) for vegetation coverage in January and August 2007, and for discharge gate in September 2006 and August 2007 ($p>0.05$).

Chapter Five

Overall Conclusions

The research in this dissertation focused on the ecohydrological impacts of SLR and other climate changes on coastal wetlands. The impacts I studied include island submergence, vegetation shift from halophytes to glycophytes, and water loss by evaporation. The changes of the island area and their vegetation cover were assessed by comparative analysis of the historical aerial images and time-series of remote sensing images. The vegetation shift was simulated in an individual-based vegetation dynamics model, and the simulation also examined if time and location of the vegetation shift can be predicted by monitoring $\delta^{18}O$ values of plant stem water. Finally, a dual-isotope model was developed to quantify evaporation from a wetland ecosystem, and examine the influences of the vegetation, water depth and distance to discharging gate on the evaporation. Here I summarize the results, and discuss possible future directions of research on the basis of my findings.

Area of mud islands and the mangrove coverage are expanding under local sea level rise

Long-term island submergence by SLR is uncertain partly because of feedbacks between vegetation and geomorphology. However, the feedbacks can be disturbed by influences including human activities. Therefore, to validate long-term resilience of island ecosystems to SLR by the biogeomorphic feedbacks, there is a need for appropriate methodology and site conditions. Mud islands in Florida Bay are unique models that have the appropriate site conditions, as they are vegetated and have a low anthropogenic impact. To measure the spatial extent of the 15 mud islands, both high-

resolution 61-yr historical aerial images and 27-yr time-series of Landsat images are available. Further, I quantified the mangrove occupied areas of these islands. Comparative spatial analysis of their historical aerial images showed that the island area significantly increased from 1953 to 2014. The pattern of the island area increase was further supported by quantification of annual total areas of the 15 islands from Landsat satellite imagery (1984 to 2011), which showed significantly increasing total area with time. With expanding island area despite SLR, a strong mangrove expansion was also observed in these islands. Mangrove expansion may benefit these islands by mitigating SLR inundation according to my observation that the islands that increased in area tend to have a greater mangrove expansion

Yearly $\delta^{18}O$ values of plant stem water may predict impending salinity stress and mortality

In order to find an appropriate predictor for the potential vegetation shift, I incorporated stable isotope ^{18}O abundance as a tracer in various hydrologic components (e.g., vadose zone, water table) of a previously published model describing ecosystem shifts between hammock and mangrove communities in southern Florida. My study shows that $\delta^{18}O$ value of plant stem water may be a promising predictor of replacement of hammocks by mangroves three years before the replacement. Three years may be sufficient time to introduce appropriate amounts of freshwater flow to cease or slow replacement of hammocks by mangroves. My predictions will be useful for improving the efficiency of current ecological restoration in southern Florida. For example, the Comprehensive Everglades Restoration Plan proposes to return freshwater flow to the Everglades closer to historic conditions (Perry, 2004).

Heterogeneous distribution of evaporation quantified from the dual-isotope model indicate the vegetation and discharging gate influecence.

Quantifying evaporation in wetlands is challenging, because it is difficult to separate evaporation from transpiration. To precisely quantify evaporation, my study developed a dual-isotope based model ($\delta^{18}O$ and δD) to calculate the remaining fraction (*f*) of water in the reservoir after evaporation. My study represents the first to use this method to quantify evaporation in a tropical wetland environment. Vegetation coverage had a positive effect, and distance to the discharge gate had a negative effect on *f* for certain months of the year, while water depth had no effect on *f*. Therefore, vegetation and distance to discharge gate are two important factors on the spatial pattern of water loss by evaporation in this tropical wetland and my results may lead to a more informed wetland management.

Future Research

1. Mangroves in Florida Bay

Mud islands of Florida Bay, surprisingly, are increasing in area under local sea level rise, and the increasing area may be the result from mangrove expansion. Therefore, information on the status and dynamics of Florida Bay mangroves in these mud islands have a practical implication for the ecological conservation of ENP. I propose that there is a need to quantify mangrove morphological (e.g., tree height) and physiological (e.g., leaf $\delta^{13}C$, $\delta^{18}O$ and nutrient content) status in mud islands of Florida Bay, to relate these measurements as potential overall physiological indicators, and finally to examine the relationship between the physiological indicators and satellite-derived vegetation indices.

2. Leaf $\delta^{13}C$ as another potential indicator of vegetation shift

I propose to examine if leaf $\delta^{13}C$ value can be used as another potential indicator of vegetation shift on the basis of my dissertation research using $\delta^{18}O$ value of plant stem water to predict vegetation shift. Leaf $\delta^{13}C$ is highly related to the salt stress on coastal vegetation (Lin and Sternberg, 1992). As salt stress reduces the stomatal conductance of the leaf, there is a corresponding decrease in CO_2 entering the leaf, and a greater proportion of $^{13}CO_2$ is forced to be fixed during photosynthesis. Therefore, as salinity of plant source water increases, more $^{13}CO_2$ would be fixed and leaf $\delta^{13}C$ values would increase. This positive relationship between the salinity and leaf $\delta^{13}C$ is observed in mangroves of southern Florida (Lin and Sternberg, 1992). Although both the stem water $\delta^{18}O$ and foliar $\delta^{13}C$ values have a similar positive relationship with the soil salinity, they differ in their assessment of the SLR impacts on the vegetation dynamics. The $\delta^{18}O$ values of stem water can change over short periods of time as plants shift their use of water sources, whereas $\delta^{13}C$ values reflect carbon assimilated over the leaf lifetime. Therefore, the $\delta^{18}O$ may be a better indicator of the instantaneous plant water use, and the $\delta^{13}C$ may be a better indicator of the long-term use. Therefore, I propose to examine the leaf $\delta^{13}C$ as a better indicator of the long-term vegetation dynamics under the long-term salt stress caused by SLR.

3. Further development of the evaporation model

I propose to apply the deuterium excess method to quantify evaporation to determine ways in which salinity can increase in coastal water bodies. Salinity of coastal water bodies can be increased with global warming by two processes: salt water intrusion

under SLR and evaporation. However, these two processes have not been separately quantified by an appropriate method. The evaporation has been quantified by a dual-isotope model in my dissertation research, because evaporation can enrich heavier oxygen and hydrogen isotopes in water. In addition to evaporation, saltwater intrusion can affect water isotopes in the coastal water bodies by mixing with saline ocean water. Therefore, I propose to disentangle these two processes, respectively, by a Stable isotope based Evaporation and Saltwater intrusion Model (SESM) that I have developed.

Works Cited

Abtew W. 1996. Evapotranspiration measurements and modeling for three wetland systems in South Florida. Journal of the American Water Resources Association 32: 465-473.

Abtew W. 2001. Evaporation Estimation for Lake Okeechobee in South Florida. Journal of Irrigation and Drainage Engineering 127: 140-147.

Abtew W, Melesse A. 2013. Evaporation and evapotranspiration: measurements and estimations: Springer Science & Business Media.

Abtew W, Obeysekera J, Iricanin N. 2011. Pan evaporation and potential evapotranspiration trends in South Florida. Hydrological Processes 25: 958-969.

Albert S, Leon JX, Grinham AR, Church JA, Gibbes BR, Woodroffe CD. 2016. Interactions between sea-level rise and wave exposure on reef island dynamics in the Solomon Islands. Environmental Research Letters 11: 054011.

Allen J. 1998. Mangroves as alien species: the case of Hawaii. Global Ecology & Biogeography Letters 7: 61-71.

Allen ST, Edwards BL, Reba ML, Keim RF. 2016. Sub-canopy Evapotranspiration from Floating Vegetation and Open Water in a Swamp Forest. Wetlands: 1-8.

Armas C, Padilla FM, Pugnaire FI, Jackson RB. 2010. Hydraulic lift and tolerance to salinity of semiarid species: consequences for species interactions. Oecologia 162: 11-21.

Asbridge E, Lucas R, Ticehurst C, Bunting P. 2016. Mangrove response to environmental change in Australia's Gulf of Carpentaria. Ecology and Evolution: n/a-n/a.

Baldwin AH, Mendelssohn IA. 1998. Effects of salinity and water level on coastal marshes: an experimental test of disturbance as a catalyst for vegetation change. Aquatic Botany 61: 255-268.

Ball MC. 1988. Ecophysiology of mangroves. Trees 2: 129-142.

Bancroft GT, Gawlik DE, Rutchey K. 2002. Distribution of wading birds relative to vegetation and water depths in the northern Everglades of Florida, USA. Waterbirds 25: 265-277.

Bellard C, Leclerc C, Courchamp F. 2014. Impact of sea level rise on the 10 insular biodiversity hotspots. Global Ecology and Biogeography 23: 203-212.

Bird ECF. 1987. The modern prevalence of beach erosion. Marine Pollution Bulletin 18: 151-157.

Brovkin V, Claussen M, Petoukhov V, Ganopolski A. 1998. On the stability of the atmosphere‐vegetation system in the Sahara/Sahel region. Journal of Geophysical Research: Atmospheres 103: 31613-31624.

Cazenave A, Cozannet GL. 2014. Sea level rise and its coastal impacts. Earth's Future 2: 15-34.

Chang SW, Clement TP. 2012. Experimental and numerical investigation of saltwater intrusion dynamics in flux-controlled groundwater systems. Water Resources Research 48, W09527.

Chapman VJ. 1976. Mangrove vegetation. Vaduz, Germany: J. Cramer.

Clark ID, Fritz P. 1997. Environmental isotopes in hydrogeology: CRC Press.

Congalton RG. 1991. A review of assessing the accuracy of classifications of remotely sensed data. Remote Sensing of Environment 37: 35-46.

Craft C, Clough J, Ehman J, Joye S, Park R, Pennings S, Guo H, Machmuller M. 2008. Forecasting the effects of accelerated sea-level rise on tidal marsh ecosystem services. Frontiers in Ecology and the Environment 7: 73-78.

Craft CB. 2012. Tidal freshwater forest accretion does not keep pace with sea level rise. Global Change Biology 18: 3615-3623.

Craig H. 1961. Isotopic variations in meteoric waters. Science 133: 1702-1703.

Dakos V, Carpenter SR, Brock WA, Ellison AM, Guttal V, Ives AR, Kefi S, Livina V, Seekell DA, Van Nes EH. 2012. Methods for detecting early warnings of critical transitions in time series illustrated using simulated ecological data. PLoS One 7: e41010.

Davis SM, Childers DL, Lorenz JJ, Wanless HR, Hopkins TE. 2005. A conceptual model of ecological interactions in the mangrove estuaries of the Florida Everglades. Wetlands 25: 832-842.

Dawson TE, Ehleringer JR. 1991. Streamside trees that do not use stream water. Nature 350: 335-337.

Dawson TE, Mambelli S, Plamboeck AH, Templer PH, Tu KP. 2002. Stable isotopes in plant ecology. Annual Review of Ecology and Systematics: 507-559.

Desantis LR, Bhotika S, Williams K, Putz FE. 2007. Sea‐level rise and drought interactions accelerate forest decline on the Gulf Coast of Florida, USA. Global Change Biology 13: 2349-2360.

Desmond G. 2007. High Accuracy Elevation Data Collection Project. USGS, phttp://sofia.usgs.gov/projects/elev_data/

Doering PH, Chamberlain RH, Haunert DE. 2002. Using submerged aquatic vegetation to establish minimum and maximum freshwater inflows to the Caloosahatchee Estuary, Florida. Estuaries 25: 1343-1354.

Donohue RJ, Roderick ML, McVicar TR, Yang Y. 2017. A simple hypothesis of how leaf and canopy-level transpiration and assimilation respond to elevated CO2 reveals distinct response patterns between disturbed and undisturbed vegetation. Journal of Geophysical Research: Biogeosciences 122: 168-184.

Doyle TW, Krauss KW, Conner WH, From AS. 2010. Predicting the retreat and migration of tidal forests along the northern Gulf of Mexico under sea-level rise. Forest Ecology and Management 259: 770-777.

Drexler JZ, Snyder RL, Spano D, Paw U, Tha K. 2004. A review of models and micrometeorological methods used to estimate wetland evapotranspiration. Hydrological Processes 18: 2071-2101.

Duarte CM, Losada IJ, Hendriks IE, Mazarrasa I, Marba N. 2013. The role of coastal plant communities for climate change mitigation and adaptation. Nature Clim. Change 3: 961-968.

Duarte CM, Middelburg JJ, Caraco N. 2005. Major role of marine vegetation on the oceanic carbon cycle. Biogeosciences 2: 1-8.

Dubbert M, Cuntz M, Piayda A, Maguás C, Werner C. 2013. Partitioning evapotranspiration – Testing the Craig and Gordon model with field measurements of oxygen isotope ratios of evaporative fluxes. Journal of Hydrology 496: 142-153.

Duvat VKE, Pillet V. 2017. Shoreline changes in reef islands of the Central Pacific: Takapoto Atoll, Northern Tuamotu, French Polynesia. Geomorphology 282: 96-118.

Egler FE. 1952. Southeast saline Everglades vegetation, Florida and its management. Vegetatio 3: 213-265.

Eisenlohr WS. 1966. Water loss from a natural pond through transpiration by hydrophytes. Water Resources Research 2: 443-453.

Ellison JC, Mosley A, Helman M. 2017. Assessing atoll shoreline condition to guide community management. Ecological Indicators 75: 321-330.

Ellsworth P, Williams D. 2007. Hydrogen isotope fractionation during water uptake by woody xerophytes. Plant and Soil 291: 93-107.

Enos P. 1989. Islands in the Bay: A key habitat of Florida Bay. Bulletin of Marine Science 44: 365-386.

Eslami-Andargoli L, Dale P, Sipe N, Chaseling J. 2009. Mangrove expansion and rainfall patterns in Moreton Bay, Southeast Queensland, Australia. Estuarine, coastal and shelf science 85: 292-298.

Ewe SML, Sternberg LdSL. 2005. Water uptake patterns of an invasive exotic plant in coastal saline habitats. Journal of Coastal Research: 255-264.

Ewe SML, Sternberg LdSL, Childers DL. 2007. Seasonal plant water uptake patterns in the saline southeast Everglades ecotone. Oecologia 152: 607-616.

Ezer T, Atkinson LP. 2014. Accelerated flooding along the U.S. East Coast: On the impact of sea-level rise, tides, storms, the Gulf Stream, and the North Atlantic Oscillations. Earth's Future 2: 362-382.

Feller IC, Dangremond EM, Devlin DJ, Lovelock CE, Proffitt CE, Rodriguez W. 2015. Nutrient enrichment intensifies hurricane impact in scrub mangrove ecosystems in the Indian River Lagoon, FL USA. Ecology.

Finch J, Hall R. 2001. Estimation of Open Water Evaporation: A Review of Methods. Bristol, UK: Environment Agency, p144.

Finn N, Barnes S. 2007. The benefits of shade-cloth covers for potable water storages. CSIRO Gale Paxific, Victoria, Australia: CSIRO Textile and Fibre Technology.

Fitterman DV, Deszcz-Pan M, Stoddard CE. 1999. Results of time-domain electromagnetic soundings in Everglades National Park, Florida. US Department of the Interior, p99-426.

Fourqurean JW, Robblee MB. 1999. Florida Bay: a history of recent ecological changes. Estuaries 22: 345-357.

Gat JR. 1995. Stable isotopes of fresh and saline lakes. Lerman A editor. Physics and chemistry of lakes. New York: Springer-Verlag, p139-165.

Gill AM, Tomlinson PB. 1977. Studies on the growth of Red Mangrove (Rhizophora mangle L.) 4. the adult root system. Biotropica 9: 145-155.

Giri C, Long J. 2016. Is the geographic range of mangrove forests in the conterminous United States really expanding? Sensors 16: 2010.

Giri C, Muhlhausen J. 2008. Mangrove forest distributions and dynamics in Madagascar (1975–2005). Sensors 8: 2104.

Gonfiantini R. 1986. Environmental isotopes in lake studies. Fritz P, Fontes JC editors. Handbook of environmental isotope geochemistry: Elsevier, p113-168.

Greaver TL, Sternberg LLdS. 2006. Linking marine resources to ecotonal shifts of water uptake by terrestrial dune vegetation. Ecology 87: 2389-2396.

Greiner La Peyre M, Grace J, Hahn E, Mendelssohn I. 2001. The importance of competition in regulating plant species abundance along a salinity gradient. Ecology 82: 62-69.

Grimm V, Berger U, Bastiansen F, Eliassen S, Ginot V, Giske J, Goss-Custard J, Grand T, Heinz SK, Huse G, Huth A, Jepsen JU, Jørgensen C, Mooij WM, Müller B, Pe'er G, Piou C, Railsback SF, Robbins AM, Robbins MM, Rossmanith E, Rüger N, Strand E, Souissi S, Stillman RA, Vabø R, Visser U, DeAngelis DL. 2006. A standard protocol for describing individual-based and agent-based models. Ecological Modelling 198: 115-126.

Guha H, Panday S. 2012. Impact of Sea Level Rise on groundwater salinity in a coastal community of South Florida. Journal of the American Water Resource Association 48: 510-529.

Gunderson LH. 1994. Vegetation of the Everglades: determinants of community composition. Davis SM, Ogden JC editors. Everglades: the ecosystem and its restoration. Boca Raton, FL: CRC Press, p323-340.

Harvey J, McCormick P. 2009. Groundwater's significance to changing hydrology, water chemistry, and biological communities of a floodplain ecosystem, Everglades, South Florida, USA. Hydrogeology Journal 17: 185-201.

Hassan MM, Peirson WL, Neyland BM, Fiddis NM. 2015. Evaporation mitigation using floating modular devices. Journal of Hydrology 530: 742-750.

Hay CC, Morrow E, Kopp RE, Mitrovica JX. 2015. Probabilistic reanalysis of twentieth-century sea-level rise. Nature.

Helfer F, Zhang H, Lemckert CJ. 2009. Evaporation Reduction by Windbreaks: Overview, Modelling and Efficiency. Urban Water Security Research Alliance Technical Report No. 16.

Herbert DA, Perry WB, Cosby BJ, Fourqurean JW. 2011. Projected reorganization of Florida Bay seagrass communities in response to the increased freshwater inflow of Everglades restoration. Estuaries and Coasts 34: 973-992.

Hoffmeister JE. 1974. Land from the sea: The geologic story of South Florida. Coral Gables, Florida, USA: University of Miami Press.

Hollins S, Ridd P, Read W. 2000. Measurement of the diffusion coefficient for salt in salt flat and mangrove soils. Wetlands Ecology and Management 8: 257-262.

Hong S-H, Wdowinski S, Kim S-W, Won J-S. 2010. Multi-temporal monitoring of wetland water levels in the Florida Everglades using interferometric synthetic aperture radar (InSAR). Remote Sensing of Environment 114: 2436-2447.

Huang T, Pang Z. 2012. The role of deuterium excess in determining the water salinisation mechanism: A case study of the arid Tarim River Basin, NW China. Applied Geochemistry 27: 2382-2388.

Ish-Shalom N, Sternberg LdSL, Ross M, O'Brien J, Flynn L. 1992. Water utilization of tropical hardwood hammocks of the lower Florida Keys. Oecologia 92: 108-112.

Jiang J, DeAngelis DL, Anderson GH, Smith III TJ. 2014. Analysis and simulation of propagule dispersal and salinity intrusion from storm surge on the movement of a marsh–mangrove ecotone in South Florida. Estuaries and Coasts: 24-35.

Jiang J, DeAngelis DL, Smith III TJ, Teh SY, Koh HL. 2012a. Spatial pattern formation of coastal vegetation in response to external gradients and positive feedbacks affecting soil porewater salinity: a model study. Landscape Ecology 27: 109-119.

Jiang J, DeAngelis DL, Teh S-Y, Krauss KW, Wang H, Li H, Smith TJ, Koh H-L. 2016. Defining the next generation modeling of coastal ecotone dynamics in response to global change. Ecological Modelling 326: 168-176.

Jiang J, Gao D, DeAngelis DL. 2012b. Towards a theory of ecotone resilience: coastal vegetation on a salinity gradient. Theoretical Population Biology 82: 29-37.

Jones JW, Price SD. 2007. Conceptual design of the Everglades Depth Estimation Network (EDEN) grid. U. S. Geological Survey.

Kadmon R, Harari-Kremer R. 1999. Studying long-term vegetation dynamics using digital processing of historical aerial photographs. Remote Sensing of Environment 68: 164-176.

Kathiresan K, Bingham BL. 2001. Biology of mangroves and mangrove Ecosystems. Advances in Marine Biology 40: 81-251.

Kenkel N, McIlraith A, Burchill C, Jones G. 1991. Competition and the response of three plant species to a salinity gradient. Canadian Journal of Botany 69: 2497-2502.

Kirwan ML, Megonigal JP. 2013. Tidal wetland stability in the face of human impacts and sea-level rise. Nature 504: 53-60.

Kirwan ML, Temmerman S, Skeehan EE, Guntenspergen GR, Fagherazzi S. 2016. Overestimation of marsh vulnerability to sea level rise. Nature Clim. Change 6: 253-260.

Kjellin J, Wörman A, Johansson H, Lindahl A. 2007. Controlling factors for water residence time and flow patterns in Ekeby treatment wetland, Sweden. Advances in Water Resources 30: 838-850.

Korkmaz S, Goksuluk D, Zararsiz G. 2014. MVN: An R Package for assessing multivariate normality. The R Journal 6(2): 151-162.

Kosten S, Huszar VLM, Mazzeo N, Scheffer M, Sternberg LdSL, Jeppesen E. 2009. Lake and watershed characteristics rather than climate influence nutrient limitation in shallow lakes. Ecological Applications 19: 1791-1804.

Krauss KW, Allen JA, Cahoon DR. 2003. Differential rates of vertical accretion and elevation change among aerial root types in Micronesian mangrove forests. Estuarine, Coastal and Shelf Science 56: 251-259.

Krauss KW, From AS, Doyle TW, Doyle TJ, Barry MJ. 2011. Sea-level rise and landscape change influence mangrove encroachment onto marsh in the Ten Thousand Islands region of Florida, USA. Journal of Coastal Conservation 15: 629-638.

Kriebel DL, Geiman JD, Henderson GR. 2015. Future flood frequency under Sea-Level Rise scenarios. Journal of Coastal Research 31: 1078-1083.

Kundu PK, Cohen IM, Dowling DR. 2012. Fluid Mechanics. 5th edition. : Academic Press.

López-Medellín X, Ezcurra E, González-Abraham C, Hak J, Santiago LS, Sickman JO. 2011. Oceanographic anomalies and sea-level rise drive mangroves inland in the Pacific coast of Mexico. Journal of Vegetation Science 22: 143-151.

Langevin CD, Zygnerski M. 2013. Effect of Sea-Level Rise on salt water intrusion near a coastal well field in southeastern Florida. Groundwater 51: 781-803.

Legendre P. 1998. Model II regression user's guide, R edition. R Vignette.

Lin G, Sternberg LdSL. 1992. Effect of growth form, salinity, nutrient and sulfide on photosynthesis, carbon isotope discrimination and growth of red mangrove (Rhizophora mangle L.). Functional Plant Biology 19: 509-517.

Lin G, Sternberg LdSL. 1994. Utilization of surface water by red mangrove (Rhizophora mangle L.): an isotopic study. Bulletin of Marine Science 54: 94-102.

Lin GH, Sternberg LdSL. 1993. Hydrogen isotopic fractionation by plant roots during water uptake in coastal wetland plants. Ehleringer J, Hall A, Farquhar G editors. Stable isotopes and plant carbon-water relations. San Diego, CA, USA: Academic Press p397-410.

Liu X, Xia J, Wright G, Arnold L. 2014. A state of the art review on High Water Mark (HWM) determination. Ocean & Coastal Management 102, Part A: 178-190.

Livingstone DM, Lotter AF. 1998. The relationship between air and water temperatures in lakes of the Swiss Plateau: a case study with pal\sgmaelig;olimnological implications. Journal of Paleolimnology 19: 181-198.

Lloyd RM. 1964. Variations in the oxygen and carbon isotope ratios of Florida Bay mollusks and their environmental significance. The Journal of Geology: 84-111.

Lovelock CE, Cahoon DR, Friess DA, Guntenspergen GR, Krauss KW, Reef R, Rogers K, Saunders ML, Sidik F, Swales A, Saintilan N, Thuyen LX, Triet T. 2015. The vulnerability of Indo-Pacific mangrove forests to sea-level rise. Nature 526: 559-563.

Lugo AE. 1980. Mangrove ecosystems: successional or steady state? Biotropica: 65-72.

Lugo AE, Sell M, Snedaker SC. 1976. Mangrove ecosystem analysis. Systems analysis and simulation in ecology 4: 113-145.

Majoube M. 1971. Fractionation of oxygen 18 and of deuterium between water and its vapor. J. Chem. Phys 68: 1423-1436.

McLean R, Kench P. 2015. Destruction or persistence of coral atoll islands in the face of 20th and 21st century sea-level rise? Wiley Interdisciplinary Reviews: Climate Change 6: 445-463.

McVicar TR, Roderick ML, Donohue RJ, Li LT, Van Niel TG, Thomas A, Grieser J, Jhajharia D, Himri Y, Mahowald NM, Mescherskaya AV, Kruger AC, Rehman S, Dinpashoh Y. 2012. Global review and synthesis of trends in observed terrestrial near-surface wind speeds: Implications for evaporation. Journal of Hydrology 416–417: 182-205.

Meeder JF, Ross MS, Telesnicki G, Ruiz PL, Sah JP. 1996. Vegetation analysis in the C-111/Taylor Slough basin. Final Report for Contract C-4244. Miami, FL, USA: Southeast Environmental Research Program, Florida International Univeristy.

Mengistu MG, Everson CS, Clulow AD. 2014. The impact of taro (Colocasia esculenta) cultivation on the total evaporation of a Cyperus latifolius marsh. Hydrological Processes 28: 620-627.

Moffett KB, Gorelick SM, McLaren RG, Sudicky EA. 2012. Salt marsh ecohydrological zonation due to heterogeneous vegetation–groundwater–surface water interactions. Water Resources Research 48: 1-22.

Mohamed YA, Bastiaanssen WGM, Savenije HHG, van den Hurk BJJM, Finlayson CM. 2012. Wetland versus open water evaporation: An analysis and literature review. Physics and Chemistry of the Earth, Parts A/B/C 47–48: 114-121.

Morris JT. 2006. Competition among marsh macrophytes by means of geomorphological displacement in the intertidal zone. Estuarine, Coastal and Shelf Science 69: 395-402.

Mykleby PM, Lenters JD, Cutrell GJ, Herrman KS, Istanbulluoglu E, Scott DT, Twine TE, Kucharik CJ, Awada T, Soylu ME, Dong B. 2016. Energy and water balance response of a vegetated wetland to herbicide treatment of invasive Phragmites australis. Journal of Hydrology 539: 290-303.

Nelsen J, Ginsburg R. 1986. Calcium carbonate production by epibionts on Thalassia in Florida Bay. Journal of Sedimentary Petrology 56: 622-628.

Neter J, Kutner MH, Nachtsheim CJ, Wasserman W. 1996. Applied linear statistical models: Irwin Chicago.

Obeysekera J, Irizarry M, Park J, Barnes J, Dessalegne T. 2011. Climate change and its implications for water resources management in south Florida. Stochastic Environmental Research and Risk Assessment 25: 495-516.

Odum WE, McIvor CC. 1990. Mangroves. Myers RL, Ewel JJ editors. Ecosystems of Florida. Orlando, Florida, USA: University of Central Florida Press, p517-548.

Odum WE, McIvor CC, Smith III TJ. 1982. The ecology of the mangroves of south Florida: a community profile. Washington D.C., USA: Fish and Wildlife Service.

Passioura J, Ball M, Knight J. 1992. Mangroves may salinize the soil and in so doing limit their transpiration rate. Functional Ecology: 476-481.

Perry W. 2004. Elements of South Florida's comprehensive Everglades restoration plan. Ecotoxicology 13: 185-193.

Peterson JM, Bell SS. 2015. Saltmarsh boundary modulates dispersal of mangrove propagules: implications for mangrove migration with Sea-Level Rise. PLoS One 10: e0119128.

Pham SV, Leavitt PR, McGowan S, Wissel B, Wassenaar LI. 2009. Spatial and temporal variability of prairie lake hydrology as revealed using stable isotopes of hydrogen and oxygen. Limnology and Oceanography 54: 101-118.

Price RM, Swart PK. 2006. Geochemical indicators of groundwater recharge in the surficial aquifer system, Everglades National Park, Florida, USA. Geological Society of America Special Papers 404: 251-266.

Price RM, Swart PK, Willoughby HE. 2008. Seasonal and spatial variation in the stable isotopic composition ($\delta^{18}O$ and δD) of precipitation in south Florida. Journal of Hydrology 358: 193-205.

Rabinowitz D. 1978. Early growth of mangrove seedlings in Panama, and an hypothesis concerning the relationship of dispersal and zonation. Journal of Biogeography 5: 113-133.

Ross MS, Meeder JF, Sah JP, Ruiz PL, Telesnicki GJ. 2000. The southeast saline Everglades revisited: 50 years of coastal vegetation change. Journal of Vegetation Science 11: 101-112.

Ross MS, O'Brien JJ, Flynn LJ. 1992. Ecological site classification of Florida Keys terrestrial habitats. Biotropica: 488-502.

Ross MS, O'Brien JJ, Ford RG, Zhang K, Morkill A. 2009. Disturbance and the rising tide: the challenge of biodiversity management on low-island ecosystems. Frontiers in Ecology and the Environment 7: 471-478.

Ross MS, O'Brien JJ, Sternberg LdSL. 1994. Sea-level rise and the reduction in pine forests in the Florida Keys. Ecological Applications: 144-156.

Sánchez-Carrillo S, Angeler DG, Sánchez-Andrés R, Alvarez-Cobelas M, Garatuza-Payán J. 2004. Evapotranspiration in semi-arid wetlands: relationships between inundation and the macrophyte-cover:open-water ratio. Advances in Water Resources 27: 643-655.

Saha AK, Saha S, Sadle J, Jiang J, Ross MS, Price RM, Sternberg LdSL, Wendelberger KS. 2011. Sea level rise and South Florida coastal forests. Climatic Change 107: 81-108.

Saha AK, Sternberg LdSL, Miralles‐Wilhelm F. 2009. Linking water sources with foliar nutrient status in upland plant communities in the Everglades National Park, USA. Ecohydrology 2: 42-54.

Saha S, Sadle J, Heiden C, Sternberg LdSL. 2014. Salinity, groundwater, and water uptake depth of plants in coastal uplands of Everglades National Park (Florida, USA). Ecohydrology 8: 128-136.

Saintilan N, Wilton K. 2001. Changes in the distribution of mangroves and saltmarshes in Jervis Bay, Australia. Wetlands Ecology and Management 9: 409-420.

Sall J, Lehman A, Stephens ML, Creighton L. 2012. JMP start statistics: a guide to statistics and data analysis using JMP: SAS Institute.

Scheffer M, Bascompte J, Brock WA, Brovkin V, Carpenter SR, Dakos V, Held H, Van Nes EH, Rietkerk M, Sugihara G. 2009. Early-warning signals for critical transitions. Nature 461: 53-59.

Scheffer M, Rinaldi S, Gragnani A, Mur LR, van Nes EH. 1997. On the dominance of filamentous cyanobacteria in shallow, turbid lakes. Ecology 78: 272-282.

Schlesinger WH, Jasechko S. 2014. Transpiration in the global water cycle. Agricultural and Forest Meteorology 189–190: 115-117.

Scholander PF. 1968. How mangroves desalinate seawater. Physiologia Plantarum 21: 251-261.

Scholander PF, Hammel HT, Hemmingsen E, Garey W. 1962. Salt balance in mangroves. Plant Physiology 37: 722.

Schoumans OF, Chardon WJ, Bechmann ME, Gascuel-Odoux C, Hofman G, Kronvang B, Rubæk GH, Ulén B, Dorioz JM. 2014. Mitigation options to reduce phosphorus losses from the agricultural sector and improve surface water quality: A review. Science of The Total Environment 468–469: 1255-1266.

Schwerdtfeger J, Johnson MS, Couto EG, Amorim RSS, Sanches L, Campelo Jr JH, Weiler M. 2014. Inundation and groundwater dynamics for quantification of evaporative water loss in tropical wetlands. Hydrol. Earth Syst. Sci. 18: 4407-4422.

Silander J, Antonovics J. 1982. Analysis of interspecific interactions in a coastal plant community—a perturbation approach. Nature 298: 557-560.

Sklar FH, McVoy C, VanZee R, Gawlik DE, Tarboton K, Rudnick D, Miao S, Armentano T. 2002. The effects of altered hydrology on the ecology of the Everglades. Porter JW, Porter KG editors. The Everglades, Florida Bay and coral reefs of the Florida keys: an ecosystem source book. Boca Raton, Florida, USA: CRC Press, p39-82.

Sklar FH, van der Valk A. 2002. Tree islands of the Everglades: Springer.

Skrzypek G, Mydłowski A, Dogramaci S, Hedley P, Gibson JJ, Grierson PF. 2015. Estimation of evaporative loss based on the stable isotope composition of water using Hydrocalculator. Journal of Hydrology 523: 781-789.

Smith III TJ, Anderson GH, Balentine K, Tiling G, Ward GA, Whelan KR. 2009. Cumulative impacts of hurricanes on Florida mangrove ecosystems: sediment deposition, storm surges and vegetation. Wetlands 29: 24-34.

Smith III TJ, Tiling-Range G, Jones J, Nelson P, Foster A, Balentine K. 2010. The use of historical charts and photographs in ecosystem restoration: examples from the Everglades Historical Air Photo Project. Cowley DC, Standring RA, Abicht MJ editors. Landscapes through the Lens: Aerial Photographs and the Historic Environment. Occasional Publication of the Aerial Archaeology Research Group. Oxford, UK: Oxbow Books, p179-191.

Snedaker SC. 1995. Mangroves and climate change in the Florida and Caribbean region: scenarios and hypotheses. Wong Y-S, Tam NY editors. Asia-Pacific Symposium on Mangrove Ecosystems: Springer Netherlands, p43-49.

Snyder JR, Herndon A, Robertson Jr WB. 1990. South Florida rockland. L. MR, J. EJ editors. Ecosystems of Florida. Orlando, Florida, USA: University of Central Florida Press, p230-279.

Sokal R, Rohlf F. 1995. Biometry: the principles and practice of statistics in biological research. New York: W. H. Freeman and Company.

Stephens DB. 1995. Vadose zone hydrology. Boca Raton, Florida, USA: CRC Press. 1-2p.

Sternberg LdSL. 2001. Savanna–forest hysteresis in the tropics. Global Ecology and Biogeography 10: 369-378.

Sternberg LdSL, Green L, Moreira MZ, Nepstad D, Martinelli LA, Victória R. 1998. Root distribution in an Amazonian seasonal forest as derived from δ13C profiles. Plant and Soil 205: 45-50.

Sternberg LdSL, Ish-Shalom-Gordon N, Ross M, O'Brien J. 1991. Water relations of coastal plant communities near the ocean/freshwater boundary. Oecologia 88: 305-310.

Sternberg LdSL, Moreira MZ, Nepstad DC. 2002. Uptake of water by lateral roots of small trees in an Amazonian tropical forest. Plant and soil 238: 151-158.

Sternberg LdSL, Swart PK. 1987. Utilization of freshwater and ocean water by coastal plants of southern Florida. Ecology: 1898-1905.

Sternberg LdSL, Teh SY, Ewe SML, Miralles-Wilhelm FR, DeAngelis DL. 2007. Competition between hardwood hammocks and mangroves. Ecosystems 10: 648-660.

Steyer GD, Cretini KF, Piazza S, Sharp LA, Snedden GA, Sapkota S. 2010. Hurricane influences on vegetation community change in coastal Louisiana. U. S. Geological Survey.

Swales A, Bentley SJ, Lovelock CE. 2015. Mangrove-forest evolution in a sediment-rich estuarine system: opportunists or agents of geomorphic change? Earth Surface Processes and Landforms 40: 1672-1687.

Swart PK, Kramer PA. 2004. Geology of mud islands in Florida Bay. Developments in Sedimentology, p249-274.

Swart PK, Sternberg LdSL, Steinen R, Harrison SA. 1989. Controls on the oxygen and hydrogen isotopic composition of the waters of Florida Bay, USA. Chemical Geology: Isotope Geoscience section 79: 113-123.

Syvitski JPM, Kettner AJ, Overeem I, Hutton EWH, Hannon MT, Brakenridge GR, Day J, Vorosmarty C, Saito Y, Giosan L, Nicholls RJ. 2009. Sinking deltas due to human activities. Nature Geosci 2: 681-686.

Teh SY, DeAngelis DL, Sternberg LdSL, Miralles-Wilhelm FR, Smith TJ, Koh H-L. 2008. A simulation model for projecting changes in salinity concentrations and species dominance in the coastal margin habitats of the Everglades. Ecological Modelling 213: 245-256.

Teh SY, Turtora M, DeAngelis DL, Jiang J, Pearlstine L, Koh HL. 2015. Application of a Coupled Vegetation Competition and Groundwater Simulation Model to Study Effects of Sea Level Rise and Storm Surges on Coastal Vegetation. Journal of Marine Science and Engineering 3: 1149-1177.

Thompson DK, Baisley AS, Waddington JM. 2015. Seasonal variation in albedo and radiation exchange between a burned and unburned forested peatland: implications for peatland evaporation. Hydrological Processes 29: 3227-3235.

Thorpe SA. 2007. An introduction to ocean turbulence: Cambridge University Press.

Tomlinson PB. 1994. The botany of mangroves: Cambridge University Press.

Vendramini PF, Sternberg LdSL. 2007. A faster plant stem‐water extraction method. Rapid communications in mass spectrometry 21: 164-168.

Volkmar K, Hu Y, Steppuhn H. 1998. Physiological responses of plants to salinity: a review. Canadian Journal of Plant Science 78: 19-27.

Wallace JM, Hobbs PV. 2006. Atmospheric science: an introductory survey: Academic Press.

Wang K, Dickinson RE. 2012. A review of global terrestrial evapotranspiration: Observation, modeling, climatology, and climatic variability. Reviews of Geophysics 50: n/a-n/a.

Wanless HR, Tagett MG. 1989. Origin, growth and evolution of carbonate mudbanks in Florida Bay. Bulletin of Marine Science 44: 454-489.

Wasson K, Woolfolk A, Fresquez C. 2013. Ecotones as indicators of changing environmental conditions: rapid migration of salt marsh–upland boundaries. Estuaries and Coasts 36: 654-664.

Webb AP, Kench PS. 2010. The dynamic response of reef islands to sea-level rise: Evidence from multi-decadal analysis of island change in the Central Pacific. Global and Planetary Change 72: 234-246.

Wei L, Lockington DA, Poh S-C, Gasparon M, Lovelock CE. 2012. Water use patterns of estuarine vegetation in a tidal creek system. Oecologia 172: 485-494.

Welch R, Madden M. 1999. Vegetation map and digital database of south Florida's National Park Service lands. Final Report to the US Department of the Interior, National Park Service, Cooperative Agreement Number 5280–4.

West JB, Bowen GJ, Dawson TE, Tu KP. 2010. Isoscapes: Springer.

Wetzel FT, Beissmann H, Penn DJ, Jetz W. 2013. Vulnerability of terrestrial island vertebrates to projected sea-level rise. Global Change Biology 19: 2058-2070.

White E, Kaplan D. 2017. Restore or retreat? Saltwater intrusion and water management in coastal wetlands. Ecosystem Health and Sustainability 3(1).

Wilcox WM, Solo-Gabriele HM, Sternberg LOR. 2004. Use of stable isotopes to quantify flows between the Everglades and urban areas in Miami-Dade County Florida. Journal of Hydrology 293: 1-19.

Wild M. 2009. Global dimming and brightening: A review. Journal of Geophysical Research: Atmospheres 114, D00D16.

Willett KM, Jones PD, Gillett NP, Thorne PW. 2008. Recent changes in surface humidity: development of the HadCRUH dataset. Journal of Climate 21: 5364-5383.

Wilson AM, Evans T, Moore W, Schutte CA, Joye SB, Hughes AH, Anderson JL. 2014. Groundwater controls ecological zonation of salt marsh macrophytes. Ecology 96: 840-849.

Wilson AM, Moore WS, Joye SB, Anderson JL, Schutte CA. 2011. Storm-driven groundwater flow in a salt marsh. Water Resources Research 47: n/a-n/a.

Wu C-L, Shukla S. 2014. Eddy covariance-based evapotranspiration for a subtropical wetland. Hydrological Processes 28: 5879-5896.

Xin P, Jin G, Li L, Barry DA. 2009. Effects of crab burrows on pore water flows in salt marshes. Advances in Water Resources 32: 439-449.

Zhai L, Jiang J, DeAngelis D, Sternberg LdSL. 2016. Prediction of plant vulnerability to salinity increase in a coastal ecosystem by stable isotope composition ($\delta^{18}O$) of plant stem water: a model study. Ecosystems 19: 32-49.

Zhang Y, Peña-Arancibia JL, McVicar TR, Chiew FHS, Vaze J, Liu C, Lu X, Zheng H, Wang Y, Liu YY, Miralles DG, Pan M. 2016. Multi-decadal trends in global terrestrial evapotranspiration and its components. Scientific Reports 6: 19124.